Studies of number-phase fluctuation effects in strongly correlated inhomogeneous conductors

A Thesis

Submitted to
Tata Institute of Fundamental Research, Mumbai, India
for the degree of
Doctor of Philosophy
in
Physics

By

Sarath Sankar
Department of Theoretical Physics
Tata Institute of Fundamental Research
Mumbai - 400005, India

September 2018
Final version submitted in December 2018

I would like to dedicate this thesis to two of my grandparents who passed away during my PhD time and to my loving parents and grandmother . . .

DECLARATION

This thesis is a presentation of my original research work. Wherever contributions of others are involved, every effort is made to indicate this clearly, with due reference to the literature, and acknowledgement of collaborative research and discussions.

The work was done under the guidance of Professor Vikram Tripathi, at the Tata Institute of Fundamental Research, Mumbai.

Sarath

Sarath Sankar

In my capacity as supervisor of the candidate's thesis, I certify that the above statements are true to the best of my knowledge.

Vikram Tripathi

Vikram Tripathi

Date: 24/08/2018

Acknowledgements

During my PhD life at TIFR I have enjoyed the help, support and guidance of numerous people. I would like to express my gratitude towards them.

First and foremost I would like to thank my thesis supervisor Prof. Vikram Tripathi for his guidance and constant support. I always get amazed by the variety and quality of the various research projects that he has in mind. He often has a very good idea on the right direction to attack a problem that is based on simple physical concepts or intuition – this really helped me in the various projects that we did and has also helped me in cultivating the habit of building proper physical intuition.

I am extremely grateful to Prof. Deepak Dhar for the various discussions we had. I have always felt that I learn something new every time I discuss with him. I am also indebted to him for making me realize the importance of clear headed thinking.

I am thankful to Prof. Rajdeep Sensarma for being part of my thesis monitoring Committee (TMC) and for the critical suggestions that has helped me to improve my research and also for emphasizing through example how to do a good scientific presentation. I would like to thank Prof. Pratap Raychaudhuri for being part of my TMC and for educating me at various stages about the fascinating research carried out in disordered superconductors. I am grateful to Prof. Kedar Damle for the various discussions we had and for giving me valuable wisdom on organizing my thoughts while giving a scientific presentation. I am also thankful to Prof. H. M Antia for the several lunch time discussions we had. I would also like to thank Prof. Valerii Vinokur for the research collaboration on one of my research projects.

My PhD life at TIFR was made more enjoyable because of some wonderful friends. I would like to thank Vishal for always being there to discuss Physics or philosophy or personal life and for the numerous times that he accompanied me to Persian for dinner. I am thankful to Jishnu and Dattaraj for being true friends right from my initial days in TIFR and for always being enthusiastic to accompany me for treks or road trips and especially for the relentless help and support they gave me when I was hampered by a broken leg. I am grateful to Pranay for the wonderful Physics and puzzles that we discussed. I would like to thank Ahana, Sounak, Sarbajaya, Ronak, Yogesh, Kirti and Meenakshi for being good friends and for some very interesting discussions we had from time to time.

Finally I would like to express my extreme gratitude and love towards my parents who always support me in all my endeavors. I am extremely grateful to my grandmother for the relentless love and care she gives me, which also inspires me to become a better person. I am also extremely thankful to my sister with whom I have always shared my ups and lows and for always motivating me to improve my personal and academic life. I would also like to thank Chaithanya for all the love and understanding she has shown and for really helping me go through some frustrating periods while writing the thesis.

List of Publications

- Sarath Sankar, and Vikram Tripathi. "Low-field magnetoresponse of strongly disordered two-dimensional superconductors" Physical Review B 94.5 (2016): 054520.
- Sarath Sankar, Valerii Vinokur, and Vikram Tripathi. "Disordered Berezinskii-Kosterlitz-Thouless transition and superinsulation" Physical Review B 97, 020507(R) (2018).
- Sarath Sankar and Vikram Tripathi. "Keldysh field theory of nonequilibrium transport in a dissipative Mott insulator" arXiv: 1808.07064 .

Table of contents

Chapter 1

Introduction

The central theme of investigation of my thesis is the interplay between the conjugate variables - **number** and **phase** - in strongly disordered or inhomogeneous systems which are also strongly correlated. In these systems the charge degrees of freedom tend to get localized in space and can be counted by the number operator, $\hat{n}$. The conjugate to $\hat{n}$ is the phase operator $\hat{\phi}$ and they satisfy the commutation relation ($\hbar$ is taken to be unity),

$$[\hat{\phi}_i, \hat{n}_j] = i\delta_{ij}, \tag{1.1}$$

where the indices i, j refer to some coarse-grained spatial points. The commutation relation expresses the fact that the quantum states cannot not have well-defined local number and phase simultaneously. One can then qualitatively identify different charge transport regimes (see also Fig 1.1) :

1. **Superconducting** - local number fluctuations are large and this leads to global phase coherence.

2. **Weakly conducting or insulating** - both the phase and number fluctuates locally.

3. **Superinsulating** - the number does not fluctuate locally where as local phase fluctuations are strong. This perfectly insulating regime is currently an area of intense theoretical and experimental research and is also a subject of my thesis work.

In a superconductor or a good metal it is well known that potential fluctuations (and hence phase fluctuations) are suppressed due to the large value of the conductivity and thus can be treated perturbatively. The phase fluctuations increase as the disorder is increased. Near the insulator transition, as the number fields become progressively well-defined the phase fluctuations become strong and can no longer be treated perturbatively. The main

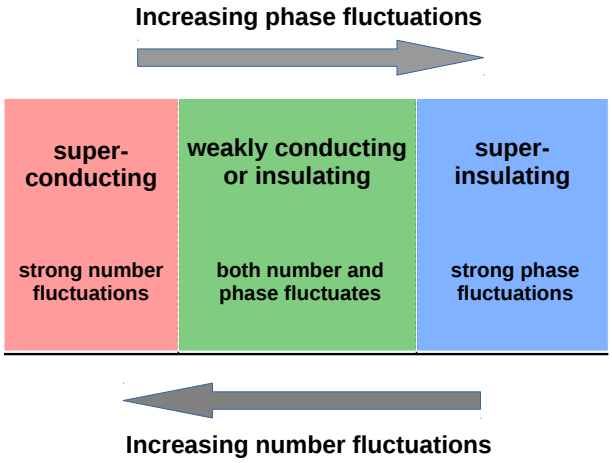

Figure 1.1 Classification of different transport regimes based on the strength of number or phase fluctuations

subject of study of my thesis work is the role of these phase fluctuations in the transitions across the various transport regimes. One common feature shared by all the model systems that I have studied is that they are granular - metallic or superconducting (SC) mesoscopic grains separated by an insulating background. This granularity can be either engineered or emergent as in the case of disordered superconductors (discussed in Chapter 2).

My thesis work consists of three different research projects related to the above mentioned theme which I briefly describe below.

1. Magneto-response in strongly disordered superconductor films

Physical Review B 94, 054520 (2016)

Strongly disordered superconductor thin films in the normal state often show a colossal positive magnetoresistance (in many cases the resistance grows by five or more orders of magnitude upon application of fields of a few Tesla) followed by a similarly large negative magnetoresistance (see e.g. Ref [124]). In the past, numerical simulations of disordered superconductors using the mean-field BdG approximation (see e.g. Ref [47]) have attributed this behavior to the changing proportions of superconducting and normal regions as a function

of the field - however, analytical studies of this phenomenon have been rare. In addition, phase fluctuation effects which are known to govern many other properties of these systems such as the field dependence of superfluid stiffness are not often taken into account.

To attack this problem, we construct a field dependent Josephson-Junction(JJ) model: strongly disordered SC films are known to have a granular structure [70, 48] consisting of SC islands in an insulating background, and connected by Josephson tunneling of Cooper pairs. To construct the model, we first study a model of weakly repulsive bosons (preformed Cooper pairs) in a disordered potential in two dimensions subjected to a uniform perpendicular magnetic field. For this we generalize *Lifshitz tail* like arguments that had been developed earlier for the zero field case (see e.g. Ref [55]) to the finite field case. The main idea is that the bosons fill the deep wells of the potential and the weak repulsion results in a spread of the Cooper pair islands across the film. The magnetic field affects the properties through enhanced localization of particles (diamagnetic orbital shrinking). We obtain the field dependence of the typical size of the islands, the typical distance between them and the typical strength of boson tunneling between neighboring islands and using these construct the aforementioned field dependent JJ model.

Analyzing the model in different parameter regimes - dominated by Coulomb blockade, thermal phase fluctuations or disorder in Ahranov-Bohm phases, we calculate magnetoresistance and field dependence of superfluid stiffness of the system. For the case of the Ahranov-Bohm phase disorder dominated regime, we use the scaling analysis of disordered classical XY models with quenched phase disorder developed earlier by Carpentier and Le Doussal [34]. We estimate the dependence of the variance of the Ahranov-Bohm phase on the magnetic field and obtain the magnetoresistance in the critical region of the superconductor to insulator transition (SIT). Using the renormalization group equations derived in the aforementioned work, we show that the superfluid stiffness in the superconducting phase drops more rapidly in this regime at small fields ($\sim \exp(-B)$) compared to that in the thermal phase fluctuation dominated regime ($\sim \exp(-B^2)$). This prediction of ours may be tested in penetration depth or AC conductivity experiments.

2. Disordered BKT transition and superinsulation

Physical Review B 97, 020507(R) (2018)

Disordered SC films in the insulating phase near an SIT sometimes show a surprising transition to a state of apparent zero conductance as the temperature falls below a critical value. The mechanism of this phenomenon and the nature of the conductance collapse is an

exciting open question. Near the SIT, the dielectric constant of a film diverges and this can result in a logarithmic interaction [83] between charge excitations in the superconducting islands. This two dimensional Coulomb gas can then undergo a charge Berezinskii-Kosterlitz-Thouless (BKT) transition and it has been proposed that the superinsulator transition is of the charge BKT type [145], analogous to the vortex BKT transition that occurs in the 2D SIT. An alternate proposal, based on the idea that the Cooper pairs are weakly coupled to phonons, is that the superinsulator is the manifestation of a many body localized (MBL) phase [113]. There are experimental reports of BKT like $(\sigma(T) \sim \exp(-1/(\sqrt{T-T_{BKT}}))$ [101] and a more singular Vogel-Fulcher-Tamann(VFT) like $(\sigma(T) \sim \exp(-1/(T-T_{VFT}))$ critical behavior of the conductivity [113] near the transition.

We investigate the possibility of VFT behavior in a charge BKT frame work. The key idea that we propose is that, the quenched random potential within a SC island can result in quenched random dipole moments of the islands. We then show that these quenched random dipole moments results in the charge excitations to experience a disorder potential that is logarithmically correlated. We further show that the strength of this disorder potential increases with increasing temperature. Then for sufficiently strong disorder, we derive the VFT critical behavior. We understand the crossover from the BKT to VFT critical behavior as a consequence of the freezing of charge dipole excitations that is known to occur in the case where dipole-dipole interactions are neglected [137];the freezing of charge dipole excitations results in poorer electrostatic screening and hence a more singular VFT behavior. Based on this, we propose the existence of an ergodic and non-ergodic regime in the superinsulator.

3. Keldysh field theory of nonequilibrium transport in a dissipative Mott insulator

arXiv:1808.07064

The problem of charge transport in regular lattice systems subjected to a uniform electric field has been extensively studied in the past. Non-interacting systems in the absence of any dissipative mechanisms are known to exhibit Bloch oscillations due to coherent Bragg reflection of particles at the Brillouin zone boundary. On the other hand the nature of non-equilibrium transport in interacting systems is not well understood. It is commonly believed that steady state transport becomes possible in these systems in the presence of inelastic relaxation processes. Most of the existing studies that take into account these dissipative mechanisms work in the regime of weak inter-particle interactions. In recent times, the problem of nonequilibrium steady state transport in the presence of dissipation and strong

correlations (e.g. in Mott insulators) has attracted considerable attention. In the absence of dissipation, it has been shown that the non equilibrium Mott insulator system also exhibit oscillatory behavior, which tends to the non-interacting Bloch oscillations at large field strengths, and not steady state transport [109]. Two different strategies have been pursued for the dissipative case: (a) Study of the Keldysh theory of a Mott-Hubbard model where the dissipation is introduced as a coupling to some environment degrees of freedom using the dynamical mean-field theory (DMFT) approximation [17], (b) Study of parity-time reversal (PT) symmetric non-Hermitian Hubbard models, where the dissipation is encoded in terms of the extent of non-Hermiticity in the Hamiltonian [140]. One shortcoming of the DMFT approach is that it is essentially a spatially local theory that may miss long range spatially correlated hopping processes. On the other hand, in PT-symmetric models, a microscopic derivation of the non-Hermitian Hamiltonian - which is their starting point - is still an open problem.

From a theoretical perspective, granular lattice systems (granular lattice refers to the sites being of mesoscopic sizes and thus can harbor many energy levels) offer an ideal playground to study non-equilibrium phenomena, since the presence of many electrons within a grain provides a natural heat bath. This system of metallic grains arranged in a regular lattice has been extensively studied in the literature in the equilibrium limit (see for e.g. Ref. [23]). Under certain conditions, these systems are well described by a dissipative Ambegaokar-Eckern-Schon (AES) action [11], formulated in terms of the fluctuating electromagnetic phases on the different grains. In the non-equilibrium case, a Keldysh generalization of this action has been considered in the context of a single quantum dot coupled to external leads [2]. However there has been no generalization of this approach to infinite granular metal systems where Mott insulator to conductor transition can be expected to occur.

In this work, we first obtain a Keldysh generalization of the AES action for the case of a one dimensional granular chain subjected to a uniform electric field. A key new ingredient in the granular chain case compared to the quantum dot case is that here higher order tunneling processes can become more relevant since co-tunneling across multiple grains can result in energy gain from the potential gradient. We calculate the electric current in this model as a function of the applied electric field that is turned on at some time say $t = 0$. After the field is turned on the current response to leading order in the inter-grain tunneling conductance, g, shows an oscillatory transient response whose primary components are the two beat frequencies, $\omega_{\pm} = |D \pm 2E_c|$., where D is the potential drop between two sites and E_C is the Coulomb blockade scale. These oscillations arise from a combination of the periodicity of the lattice, Coulomb correlations, and charge quantization. These beat frequencies have also been observed [17] in DMFT calculations of the dissipative Hubbard model in the form of

"island" features in the spectral function, and in the dissipationless Bose-Hubbard model [30]. In the absence of correlations ($E_C = 0$), these oscillations would correspond to the Bloch oscillation frequency $\omega_B = |D|$. At long times, we show that the amplitude of these oscillations decays in accordance with an inverse square law. Remarkably, the dissipation, which is responsible for the decay of the amplitude of these oscillations, is nevertheless unable to suppress the coherent quantum effects in a finite time scale. Apart from these oscillations, the current also has a finite DC component for $|D| > 2E_C$, ($2E_C$ is the energy required to create a particle-hole excitation in neighboring grains) and is a direct consequence of the presence of dissipation.

Next, to understand the nature of the DC response at small fields, $|D| < 2E_C$, we consider the long time limit of the current response. For this purpose, we take into account higher order co-tunneling processes over multiple dots such that the Coulomb blockade is offset by the extra potential energy gain. We obtain analytic expressions for the field dependence of current up to $O(g^2)$. The analysis of higher order terms at arbitrary field strengths rapidly becomes very complicated; however we infer some general features. In the zero temperature limit, there is a hierarchy of thresholds, $D_{\rm th}^{(n)} = 2E_C/n$, with the $n^{\rm th}$ order current corresponding to the matching of the Coulomb scale with the electrostatic potential energy gain from co-tunneling over n successive dots. The leading order in g contributions to the current near these thresholds has the form

$$j^{(n)}(D) \sim nDg^n(1-2E_C/nD)^{2n-1}\Theta(nD-2E_C), \tag{1.2}$$

where Θ is the Heaviside step function. Based on this expression, we show that at low fields and small g, the field dependence of the current has the LZS form, $j(D) \sim D[g/\ln^2(1/g)]^{2E_C/D}$, but with qualitative differences from the LZS particle-hole pair production probability $P \sim e^{-E_C^2/cD}$ for the non-dissipative Hubbard chain at half filling [109] deep in the Mott insulator phase.

An important question relates to the nature of the transition from the Mott insulating state to a conducting state as a function of the field. In the dissipation free case, it is evident from the expression for the LZS pair production probability that it is a crossover, howsoever sharp, and not a true phase transition. A true phase transition to a metallic state is indicated if the perturbation expansion for the current made from within the Mott insulator phase diverges as a function of $g(\leq 1)$ or $D(< 2E_C)$. If the form of the current is assumed to have the form shown in Eq. (5.7) for a finite but small field strength away from the

thresholds, then the criterion for divergence of the perturbation expansion for the current is $D > D_C = 2E_C(1 - \sqrt{g/g_0})$.

The rest of this thesis is organized as follows. Chapter 2 gives a quick overview of the phenomenology of disordered superconductors that is relevant to the first two projects. Here I discuss the emergent granularity and importance of phase fluctuations in strongly disordered superconductors and is followed by a discussion on the Josephson-junction model that we use to study the various phenomena. Chapters 3, 4 and 5 respectively discuss the three research projects mentioned above. Finally I conclude by summarising the main findings of my thesis research projects.

Chapter 2

Disordered superconductors

2.1 Introduction

Superconductivity is a fascinating macroscopic quantum phenomenon that is characterized by a vanishing electrical resistance and expulsion of magnetic fields when certain materials are cooled below a critical temperature. The experimental discovery of superconductivity by H. K. Onnes [112] in 1911 and its understanding in the form of a microscopic theory by J. Bardeen, L. Cooper and J. R. Schrieffer (BCS Theory [20]) in 1957 are important milestones of the 20th century Physics. According to BCS theory (a short summary of BCS theory is given in Appendix C), in the presence of an attractive interaction the electrons near the Fermi surface become unstable against the formation of Cooper pairs (CPs) at sufficiently low temperatures. The Cooper pairing results in a gap in the single particle electronic density of states (DoS), called the superconducting(SC) gap, $E_{\rm gap}$. Below the SC transition temperature, T_c, CPs condense into a phase coherent macroscopic ground state. This SC state is characterized by an order parameter, $\Delta = \langle c_\uparrow c_\downarrow \rangle$, where c is the annihilation operator for electrons from the filled Fermi sea and $\{\uparrow,\downarrow\}$ denotes the spin. In the BCS theory, $E_{\rm gap} = |\Delta|$. The vanishing of electrical resistance follows from the fact that this ground state can support a finite electric current and the single particle excitations from the ground state are gapped. Much of the properties of superconductivity can similarly be traced back to the existence of this macroscopic phase coherent ground state and the presence of a gap in the single particle DoS.

In conventional BCS theory, the attractive interaction responsible for Cooper pairing is mediated by phonons. A qualitative picture of this phenomenon is as follows: the motion of an electron through a metal causes a dynamic local distortion of the crystal and results in a local excess positive charge. There are two widely separated time scales associated with this : E_F^{-1} and ω_D^{-1}. The inverse Fermi energy, E_F^{-1}, is the time scale for an electron

to traverse the immediate vicinity of a lattice ion and to trigger the distortion. The inverse Debye frequency, ω_D^{-1}, is the typical time for the lattice distortion to relax to its equilibrium position. Typically, $\omega_D^{-1} \gg E_F^{-1}$. Thus long after the first electron has passed, a second electron may feel the excess local positive charge of the lattice distortion. This effectively results in a net effective attraction between the two electrons. Since the maximum energy scale for the ionic excitations is ω_D, the range of this attractive interaction is limited to energies $\sim \omega_D$ around the Fermi surface.

Disorder is ubiquitous in condensed matter systems. It often arises due to imperfections in the crystal structure, presence of impurities (magnetic or non-magnetic) etc. Depending upon the strength of disorder, its effect on the physical properties of a system may vary from minor quantitative corrections of some physical quantities, to severe qualitative changes, for example as in the case of Anderson localization [13] - for sufficiently strong disorder (for any strength of disorder in one and two dimensions [1]), the single particle eigenstates will be localized as opposed to being extended like in the plane wave case. Low dimensionality and finite size effects are known to enhance the effect of disorder. How disorder effects superconductivity is naturally a central question of research in the subject. In many cases, like high T_c cuprates or superconductor thin films, disorder is intrinsic and cannot be neglected.

In metals, increasing disorder results in the decrease of conductivity, primarily due to the decrease in the mean free path of electrons. $(K_F l)^{-1}$ is typically considered as a measure of the disorder strength, where K_F is the Fermi momentum and l is the mean free path; it is essentially a measure of the inverse mean free time between scattering, which is expected to increase with increasing disorder. One might think that disorder even if weak might have an adverse effect on superconductivity and in particular increasing disorder strength might lead to a decreasing T_c. Soon after the proposal of BCS theory, Anderson argued that this is not the case [14]. The central idea behind his theory of “dirty superconductors" is that superconductivity is insensitive to perturbations that do not destroy time reversal invariance and hence will not result in the breaking of CPs. This is usually referred to as Anderson’s theorem. He showed that in a disordered environment, instead of forming CPs from plane wave states of opposite momenta, as is done in conventional BCS theory, one can form CPs from the time-reversed eigenstates of the single particle in the disordered potential; $|\Delta(\mathbf{r})|$ (defined locally as $< c_\uparrow(\mathbf{r}) c_\downarrow(\mathbf{r}) >$) remains spatially uniform and the ensuing $E_{\rm gap}$, then attain the same value as the disorder-free case and thus the T_c remains unaltered. The above considerations were given a rigorous treatment by Gor’kov [74] who explicitly showed to leading order in $(K_F l)^{-1}$ that the two-particle propagator is unaffected by disorder.

Anderson’s theorem is only valid in the case of weak disorder. This is because it fails to take into account two main effects of disorder - (1) Anderson localization and (2) enhanced

Coulomb interaction due to weaker screening. Let us first discuss (1) neglecting (2) for the time being. The fact that localization can have a dramatic effect on superconductivity can be inferred by looking at the extreme limit of site localization. In this case the wave functions of neighboring sites will not have any overlap so as to form a macroscopic phase coherent state - and thus superconductivity will be entirely destroyed. This then points to the possibility of having a SIT as the disorder strength is increased.

Early studies of the effects of localization on superconductivity were generally mean-field approaches based on extending Anderson's idea of pairing time-reversed eigenstates by accounting for the possible localized nature of wave functions. One of the key findings is that sufficiently strong disorder can result in the spatial fluctuation of $|\Delta(\mathbf{r})|$. The criterion for the setting in of the spatial fluctuation of $|\Delta(\mathbf{r})|$ is [98]

$$\rho\Delta_0 L^D < 1, \tag{2.1}$$

where ρ is the averaged density of states at the Fermi surface, Δ_0 is the BCS gap , D is the dimensionality of the system and L is the localization length (typical extend of a localized wave function). Interestingly the above criterion says that superconductivity persists far into the localized phase.

A three dimensional disordered metal is characterized by the existence of a mobility edge - the energy density below which all single particle eigenstates are localized. There exists a metal-insulator transition (MIT) as the Fermi energy is tuned across the mobility edge – increasing the disorder strength results in the decrease in mobility edge and eventually it will cross the Fermi energy. The localization length in the insulating phase diverges near the MIT. The corresponding length scale that diverges in the metallic side near the MIT is the correlation length for the conductivity scaling. The setting in of spatial fluctuation of $|\Delta(\mathbf{r})|$, as described by the condition in Eq. (2.1), then occurs deep inside the localized phase.

An hallmark of superconductivity is the existence of a finite superfluid stiffness, ρ_s, which is a measure of the response of the system to a phase twist at the boundary. Thus the SC state is clearly sensitive to boundary conditions - which again follows from its macroscopic phase coherent nature. On the other hand, the localized wave functions are insensitive to boundary conditions. Thus the formation of the coherent SC state from these underlying localized eigenstates in the localized phase is puzzling. One can understand this and the criterion, $\rho\Delta_0 L^D < 1$, roughly as follows : Imagine dividing the system into boxes of size L. ρL^D is the measure of the mean energy level spacing between the energy levels localized within L. Thus, if $\rho L^D < \Delta_0^{-1}$, then it implies the existence of several states localized in the box with energy within Δ_0 of the Fermi surface. These can then be organized coherently into a local superconductivity fluctuation, and the localized states connecting adjacent boxes

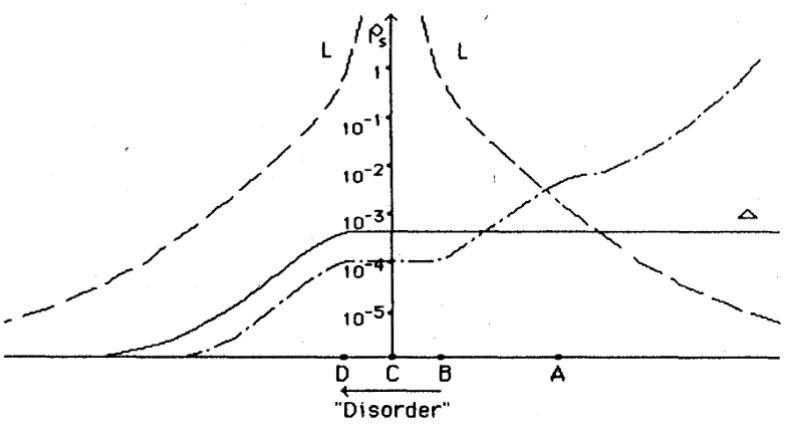

Figure 2.1 Schematic summary of the results in [98] describing the effect of localization on superconductivity. The horizontal axis measures the disorder strength with increasing disorder to the left. Point C denotes the disorder strength at which MIT occurs. The localization length on the insulating side and the corresponding correlation length of conductivity scaling in the metallic side, as depicted by the dashed lines, diverge at the MIT. Point A denotes the onset of the strong disorder regime. Point D denotes where the criterion for the spatial fluctuation of Δ as given in Eq. (2.1) holds and point B is the mirror image of D about C. The spatial average of Δ and ρ_s are shown as solid and dotted lines respectively. (Figure shown from Ref [98] with permission)

can allow Josephson tunneling (tunneling of CPs). This then allows for the communication between the local fluctuations and the stabilization of them into a global SC ground state. Figure 2.1 summarizes the above discussion.

A more rigorous study of the effect of Anderson localization on superconductivity was done by Feigelman et. al. in [57]. They showed that in weak Anderson insulators with an attractive BCS interaction, the fractal nature of the single particle wave functions near the mobility edge leads to a large single particle gap in the SC state near the SIT that persists and even increases in the insulating state. This is reminiscent of the pseudogap that is observed in the cuprates. They also predicted that in the SC ground state, the correlations are inhomogeneous in real space.

The effects of interaction between electrons in a disordered metal in the weak disorder limit is usually described within the Landau Fermi-liquid theory [90] according to which the interaction effects can be represented by the introduction of a number of Fermi-liquid parameters describing the renormalization of various physical quantities. Even though these renormalizations could be large they are always finite and hence do not result in any singular behavior. However, Altshuler and Aronov [6] showed that interactions in a disordered Fermi liquid can lead to strong singularities near the Fermi level. For example, in the case of a 3D disordered metal, a singularity of the form $(\omega - E_F)^{1/2}$ is predicted for the tunneling DoS

and $T^{1/2}$ and $T^{3/2}$ low-temperature corrections are predicted for the electronic conductivity and specific heat, respectively. The calculations were carried out in the regime of weak disorder ($K_F l \gg 1$) and consequently localization effects were neglected (diagrams with crossed impurity lines were neglected). The main physical idea here is that in a disordered environment, the electron motion is diffusive and hence the electrons spend a longer time in a given region of space, which in turn enhances the Coulomb interaction between electrons.

An enhanced Coulomb repulsion between electrons results in reducing the effective phonon mediated electron-electron interaction which results in Cooper pairing. This then leads to the suppression of T_c as the disorder strength increases. In the weak disorder regime, a perturbative analysis of interaction effects in the suppression of T_c has been carried out in Ref [99] where the authors consider the two dimensional case and find that the corrections to the pair density of states and to the interaction vertex both affect T_c and is given by,

$$\ln\left[\frac{T_c}{T_c^0}\right] = -\frac{(g_1-3g_0)N(0)}{4\pi E_F\tau}\left(\ln\frac{1}{T_c^0\tau}\right)^2 - \frac{(g_0+g_1)N(0)}{6\pi E_F\tau}\left(\ln\frac{1}{T_c^0\tau}\right)^3, \tag{2.2}$$

where T_c^0 is the transition temperature in the absence of disorder, $N(0)$ is the DoS at the Fermi surface, τ is the mean free time between scattering, g_1 is the electron repulsion and g_0 is the phonon-mediated coupling. Retardation effects due to phonon-mediated interactions and dynamic screening and extensions of the calculations in the weak disorder regime to three dimensions was reported in [67]. A non-perturbative calculation of the suppression of T_c using a renormalization group (RG) analysis of the disordered electron gas was reported in [58]. For two dimensional films the disorder strength can be captured in terms of the dimensionless conductance $g = 2\pi\hbar/e^2R_S$, where R_S is the sheet resistance. Finkelstein's result is up to leading order in $g^{-1/2}$ and is,

$$T_c = \frac{h}{\tau^*}\left[\frac{\sqrt{2\pi g}-\ln(\hbar/T_c^0\tau^*)}{\sqrt{2\pi g}+\ln(\hbar/T_c^0\tau^*)}\right]^{\sqrt{\pi g/2}}, \tag{2.3}$$

where $\tau^* = \max\{\tau, \tau(d/l)^2\}$ with d being the film thickness and l the mean free path.

The effects of enhanced electron repulsion in the strong disorder regime was reported in Ref [12] where the authors pointed out that in a three dimensional system close to critical disorder, the strongly scale-dependent diffusion enhances the repulsive Coulomb pseudopotential and thus decreases T_c. Contrary to the weak disorder regime, here localization effects - manifest through the slowness of the electron diffusion - play a key role in the enhancement of Coulomb repulsion and thereby the suppression of T_c.

2.2 Granularity and phase fluctuations in disordered superconductor thin films

The case of disordered superconductor films is very interesting because the lower critical dimension for both superconductivity and localization is two - global phase coherence is just possible in two dimensions and for arbitrary strength of disorder, all underlying single particle states are localized. The thin film case is also characterized by the presence of multiple length scales : lattice spacing a (1-2 Å), film thickness d ($\sim$ 10 nm), mean free path l ($l \gg a$, unless disorder is very strong), zero temperature coherence length (spatial extend of CPs) for clean system ξ_0 ($\sim 1\mu m$) and the same for the disordered system ξ ($\sim$ 10 nm). A film is considered two-dimensional if $d < \xi$.

The effect of disorder on superconductivity in thin films has been extensively studied both theoretically and experimentally. Spatial fluctuation of amplitude of the SC order parameter and the related effects were studied in [70] by numerically solving the Bogoliubov-de Gennes (BdG) mean field equations. The BdG approach is essentially a real space version of the mean-field BCS theory and in particular the order parameter $(\Delta(\mathbf{r}))$ is taken to be a function of the spatial coordinates. Disorder is introduced through a potential for single particles - the potential at each site is chosen from some distribution (e.g a uniform distribution , $[-V,V]$, with V acting as a measure of the disorder strength). The resulting mean-field equations are then numerically solved until self consistency is achieved. One of the main findings of this analysis was that a granular structure emerges at sufficiently high disorder strength (V): some regions with appreciably high values of $|\Delta|$ acting as SC islands and the in-between region with very small $|\Delta|$ acting as an insulator background. These SC islands are then found to shrink upon increasing disorder. Figure 2.2 illustrate these results.

Another interesting finding of this analysis was that the gap in the single particle DoS, E_{gap} persists at higher disorder strengths; infact E_{gap} starts increasing after some disorder strength. On the other hand, the average amplitude of the SC order parameter was found to decrease monotonously with increasing disorder. This apparently puzzling finding can be understood by realizing that E_{gap} and $|\Delta|$ are the same only in the clean limit. The strength of the order parameter clearly falls with increasing disorder. The insulator background has also a gap in the DoS . This gap increases with the disorder strength and this combined with the shrinking of SC islands with increasing disorder strength explains the non-monotonic behavior of E_{gap}.

The mean field approach in [70] does not take into account the fluctuations of the phase of the order parameter. The BdG analysis in [70] was extended to include thermally induced fluctuations of the phase but neglecting the quantum fluctuations of the order parameter in

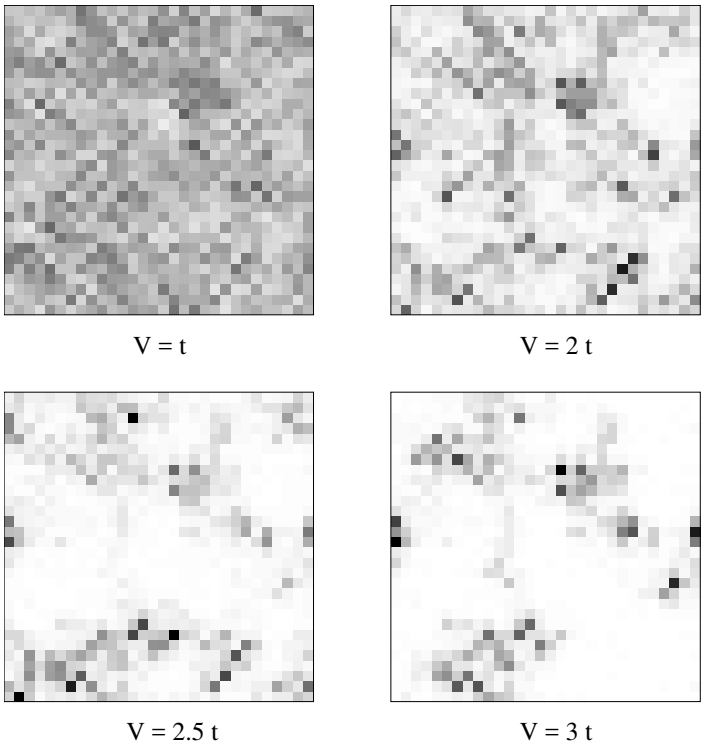

Figure 2.2 Emergence of a granular structure reported in [70] by numerically solving the mean field BdG equations. V (measured in terms of the tunneling amplitude t) is a measure of the strength of disorder. The spatial variation of $\Delta(\mathbf{r})$ is shown for different disorder strengths with increasing darkness indicating higher $\Delta(\mathbf{r})$. For low V, the spatial texture is more or less homogeneous where as for large V, regions with large $\Delta(\mathbf{r})$ - the SC islands - are clearly separated by regions with vanishing $\Delta(\mathbf{r})$ - the insulating background. The SC islands are also found to shrink with increasing V. (Figure shown from Ref [70] with permission.)

[48]. In addition the authors also studied the effects of a perpendicular uniform magnetic field. For a fixed disorder strength, an increasing magnetic field results in the system separating into SC islands with an insulating background and a consequent shrinking of the islands. The phase correlations between different islands were suppressed with the increasing field where as that within an island sustained. An SIT occurs at a critical magnetic field, which is captured by the vanishing of the phase correlation function between the edges of the sample.

The nature of the SIT is found to be different for the weak and strong disorder regimes (see Figure 2.3). In the weak disorder regime, both the spatially averaged amplitude of the order parameter Δ and the phase correlation between the edges of the sample tend to vanish at the same field strength. This is similar to the usual BCS scenario and this type of SIT caused by the vanishing of Δ is called the " Fermionic mechanism". On the other hand, in the strong disorder regime, the phase correlations between the edges vanish first at some critical

field B_c where as Δ remains finite and does not show any appreciable feature around B_c. This clearly shows that here the SIT is driven by the phase fluctuations and this type of SIT is often referred to as the “Bosonic mechanism". Quantum Monte-Carlo studies [27] that take into account the thermal and quantum fluctuations of the amplitude and phase of the order parameter also support that the “Bosonic mechanism" drives the SIT at strong disorder.

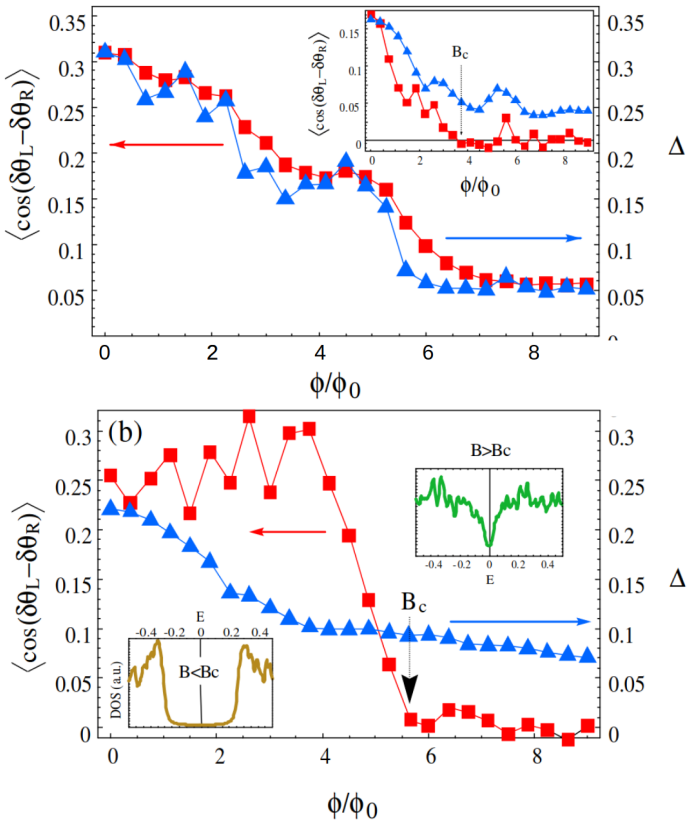

Figure 2.3 Difference in the nature of magnetic field driven SIT for weak and strong disorder regimes as obtained in [48]. The evolution of spatially averaged Δ and the phase correlation between the edges of a sample with an increasing perpendicular magnetic field (measured in terms of flux per square) are shown for (a) weak disorder and (b) strong disorder regimes. In (a) both Δ and the phase correlations tends to vanish together and hence the SIT here is characterized by a vanishing Δ like in the usual *BCS* scenario. But in (b) the phase correlations vanish at lower field strength B_c whereas Δ is finite there and does not show any appreciable features. This clearly shows that here the SIT is driven by phase fluctuations. The inset in (b) shows the DoS displaying a pseudo-gap feature. (Figure is shown from Ref [48] with permission.)

The physical picture of the SIT via the “Bosonic mechanism" is as follows: the phase within an individual island does not fluctuate spatially and the Josephson tunneling between neighboring grains tends to align their phases. On the SC side, Josephson tunneling leads to global phase coherence where as in the insulating side, the Josephson tunneling is not strong

enough to cause a phase coherence at a macroscopic scale. The mesoscale phase fluctuations then crucially determine the critical properties of the SIT.

The numerical BdG approach to study the effect of disorder on superconductivity has several drawbacks. The biggest drawback is that despite being able to shed some qualitative insights, the approach can hardly say something about the critical behavior near the SIT. This is primarily because the SIT in the strong disorder regime is governed by the phase fluctuations as discussed above and the BdG approaches do not faithfully account for the fluctuations of the phase. Even though Quantum Mont-Carlo studies take into account the full effect of phase fluctuations, currently the method is only applicable to small system sizes and hence any reliable information about the critical behavior cannot be extracted. A further drawback is that these appraoches do not take into account Coulomb repulsion, which has a detrimental effect on superconductivity especially in the insulating regime where the Coloumb screening is expected to be weaker. Phenomenolgical phase models like the the Josephson-junction (JJ) model are often used to study the critical properties near the SIT and is discussed in detail in the next section.

I now discuss briefly the experimental situation. The spatial inhomogeneities in disordered SC films were studied using scanning tunneling spectroscopy (STS) [38, 82, 120] by analyzing the local DoS obtained from the tunneling conductance. Even though the gap in the local single particle DoS varies spatially, it does not capture the granular structure, owing to the presence of a spectral gap in the insulating regions as well. Another strategy is to study the coherence peak after subtracting the Altshuler-Aranov background [38, 82] (see Figure 2.4). Topographic image of the spatial inhomogeneities that reveals the granular structure is then constructed by scanning the film surface .

Complex AC conductivity studies also give strong evidence for the existence of the CPs in the insulating regime. A significant local superfluid stiffness is resolved in the insulating state which persists well into the strongly insulating regime [40]. Another line of evidence comes from the observation of magnetoresistance oscillations in the insulating regime [135], dictated by the SC flux quantum, $h/2e$; the occurrence of $2e$ as opposed to e shows the existence of Cooper pairs. The observation of steep magnetoresistance [124, 134] in the insulating side of the SIT and its further non-monotonic dependence on the external magnetic field finds its explanation in the existence of CPs in the insulating phase and the shrinking of the SC islands [47]. The next chapter discusses this aspect in detail.

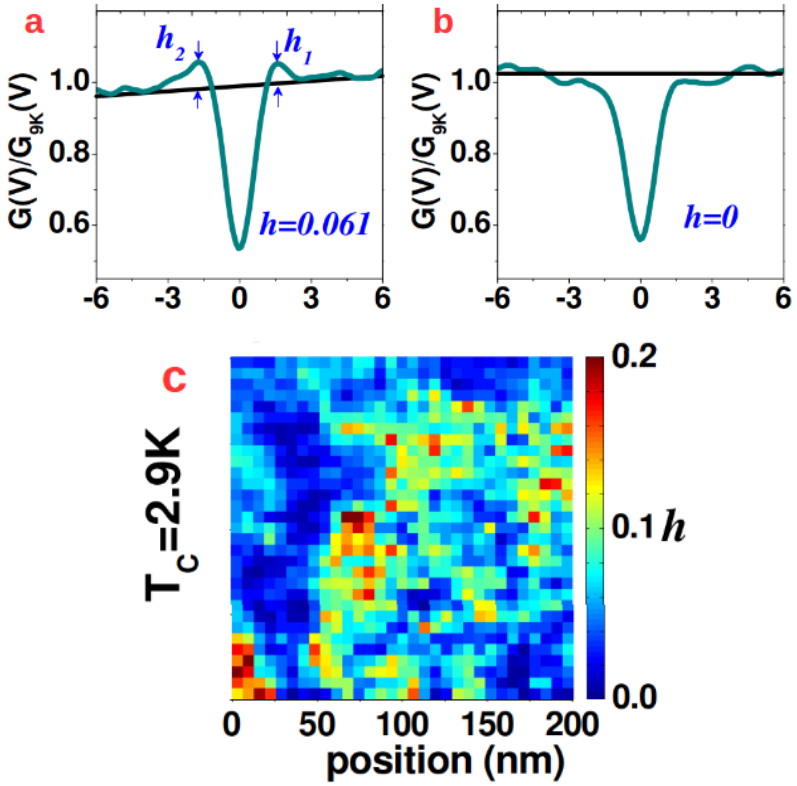

Figure 2.4 Scanning tunneling spectroscopy of disordered SC thin films reported in [82] (a) The local single particle DoS with the Altshuler-Aronov background removed with a prominent coherence peak indicating a SC region (b) coherence peak absent indicating a non-SC region (c) topographic image showing the spatial variation of the coherence peak height. (Figure shown from Ref [82] with permission.)

2.3 Josephson-junction model

The JJ model is a good starting point to understand the role of phase fluctuations near the SIT, especially for SC films in the strongly disordered regime where a granular structure emerges as discussed in the previous section. Josephson-Junction refers to an arrangement of a non-SC material sandwiched between two layers of SC material. It is named after B. D. Josephson, who predicted that CP could tunnel through the non-SC barrier from one superconductor to another - this is called the Josephson effect [81] . The voltage across the junction (V) and the current through the junction (I) is related to the difference in the phases of the complex order parameter of the two superconductors. This phase difference is denoted by ϕ. The relations are :

$$V(t) = \frac{\Phi_0}{2\pi}\frac{\partial\phi}{\partial t}, \tag{2.4}$$
$$I(t) = I_c \sin(\phi(t)). \tag{2.5}$$

Here I_c denotes the critical current of the junction and Φ_0 denotes the magnetic flux quantum, $h/2e$. In the JJ model, the SC grains are arranged in a lattice (we will consider a square lattice), and Josephson tunneling happens between neighboring grains. The charge dynamics is governed by both the Josephson tunneling and Coloumb repulsion between the CPs. The Hamiltonian is given by:

$$H = \frac{1}{2}\sum_{<ij>}(\hat{n}_i - n_0)V_{ij}(\hat{n}_j - n_0) - J\sum_{<ij>}\cos(\hat{\phi}_{ij}), \tag{2.6}$$

where, $\phi_{ij} = \phi_i - \phi_j$, J denotes the Josephson energy, V_{ij} denotes the Coloumb interaction, $\hat{n}$ is the number operator for the CPs and $2en_0$ is the background charge with e being the electron charge. The tunneling term is the potential energy accumulated due to Josephson tunneling and its form is easily derived by integrating the power,

$$\int_0^t IV\,\mathrm{dt} = \frac{\Phi_0}{2\pi}\int_0^\phi I_c \sin(\phi)d\phi = \frac{\Phi_0 I_c}{2\pi}(1-\cos(\phi)). \tag{2.7}$$

Generally the long range Coulomb interaction is well screened and then one can simply restrict to Coulomb interaction within a grain. Using the commutation relation between the charge and the phase operators, the Lagrangian density of the model can then be written as,

$$L = \frac{1}{4E_c}\sum_i(\partial_t\phi_i)^2 + J\sum_{<ij>}\cos(\phi_{ij}) \tag{2.8}$$

where $E_C = 2e^2/C$ is the capacitive energy with C being the capacitance of the grain. To understand the Physics captured by the JJ model, let us first look at the limiting cases of the two energy scales, J and E_C.

2.3.1 Coulomb blockade regime ($E_C \gg J$)

In this regime the dynamics will be dominated by the temporal fluctuations of the phases in the individual grains. To leading order, we can neglect the tunneling part and then the model describes a classical capacitor that can only be charged in discrete charge steps of $2e$. The partition function in thermal equilibrium at some temperature, T, is given by,

$$Z = \sum_n e^{-\beta E_c (n-n_0)^2} \tag{2.9}$$

At this order, clearly no charge transport is possible in the problem. To understand the electrical conductivity in this regime, we can treat the tunneling part perturbatively by taking the charging part as the bare action. A Kubo formula analysis then obtains [141, 136],

$$\sigma \sim J^2 e^{-\beta E_c}. \tag{2.10}$$

Thus the conductivity shows an activated behavior with characteristic energy scale, E_c.

2.3.2 Tunneling dominated regime ($J \gg E_C$)

In this regime, we can neglect the temporal fluctuations of the phases in a grain and hence the dynamics is governed by the Hamiltonian,

$$H = -J \sum_{<ij>} \cos(\phi_i - \phi_j) \tag{2.11}$$

This has the same form of the classical XY model in two dimensions. The 2D XY model is famously known to undergo the Berezinskii-Kosterlitz-Thouless (BKT) transition at a finite temperature [88, 24]. The Mermin-Wagner theorem [100] predicts that true long range order is not possible for systems with a continuous symmetry in dimensions, $D \leq 2$. The BKT transition happens between a high temperature and a low temperature phase, each of which are characterized by a distinct form for the correlation function,

$$\chi_{ij} = \left\langle \cos(\phi_i - \phi_j) \right\rangle, \tag{2.12}$$

where $<>$ denotes the thermal average. In the high temperature phase, the correlation function decays exponentially,

$$\chi_{ij} \sim e^{-|i-j|/\xi}, \tag{2.13}$$

where $\xi^{-1} = \ln(2T/J)$ and we have taken the lattice spacing to be unity. This exponential decay of the correlation function shows that the high temperature phase does not possess any long range order. On the other hand the low temperature phase exhibits a power law decay for the correlation function,

$$\chi_{ij} \sim \left(\frac{1}{|i-j|} \right)^{T/2\pi J} \tag{2.14}$$

This power law decay is often considered to show that the system possesses a quasi-long range order. The BKT phase transition from this quasi-ordered phase to the disordered phase is brought out by the proliferation of topological defects in the model called vortices. These topological excitations can be easily studied in the continuum description of the model.

In the continuum limit, we keep the leading order gradient expansion of the model (2.11),

$$H = \frac{J}{2}\int d^2\mathbf{r}\,(\nabla\phi)^2 \tag{2.15}$$

It is easy to see that for any closed loop in 2D,

$$\oint \nabla\phi.d\mathbf{l} = 2\pi n, \tag{2.16}$$

where n is an integer. The topological excitations with non-zero n are called vortices and n is called the charge of a vortex; the topological nature is evident from n being an integer since any smooth deformations in the model cannot change n as it can only change in discrete steps. The energy cost for the creation of a single vortex of charge n is given by,

$$E_n = E_n^0(a) + \frac{J}{2}\int_a d^2\mathbf{r}\,(\nabla\phi)^2 = E_n^0(a) + \pi J n^2 \ln\left(\frac{L}{a}\right), \tag{2.17}$$

where L, denotes the system size, a denotes a short length cutoff scale below which the continuum approximation is not valid owing to the lattice structure, and $E_0(a)$ denotes the associated vortex core energy. Note that the energy diverges logarithmically with the system size and hence at low temperatures the probability of occurrence of a single vortex vanishes. The entropy contribution for a vortex to appear also scales logarithmically with the system size, since there are $\sim L^2$ sites for the vortex to appear. One can then obtain an estimate of the transition temperature by looking at $n = \pm 1$ and taking the ratio of the energy and entropy. Such an estimate is only a upper bound of the transition temperature since we have neglected the possibility of the occurrence of dipoles - vortices of opposite charges in close proximity. In fact the BKT theory classifies the two phases as follows : the quasi-ordered phase is a gas of tightly bound dipoles whose density and size increases with temperature. The disordered phase constitutes a plasma of unbound vortices. The BKT transition is then usually visualized as the unbinding of vortex dipoles. This picture should be seen at a qualitative level and one should exercise caution in pushing it too far as is discussed in Ref 44.

Coulomb gas description and the BKT transition

The BKT transition can be clearly understood by going to the Coulomb gas description. The velocity field $\mathbf{u} = \nabla\phi$ can be decomposed to a curl-free and divergence-free part, $\mathbf{u}_0$ and $\mathbf{u}_1$ respectively. Using Stokes' theorem, we can relate the curl of $\mathbf{u}_1$ to the distribution of vortices of charge $\{n_i\}$ at locations $\mathbf{r}_i$ as,

$$\nabla \times \mathbf{u}_1 = 2\pi\hat{z}\sum_i n_i \delta^2(\mathbf{r} - \mathbf{r}_i) \tag{2.18}$$

The above equation can be written in the form of Poisson equation, by setting, $\mathbf{u}_1 = -\nabla \times (\hat{z}\psi)$. Thus we get,

$$\nabla^2\psi = 2\pi\sum_i n_i \delta^2(\mathbf{r} - \mathbf{r}_i). \tag{2.19}$$

The solution in two dimensions to the above Poisson equation for the potential due to a set of charges $\{2\pi n_i\}$ is given by,

$$\psi(\mathbf{r}) = \sum_i n_i \ln\left(|\mathbf{r} - \mathbf{r}_i|\right). \tag{2.20}$$

Now setting the curl-free part as $\mathbf{u}_0 = \nabla\theta$, we can write the continuum Hamiltonian in eq.(2.15) as a sum of spin wave part and vortex part, $H = H_{\rm SW} + H_{\rm Q}$, where,

$$H_{\rm SW} = \frac{J}{2}\int d^2\mathbf{r}\,(\nabla\theta)^2, \tag{2.21}$$

$$H_Q = \sum_i E^0_{n_i} - 2\pi J\sum_{i<j} n_i n_j \ln(|\mathbf{r}_i - \mathbf{r}_j|). \tag{2.22}$$

Thus the partition function can be factorized into the spin-wave part and the vortex part as, $Z = Z_{\rm SW}Z_Q$. In obtaining the above form of H_Q, an integration by parts was performed and a surface integral was ignored; the surface integral actually grows with the system size as, $(\sum_i n_i)\ln L$. Thus in the partition function Z_Q, only overall charge neutral contributions are included. Further, the BKT transition from the quasi-ordered state will be dominated by the proliferation of the lowest excitations, i.e , $n = \pm 1$ and hence in Z_Q, we restrict to these. Thus, we have,

$$Z_Q = \sum_{N=0}^{\infty} y_0^N \int\prod_{i=1}^{N} d^2\mathbf{r}_i \exp\left[2\pi K\sum_{i<j} n_i n_j \ln(|\mathbf{r}_i - \mathbf{r}_j|)\right], \tag{2.23}$$

where $K = \beta J$, the bare vortex fugacity $y_0 = e^{-\beta E^0_{\pm 1}}$, and N counts the total number of vortices such that, $n_i = \pm 1$ and $\sum_i n_i = 0$.

The nature of the BKT transition and its associated critical behavior can be obtained from a RG analysis of Z_Q and was first reported in Ref 87. The Kosterlitz-RG analysis is performed in the real space. Here, in each RG step, the vortex core cutoff scale, a is increased infinitesimally, $a \to ae^{dl}$, and all the vortex dipoles in the annulus between a and ae^{dl} are integrated out. This coarse-graining results in the renormalization of the fugacity and the coupling constant K, and are captured by the following RG equations, (the RG analysis for the case of a phase-disordered XY model is discussed in the Appendix A. The RG equations given below can be obtained from those discussed in the Appendix A by setting the disorder strength parameter to zero.)

$$\frac{dK^{-1}}{dl} = 4\pi^3 a^4 y^2 + O(y^4) \tag{2.24}$$

$$\frac{dy}{dl} = (2 - \pi K)y + O(y^3) \tag{2.25}$$

The RG flows described by the above equations are governed by two distinct classes of fixed points (see Fig 2.5) : (1) $\{y = 0, \{K^{-1} < \frac{\pi}{2}\}\}$ and (2) $\{y = \infty, K^{-1} = \infty\}$. For parameters below the critical line, $K^{-1} = \pi/2 - \pi^2 y a^4$, the flows approach the fixed point(s) (1). The fixed point $y = 0$ shows that the vortex core energy becomes infinite - that is the occurrence of a free vortex is improbable. Thus this regime describes the quasi-ordered phase. The coupling constant K here flows to a line of fixed points. On the other hand for parameter values above the critical line, the flows go towards the fixed point at infinity. This describes the high temperature disordered phase.

To find the critical behavior near the transition, we expand the RG equations in the vicinity of the fixed point $(y = 0, K^{-1} = \pi/2)$. Setting $x = K^{-1} - \pi/2$, $y = a^2 y$, and expanding to the lowest order, we get,

$$\frac{dx}{dl} = 4\pi^3 y^2 \tag{2.26}$$

$$\frac{dy}{dl} = \frac{4}{\pi} xy \tag{2.27}$$

From the above equations we can easily see that $\frac{d}{dl}(x^2 - \pi^4 y^2) = 0$. Thus in the vicinity of the fixed point, the flows proceed along hyperbolas given by, $x^2 - \pi^4 y^2 = c$. The critical trajectory separating flows to zero and infinite y corresponds to $c = 0$.

One important prediction of the RG analysis is that, at the BKT transition, the coupling constant undergoes a universal jump : at the transition temperature, T_{BKT}, the reduced

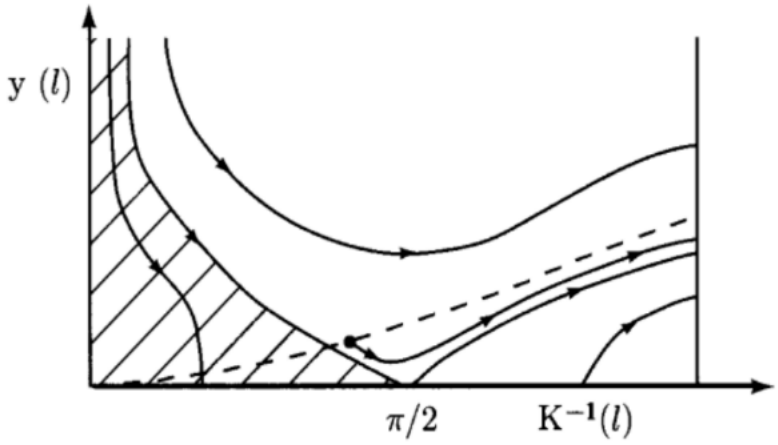

Figure 2.5 The RG flows described by Eqs. 2.24 and 2.25. The shaded region denotes the XY phase where the flows end at a line of fixed points on the horizontal axis. Outside the shaded region, the flows are towards the high temperature fixed point. The dashed line is the line of initial conditions as T increases. The critical temperature is determined by the crossing of the dotted line and the seperatrix.

superfluid stiffness, $K = J/T$, shows a sharp jump from a finite value to zero given by,

$$\lim_{l\to\infty} K(T_{\rm BKT}^{-}) = \frac{\pi}{2} \tag{2.28}$$

$$\lim_{l\to\infty} K(T_{\rm BKT}^{+}) = 0 \tag{2.29}$$

This jump in the reduced superfluid stiffness is system independent and hence represents the universal nature of the BKT transition.

To understand the form of the correlation length in the disordered phase near the transition, we write the parameter $c = b^2(T - T_c)$, where b is some constant. Physically, this is a measure of closeness to the transition. The RG equation, (2.27) then reads,

$$\frac{dx}{dl} = \frac{4}{\pi}(x^2 + b^2(T - T_c)). \tag{2.30}$$

Integrating the above we get,

$$\frac{4}{\pi}l = \frac{1}{b\sqrt{T - T_c}} \arctan\left(\frac{x}{b\sqrt{T - T_c}}\right). \tag{2.31}$$

The integration has to be terminated when $x(l) \sim y(l) \sim 1$, since the perturbative nature of the RG equations is not valid beyond this. This termination length scale is given by,

$l^* \approx \frac{\pi^2}{8b\sqrt{T-T_c}}$. The form of the correlation length is given by,

$$\xi \approx a e^{l^*} \approx a \exp\left(\frac{\pi^2}{8b\sqrt{T-T_c}}\right). \tag{2.32}$$

2.3.3 Long range Coulomb interaction

The JJ model in Eq. (2.8) is a special case of the general model in Eq. (2.6), where only Coulomb interactions within a grain are considered. Such a model is good for capturing the Physics of a system where the long-range Coulomb interaction is weak compared to the interaction within a grain. This comparison can be made quantitative [56] in terms of the quantity $\Lambda' = a\left(\frac{C}{C_0}\right)^{1/2}$, where C is the nearest neighbor capacitance (neglected so far), C_0 is the capacitance of a grain with ground and a is the lattice spacing. The model described in Eq.(2.6) is good for systems with $\Lambda' \ll L$, where L is the system size. On the other hand for $\Lambda' \gtrsim L$, it is necessary to take into account the long-range nature of the Coulomb interaction. In a model where only the capacitances with the ground and the nearest neighbor capacitances are considered, Λ' plays the role of screening length; in particular the potential due to a test charge at the origin is given by,

$$V(\mathbf{r}) = \frac{1}{C} K_0\left(\frac{r}{\Lambda'}\right), \tag{2.33}$$

where, K_0 is the modified Bessel function. For $r \ll \Lambda'$, the potential falls logarithmically as, $V(\mathbf{r}) = (1/C)\ln(r/\Lambda')$ and falls exponentially for $r \gg \Lambda'$.

The exponential decay at large distances is actually an artifact of neglecting the higher order capacitances (next nearest neighbor and so on) in the system. A better way to understand the long-range nature of the Coulomb interaction and also the range of validity of the logarithmic nature is to study the nature of Coulomb interaction in a film of thickness t with an average dielectric constant k. L. V. Keldysh [83] studied the problem of potential due to a unit charge at origin in a film of thickness t and dielectric constant k sandwiched between two semi-infinite media of dielectric constants k_1 and k_2. The potential within the film at a distance $r \gg t$ is found to be,

$$V(r) = \frac{1}{4\varepsilon_0 kt}\left[\mathscr{H}_0\left(\frac{k_1+k_2}{k}\frac{r}{t}\right) - \mathscr{N}_0\left(\frac{k_1+k_2}{k}\frac{r}{t}\right)\right], \tag{2.34}$$

where $\mathscr{H}_0$ and $\mathscr{N}_0$ are the Struve and Neumann functions respectively. Here the logarithmic nature of the interaction,

$$v(r) = \frac{1}{2\pi\varepsilon_0 kt}\ln\left(\frac{r}{t}\right), \tag{2.35}$$

is then valid for $t \ll r \ll \Lambda$, where $\Lambda = kt/(k_1+k_2)$. Thus the charge excitations in the SC grains will interact logarithmically if the system size is much less than kt $(k_1, k_2 \simeq 1)$ and then the system would be a realization of the 2D Coulomb gas. The dielectric constant of a film diverges as one approaches the SIT from the insulating side and thus close to the SIT, we see that it is important to consider the long range logarithmic nature of the Coulomb interaction. The Lagrangian density in the imaginary time of the coupled charge and phase degrees of freedom is then given by,

$$L = \sum_{j \neq k} n_j V_{jk} n_k + i \sum_j n_j \frac{\partial \phi_j}{\partial \tau} + \sum_{<jk>} J \cos(\phi_{jk}), \tag{2.36}$$

where, $V_{jk} = E_C \ln(|\mathbf{r}_j - \mathbf{r}_k|)$, with $E_C = 1/2\pi\varepsilon_0 kt$. Integrating out the spin-wave excitations of the phase fields and retaining the vortex excitations, one obtains a coupled Coulomb gas of charges and vortices. Labelling the charges as q and the vortices as n, the coupled Coulomb gas model can be written as,

$$L = \sum_{j,k} \left(E_C q_j U_{jk} q_k + J n_j U_{jk} n_k + i q_i \Theta_{ij} \partial_\tau n_j + \frac{1}{2J} \partial_\tau q_i U_{ij} \partial_\tau q_j \right), \tag{2.37}$$

where, $U_{ij} = \ln(|\mathbf{r}_i - \mathbf{r}_j|)$ and $\Theta_{ij} = \arctan[(y_i - y_j)/(x_i - x_j)]$. This coupled Coulomb gas can display a vortex BKT transition if $J \gg E_C$ or a charge BKT transition if $E_C \gg J$ [56]. The next two chapters discuss various aspects of this vortex and charge BKT transition and in particular the role of disorder in these. An interesting scenario arises when $J \simeq E_C$. The two BKT transitions compete and at $J = E_C$ the transition temperature is driven all the way to zero resulting in a quantum phase transition between a 'superinsulating' phase for $J < E_C$ where charge dipoles are tightly bound to a superconducting phase for $J > E_C$ where the vortex dipoles are tightly bound.

Chapter 3

Magneto-response of strongly disordered superconductor thin films

3.1 Introduction

One of the most challenging problems in strongly disordered superconductors relates to understanding the nature of the magnetic field-induced superconductor-normal state transition (SNT). Experimental and theoretical studies over the past two decades have opened a large number of puzzling questions such as the origin of the giant non-monotonous magnetic field dependence of the resistivity [124, 134, 130, 47, 117, 69, 97] (see also Fig 3.1), flux quantization in the insulating state [135] and the universality class governing the field-induced SNT [29, 115, 59, 130]. The two-dimensional (2D) case has in particular attracted intense theoretical attention and it is the focus of this work.

As discussed in the previous chapter, in the absence of a magnetic field, it is well-known that strong homogeneous disorder introduces granularity in the form of SC islands embedded in an insulating matrix [80, 60, 70, 120, 38]. However the relative importance of diamagnetic (orbital) shrinking effects [117, 47] and phase frustration effects brought in by the Aharonov-Bohm (AB) phases of the Cooper pairs tunneling across the islands [37, 84] is not well-understood.

Mean-field analyses of the field-sensitivity of the distribution of SC regions go back nearly two decades for weakly-disordered metals [133, 68], and more recently [47], for strongly-disordered insulators. Standard, perturbative approaches fail in the strongly-disordered regime but numerical mean-field solutions of the appropriate BdG equations [47], reveal a picture of shrinking SC regions in increasing fields, a downward shift of the distribution of the local SC gaps, and through the Ambegaokar-Baratoff relation [10], a corresponding decrease

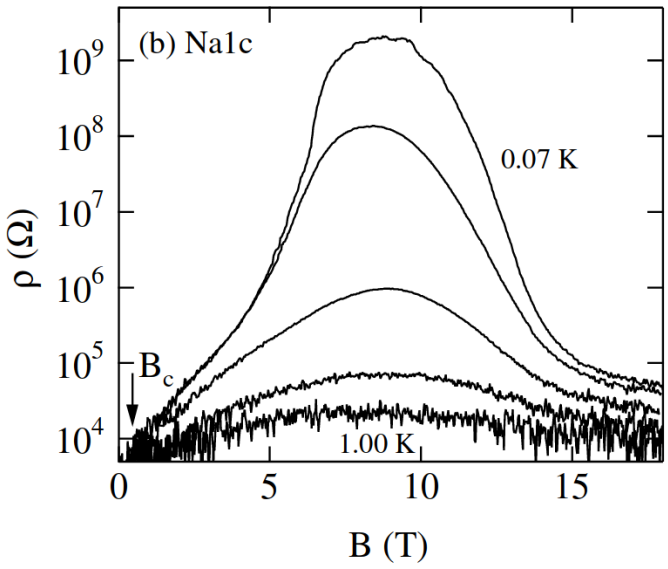

Figure 3.1 Magnetoresistance observed in amorphous Indium oxide thin films as reported in Ref. [124]. The magentoresistance is shown for different temperatures. At the lowest temperature the magnetoresistance grows upto five orders of magnitude upon increasing a few Teslas. The positive magnetoresistance then gives way to a negative magnetoresistance. (Figure shown from Ref. [124] with permission.)

in the Josephson couplings J between neighboring grains. To understand the physical origin of these effects, we study a phenomenological model of repulsive bosons (CPs) subjected to a disordered potential and a perpendicular magnetic field. The approach is reminiscent of earlier work on Lifshitz states [95] in disordered Bose systems [93, 55, 117].

We show that orbital shrinking in the presence of a magnetic field suppresses the Josephson couplings as $J(B) \sim \exp[-(B/B_J)^2]$, and is a primary cause of the strong magnetoresponse seen in experiments.

To understand magnetoresponse of these 2D granular superconductors, we study the standard Josephson-junction (XY) model,

$$L = \frac{1}{4E_c}\sum_{\mathbf{i}}(\partial_\tau \phi_{\mathbf{i}})^2 - \sum_{\langle \mathbf{ij}\rangle} J_{\mathbf{ij}}(B)\cos(\phi_{\mathbf{ij}} + A_{\mathbf{ij}}), \tag{3.1}$$

where E_c represents the Coulomb blockade scale, $\phi_{\mathbf{ij}} = \phi_{\mathbf{i}} - \phi_{\mathbf{j}}$ is the SC phase difference between neighboring grains at positions $\mathbf{i}$ and $\mathbf{j}$ respectively, and $A_{\mathbf{ij}} = (2e/\hbar)\int_{\mathbf{i}}^{\mathbf{j}} \mathbf{A}\cdot d\mathbf{r}$ are the AB phases acquired by the hopping Cooper pairs. Disregarding the contribution of normal quasi particles means the model can provide a good description of the magnetoresponse only at lower fields where CP breaking is not important. Spatial disorder in the grain positions introduces randomness in the Josephson couplings as well as the AB phases. Studies of

the 2D classical limit of Eq.(3.1) in the $B = 0$ limit [47] have shown that strong disorder in J does not alter the universality class of the SNT from the homogeneous case (where it is known to be of BKT type) but is nevertheless dominated by a percolating backbone of paths with the largest local superfluid stiffnesses. Likewise the transition in the quantum 1D disordered counterpart at $B = 0$ also obeys a KT like scaling [4, 71, 5, 79]. Therefore for simplicity we will work with the typical value of J ignoring its spatial disorder.

In regular lattices, the AB phase is associated with flux threading the plaquettes, and depending on the amount of frustration f (measured as a fraction of a flux quantum), leads to oscillations in properties such as the critical current and the resistance [138, 144]. Such matching (commensuration) effects are absent in the disordered case as there is random flux penetration in different plaquettes. Phase transition in the classical quenched random phase XY model on a square lattice close to integer f is well studied [36, 105, 33, 34]. The presence of disorder results in rare favorable regions for the occurrence of vortices at low temperatures. At sufficiently low temperatures, [105, 33, 34]found that the disorder-induced phase transition is not in the KT universality class. Very similar results were also obtained earlier [71] in a study of the Anderson localization in one-dimensional Luttinger-liquids subjected to quenched phase disorder. The similarity is puzzling since quenched disorder in 1D is equivalent to columnar disorder in the two-dimensional case. Quantum Monte Carlo studies [84] of the interplay of phase frustration and Coulomb blockade suggest a zero temperature field-driven SNT with dynamic exponent $z \approx 1.3$, placing the transition in a different universality class from 3D XY.

We study the effect of three dominant mechanisms governing loss of phase coherence and their specific signatures on the magnetoresistance and superfluid stiffness. These are (a) quantum phase fluctuations originating from Coulomb blockade, (b) thermal fluctuations of the phase and (c) frustration effects due to disorder in AB phases. We show that Coulomb blockade effects impart a specific signature to the magnetoresistance, $\rho(B) \sim \exp[(B/B_0)^2]$. Where the SNT is driven by thermal fluctuations, we find a KT transition, with $\rho(B) \sim \exp[-1/\sqrt{B - B_{KT}}]$ in the critical region. In the AB phase frustration dominated regime, we find a new, non KT critical behavior, $\rho(B) \sim \exp[-1/(B - B_{AB})]$. The field-dependent superfluid stiffness Υ also shows a surprising behavior: at small fields, we predict that phase frustration effects on Υ are more significant than the field dependence of Josephson couplings. In the Coulomb blockade regime away from the critical region, our predicted magnetoresistance is in excellent accord with experimental data [124, 134]. However in the critical scaling region, existing experimental data is somewhat less clear, and while there is some evidence for mechanism (c) for the field-tuned SNT in oxide heterostructures[25] , further study is needed and we propose additional probes to distinguish between the two.

3.2 Disordered Boson model

We now analyze the effect of a transverse magnetic field on the distribution of the SC islands in the granular superconductor. Consider a model of repulsive bosons (Cooper pairs) with average density n subjected to a random potential with a Gaussian white noise distribution:

$$H = \sum_{\mathbf{p}} \frac{\Pi^2}{2m} a^{\dagger}_{\mathbf{p}} a_{\mathbf{p}} + \int_{\mathbf{r}} \left[\frac{g}{2} |\Psi(\mathbf{r})|^4 + U(\mathbf{r}) |\Psi(\mathbf{r})|^2 \right], \tag{3.2}$$

where $\Psi(\mathbf{r}) = \frac{1}{\sqrt{V}} \sum_{\mathbf{p}} a_{\mathbf{p}} \exp[i\mathbf{p}\cdot\mathbf{r}/\hbar]$, $\Pi = (\mathbf{p} - q\mathbf{A})$, $U(\mathbf{r})$ is the random potential, $\langle U(\mathbf{r}) \rangle = 0$ and $\langle U(\mathbf{r}) U(\mathbf{r}') \rangle = \kappa^2 \delta(\mathbf{r} - \mathbf{r}')$, $q = 2e$ is the boson charge and g, parametrizes the boson repulsion. We choose the gauge $\mathbf{A} = \frac{1}{2}(\mathbf{B} \times \mathbf{r})$ with the field in the transverse z direction. This model is equivalent to earlier studied (for $B = 0$) Ginzburg-Landau models with disorder in critical temperature [80]. The important length scales in the model are the single particle localization length $\mathscr{L} = \hbar^2/m\kappa$ characterizing the disorder, and the magnetic length $l_B = \sqrt{\hbar c/(eB)}$. At finite temperatures, the model has at least three parameters, $\gamma_1 = \mathscr{L}/l_B$, $\gamma_2 = 2mg/\hbar^2$ and $\gamma_3 = \mathscr{L}/\lambda_T$, where λ_T is the De Broglie wavelength. We are specifically interested in the regime where all the three parameters are small. At low densities, the interplay of disorder and interparticle repulsion leads to the formation of disconnected islands of localized bosons [55] whose typical size and separation may be estimated as follows. The optimal potential fluctuation that has a bound state at energy $E < 0$ is found by minimizing $\frac{1}{2} \int U^2 d\mathbf{r} + \lambda (E - H)$, where λ is a Lagrange multiplier. We choose Ψ to be real, assuming a spherical fluctuation and zero angular momentum bound state. Varying with respect to U, we obtain $U = \lambda \Psi^2$; thus the size R of the optimum potential well is also of the same order as the wave function. The energy of a particle in an island, in the mean-field approximation, is thus of the order of

$$E \sim -\frac{\hbar^2}{2mR^2} + \frac{(qBR)^2}{8m} + gN_p/(\pi R^2), \tag{3.3}$$

where N_p is the number of bosons in the island. The density $n_w = n/N_p$ of these islands is determined by the Gaussian factor, $\exp[-\frac{1}{2\kappa^2} \int_{\mathbf{r}} U^2]$, whence

$$n_w \sim \left(\frac{1}{\pi R} \right)^2 \exp[-(\mathscr{L}/R)^2]. \tag{3.4}$$

Minimizing the energy with respect to R, the size of the typical island, to logarithmic precision, is

$$R(B) \sim \frac{\mathscr{L}}{\sqrt{\ln[n_c(B)/n]}}, \tag{3.5}$$

where for small fields,

$$n_c(B) \approx \frac{\hbar^2}{2gm\mathscr{L}^2}\left(1+\frac{(qB\mathscr{L}^2/\hbar)^2}{4}\frac{1}{\ln^2(n_c(0)/n)}\right), \tag{3.6}$$

is the critical density for percolation of the islands and $n_c(B)/n > 1$. For future convenience we introduce $w(B) = n_c(B)/n$. Clearly the magnetic field shrinks the islands but the field-dependence is very different from a simple expectation from wave function shrinking of a localized noninteracting particle. The distance $D \sim 1/\sqrt{n_w}$ between the islands can be estimated as

$$D(B) \sim R(B)e^{\frac{1}{2}(\mathscr{L}/R(B))^2} \sim \mathscr{L}\frac{\sqrt{w(B)}}{\sqrt{\ln w(B)}}. \tag{3.7}$$

The strength of tunneling of the bosons across nearest islands can be estimated from the semi-classical formula, $t = \exp(-1/\hbar\int|p|\mathrm{dl})$, where the integral path connects the two wells. The integral can be estimated using $|p| \sim \sqrt{2m|E|} \sim \hbar/R(B)$ and the length of the path is $\sim D(B)$. This leads to $t \sim \exp(-D(B)/R(B))$. The Josephson coupling between the nearest islands is, $J \propto t^2$. Thus we obtain,

$$J(B) \sim e^{-2\sqrt{w(B)}}. \tag{3.8}$$

Note that even when at small magnetic fields, $\mathscr{L}/l_B \ll 1$, the exponent in Eq. 3.8 can be large at low boson densities, $w(B) \gg 1$. For such fields we have $J(B)/J(0) \sim e^{-(B/B_J)^2}$, where $B_J^{-2} \approx \frac{\sqrt{w(0)}}{\ln^2 w(0)}(q\mathscr{L}^2/2\hbar)^2$.

Even though the value of R is fixed in our mean-field analysis, D and J nevertheless fluctuate since the wells have a finite probability density n_w to appear in any part of the system. It is straightforward to show that the distance D between neighboring grains has the distribution,

$$P(D) \sim 2\pi D n_w e^{-n_w\pi D^2} \tag{3.9}$$

We now analyze the effects of the three different mechanisms that lead to loss of global phase coherence in their regimes of dominance which are determined by the dimensionless

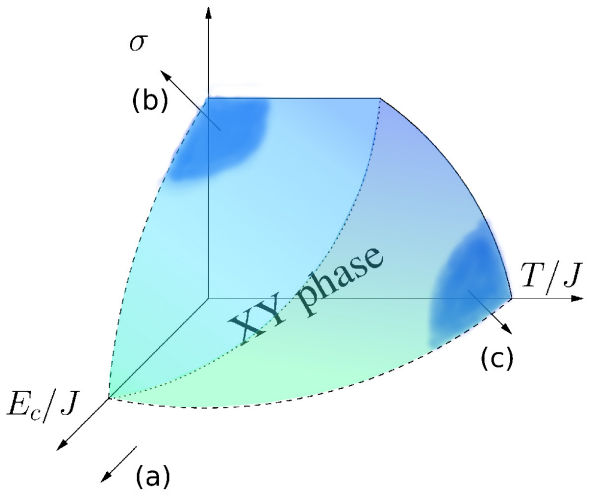

Figure 3.2 Schematic phase diagram for the 2D superconductor-normal state transition, with the XY superfluid phase in the interior of the surface, as a function of dimensionless temperature T/J, Coulomb blockade scale E_c/J and the Aharanov-Bohm (AB) phase disorder σ for the model described in Eq. (3.1). Here J is the (field-dependent) Josephson coupling estimated in the paper. (a) refers to the Coulomb blockade dominated regime. The shaded regions (b) and (c) denote transitions driven by AB phase frustration and thermal phase fluctuation respectively. The dotted line on the surface separates these two different critical scaling regimes. The critical disorder at low T and E_c is independent of T and scaling of the correlation length is not of the BKT type [34].

parameters E_c/J, T/J and σ, with the latter a measure of disorder in the fluxes through elementary plaquettes. Figure 3.2 shows the phase diagram and the regimes of our study. In order to carry on this analysis it is convenient to work with an effective Hamiltonian which has only the collective phases of different grains as the degrees of freedom. It is well known that our system can be described by a Josephson Junction model with the Hamiltonian corresponding to the Lagrangian in (3.1). The magnetic field dependent parameters of the Hamiltonian is obtained from our analysis above. $E_c(B) = q^2/2C$ is the typical charging energy of the grains where C is the typical capacitance of the grains; $C \sim \varepsilon R(B)$, ε being the dielectric constant. Denoting the plaquette area fluctuation by $(\delta D)^2$, we identify $\sigma \sim B^2(\delta D)^4$. From eq.(3.9) it follows that, $(\delta D)/D < 1$

3.3 Analysis of the effective Josephson-junction model

We now proceed to the analysis in the three different regimes mentioned above.

(a) Quantum phase fluctuations dominated insulating regime ($E_c/J, E_c/T \gg 1$)

We treat the Josephson term in Eq.(3.1) as a perturbation, and calculate the conductivity using the Kubo formula [141, 136]. Transport in this model proceeds through Arrhenius activation and incoherent sequential hopping of charges between neighboring islands - this leads to a resistivity of the form

$$\rho(B) \sim J(B)^{-2} e^{E_c(B)/T} \sim e^{[4\sqrt{w(B)}+(q^2/\mathscr{L}T)\sqrt{\ln w(B)}]}. \tag{3.10}$$

The above behavior shows the insulating nature of the normal state. For small fields, the magnetoresistance obeys the law $\rho(B)/\rho(0) \sim \exp[(B/B_0)^2]$, where $B_0^{-2} \approx \frac{(q\mathscr{L}^2/2\hbar)^2}{2\ln^2 w(0)}[\sqrt{w(0)} + \frac{q^2}{\mathscr{L}T\sqrt{\ln w(0)}}]$. More accurately, one must also take into account the renormalization of the charging energy by Josephson coupling [136, 61], $E_c \to E_c - J$. It is interesting to note that a similar field dependence of resistivity $\rho(B) \sim e^{(B/B_c-1)^2}$ has been obtained in the context of a superconductor to Hall insulator transition [131].

(b) AB phase frustration dominated regime ($E_c/J \ll 1$, $T/J \ll 1$, $\sigma/\sigma_c \sim 1$)

To study this regime, it is useful to consider the Coulomb gas representation of the model in Eq. (3.1). Following earlier works [34, 116] we assume a Gaussian white noise distribution for the AB phases on the links, reckoned from a background average corresponding to a typical separation of islands, D. In the Coulomb gas representation, such disorder translates to a random flux threading elementary plaquettes, corresponding to an external potential $V_{\mathbf{r}}$ acting on the "charges" (vortices) with a Gaussian distribution $\langle (V_{\mathbf{r}} - V_{\mathbf{r}'})^2 \rangle = 4\sigma J^2 \ln|\mathbf{r} - \mathbf{r}'| + O(1)$. It is crucial that the random background potential has long-range (logarithmic) correlations. In the continuum description of the model with a lower cutoff scale a_0, $V_{\mathbf{r}}$ has a local part $v_{\mathbf{r}}$: $\langle (v_{\mathbf{r}} - v_{\mathbf{r}'})^2 \rangle \sim \sigma J^2$ and a long-range correlated part $V_{\mathbf{r}}^{>}$ with no cross-correlation between these two parts. The Coulomb gas Hamiltonian then reads

$$H = -J \sum_{\mathbf{r} \neq \mathbf{r}'} n_{\mathbf{r}} n_{\mathbf{r}'} \ln\left(\frac{|\mathbf{r} - \mathbf{r}'|}{a_0}\right) - \sum_{\mathbf{r}} \left[n_{\mathbf{r}} V_{\mathbf{r}}^{>} - \ln Y[n_{\mathbf{r}}, \mathbf{r}] \right], \tag{3.11}$$

where $n_{\mathbf{r}}$ represents integer charge at $\mathbf{r}$ and the spatially dependent fugacities have the bare value, $\ln Y[n_{\mathbf{r}}, \mathbf{r}] = \gamma J n_{\mathbf{r}}^2 + n_{\mathbf{r}} v_{\mathbf{r}}$, and γ is a constant of order unity. We have dropped the background term as it just sets the chemical potential of the vortices and does not affect the scaling equations [106].

In the absence of disorder, the usual RG procedure consists of (i) increasing the short scale cutoff, $a_0 \to a_0 + dl$, and eliminating all dipoles in the annulus of thickness dl, and (ii) disregard all configurations that increase the net charge within the cutoff region. The RG

procedure is perturbatively controlled by small dipole fugacities. For the disordered case, we follow Ref.[34] and introduce replicas which allows us to perform the average over Gaussian disorder. The lowest excitations continue to carry charges $0, \pm 1$ but now the $n_{\mathbf{r}}^{\alpha}$ also carry a replica index α. An important difference from the RG procedure of the disorder-free case is that now when the cutoff is increased, one must, apart from considering annihilation of replica charges, also take into account "fusion" of unit charges in different replicas (see appendix A). Another important difference that invalidates the usual perturbative expansion in small dipole fugacities is that the random potential creates favorable regions for single vortex formation. Hence we study the scale dependence of the single vortex fugacity distribution identifying the density of rare favorable regions, $\rho_{a_0}^{v}$, for the occurrence of vortices as the perturbation parameter. By studying the scaling of $\rho_{a_0}^{v}$, two distinct regimes can be identified for $T/J \ll 1$: (a) an XY phase phase at sufficiently low bare disorder where $\rho_{a_0}^{v}$ scales to zero, and (b) a disordered phase beyond a critical bare disorder where $\rho_{a_0}^{v}$ diverges (see appendix for details). In the disordered phase, the phase correlation length has a surprising non-BKT behavior, $\xi \sim e^{1/(\sigma-\sigma_c)}$, which in our context translates to a field dependence $\xi \sim e^{1/(B-B_{AB})}$, with $B_{AB} \sim \hbar/q(\delta D)^2$. Such a non-BKT behavior is a direct consequence of the logarithmic scaling of the disorder potential correlations. Another peculiarity is that over a range of low temperatures up to a scale of order J, the critical disorder σ_c is independent of the temperature [34].

We obtain the magnetic field dependence of the superfluid stiffness by solving the scaling equations in the critical region at low temperatures for the coupling constant J_l and the effective disorder σ_l. Taking the ratio of the scaling equations for J_l and σ_l obtained in Ref.[34], we get

$$\frac{\partial_l J_l^{-1}}{\partial_l \sigma_l} \sim \frac{1}{J_l \sqrt{\sigma_l}},$$

and from the solution $J_l \sim e^{-2\sqrt{\sigma_l}}$ it follows that the superfluid stiffness $\Upsilon(B)$ has the behavior

$$\Upsilon(B) \sim J(B) e^{-2\sqrt{\sigma(B)}} \sim e^{-(B/B_1)-(B/B_J)^2}, \tag{3.12}$$

where B_1 is of the order of B_{AB}. Phase frustration effects thus play a more important role in determining the low-field dependence of superfluid stiffness in the AB phase-frustration dominated regime compared to the effect coming from orbital shrinking.

Now we analyze magnetoresistance in the disordered phase at low temperatures and close to the field-induced transition. Following Halperin and Nelson [76] we estimate the electrical resistivity (which is essentially the vortex conductivity) as $\rho(B) = \mu_v n(B)$, where μ_v is the

temperature and field-dependent mobility of the vortices, and $n(B) \sim 1/\xi^2$ is the vortex density. We make an assumption that $\mu_v(B)$ is well-behaved near $B = B_{AB}$, which allows us to neglect its field dependence in comparison to the singular behavior of $\xi(B)$. The temperature dependence of resistivity is governed by the temperature dependence of the mobility, and we believe it shows an activated behavior given the logarithmic Coulomb interaction of the vortices[132]. The magnetoresistance in this AB phase frustration dominated regime thus grows as

$$\rho(B) \sim \mu_v(T) e^{-1/(B-B_{AB})}. \tag{3.13}$$

(c) Thermal phase fluctuations dominated BKT regime
$(E_c/J \ll 1, \sigma/\sigma_c \ll 1, T/J(B) \sim 1)$

In this regime, the transition is brought about by the proliferation of thermally activated vortices. The superfluid stiffness now has a field dependence$\Upsilon(B) \sim J(B) \sim e^{-(B/B_J)^2}$ arising from orbital shrinking of the SC islands. For the resistivity we again consider the correlation length in the disordered phase, which has the well-known form, $\xi \sim e^{1/\sqrt{T-T_{KT}}}$, with $T_{KT} \propto J(B)$. Near the transition, this is equivalent to a field-dependent correlation length, $\xi \sim e^{1/\sqrt{B-B_{KT}}}$. Thus the resistivity in this regime has the form

$$\rho(B) \sim \mu_v(T) e^{-1/\sqrt{B-B_{KT}}}. \tag{3.14}$$

For regimes (b) and (c), the normal state has a "metallic" temperature dependence since enhancement of vortex mobilities at higher temperatures translates to higher resistivity.

3.4 Relation to experiments

Figure 3.3 shows the low-temperature and low-field magnetoresistance of disordered InO_x thin films extracted from two different experiments [124, 134]. The two sets of the positive magentoresistance data are fitted to the form $\ln(\rho) = aB^n + b$. For the data from Ref [124], we get $n = 2.834 \pm 0.024$ and for the data from Ref [134], we get $n = 2.542 \pm 0.131$. In the Coulomb blockade dominated regime according to the predicted form given in Eq. (3.10), n should be equal to 2. This difference could be due to various reasons. The form in Eq. (3.10) is only valid if we treat Josephson tunneling perturbatively to leading order. We have made some crude simplifying assumptions while estimating the properties of the SC islands from the disordered Boson model subjected to a magnetic field. Hence the exact form in Eq. (3.10) may not hold; but a crucial outcome of the analysis is that the resistance is exponentially

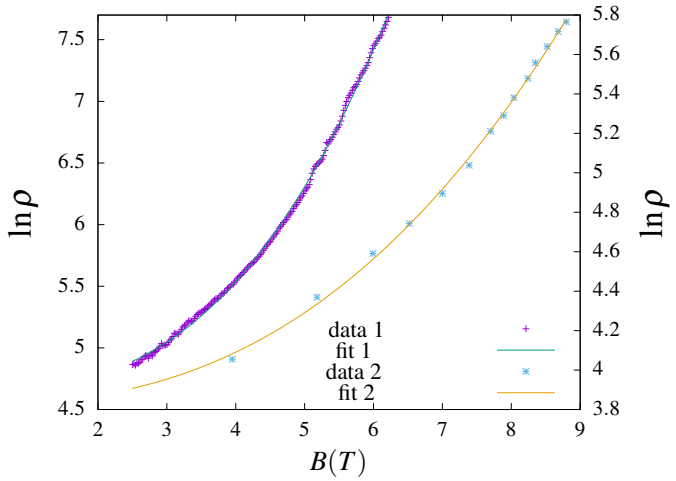

Figure 3.3 Resistivity ρ as a function of perpendicular magnetic field B for disordered InO_x thin films as reported in Ref.[124] (data 1) and Ref. [134] (data 2) in the low-field region where the fits are to the form $\ln(\rho) = aB^n + b$. In the region where Coulomb blockade is dominated we predicted $n = 2$. Here for data 1 we get $n = 2.834 \pm 0.024$ and for data 2, $n = 2.542 \pm 0.131$. The possible reasons for deviations from the predicted form are discussed in the main text, but the main point is that the resistance is exponentially sensitive to the magnetic field.

sensitive to the magnetic field in the Coloumb blockade regime and this aspect is nicely obeyed in the two sets of experimental data. Finally the deviations from the predicted form can also occur due to the opening up of a quasiparticle transport channel which we have totally ignored. This can be more prominent as we approach the magnetoresistance peak since the very existence of the peak is thought to be due to the presence of a quasiparticle channel as well.

In samples with lower disorder [134], unsurprisingly, Coulomb blockade does not adequately explain the data; however, the other critical scaling regimes (AB phase frustration and BKT) show better agreement even though we were unable to distinguish between the two. In Fig.3.4, we show the sheet resistance $R_\square$ vs. magnetic field data near a field-driven SNT in a homogeneously-disordered InO_x thin film from Ref. [134], and attempt fits of this data to the BKT behavior ($R_\square = R_0 e^{-1/\sqrt{B-B_{KT}}}$) and the non-BKT behavior ($R_\square = R_0 e^{-1/(B-B_{AB})}$) . It is difficult to say which of these two laws describes the data better; however, we argue that the non-BKT fit might be a bit better on account of a more reasonable value for the high-field resistance R_0.

In a recent study of the field-tuned SNT at 2D interfaces of gated oxide heterostructures [25], it was reported that for certain gate voltages, the critical magnetic field at low temperatures was independent of the temperature, suggestive of the phase frustration driven

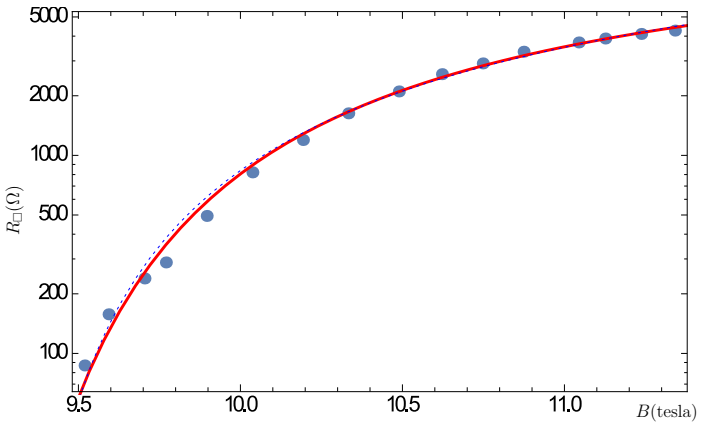

Figure 3.4 Sheet resistance $R_\square$ of homogeneously-disordered InO_x thin films as a function of perpendicular magnetic field B near the field driven SIT (data extracted from Ref. [134]). The fits are to a BKT law $R_\square = 5.02 \times 10^4 e^{-16/\sqrt{B^2-9.2^2}}$ (solid red curve) and the non-BKT law $R_\square = 1.53 \times 10^4 e^{-61.2/(B^2-8.9^2)}$ (blue dashed curve). The BKT transition is driven by thermal phase fluctuations while the non-BKT transition is driven by phase frustration. Both the laws fit the data equally well; however the pre-factor of the exponential, which represents the high-field sheet resistance, is a more reasonable number in the non-BKT case since in the actual data, the peak value of resistance is of a comparable order.

SNT mechanism. Finally, our predictions for superfluid stiffness in the XY regime can possibly be tested through studies of field-dependent ac conductivity[102] and may provide an independent means for distinguishing between the two regimes in the XY phase.

3.5 Discussion

In summary, we studied the field-dependence of the distribution of SC islands in strongly disordered superconductors and constructed an effective Josephson-junction model with field-dependent parameters. Analyzing the model in different physical regimes - dominated by Coulomb blockade, thermal phase fluctuations or Aharanov-Bohm phase fluctuations - we obtained the field-dependence of resistivity and superfluid stiffness. In the Coulomb blockade regime, available experimental data is in excellent agreement with our prediction $\rho(B) \sim e^{(B/B_0)^2}$, while in the critical scaling region, available magnetoresistance data [134] is insufficient to distinguish between BKT and AB phase frustration regimes.

At very low temperatures, the critical behavior in the vicinity of the quantum critical point ($E_c/J(B) \sim 1$) is expected to be that of the 3D XY universality class. For the field-tuned transition in systems with homogeneous potential disorder, the rapid decrease of the Josephson coupling $J(B)$ with field implies that the likely experimental trajectories in the T/J vs.E_c/J plane rapidly move out of the quantum critical region into the Coulomb-

blockade dominated region where $E_c/J \gg 1$. In contrast, in systems such as nanopatterned SC proximity arrays, the fabrication technique is such that the separation of SC regions (and thus $J(B)$) is not as field-sensitive. Such systems look attractive from the point of view of studying the critical behavior near the field-tuned SNT, especially in the quantum critical region $E_c/J(B) \sim 1$. In our study we neglected pair-breaking effects which likely play a crucial role in explaining the giant negative magnetoresistance observed at higher fields [117, 47]. Pair breaking opens up an additional quasi particle transport channel, and it would be interesting to study magnetic field effects in phase models with both quasi particle and Cooper pair tunneling.

Chapter 4

Disordered BKT transition and superinsulation

4.1 Introduction

Strongly disordered superconductor thin films in the insulating side of a magnetic field tuned SIT, show a surprising phenomenon at very low temperatures: an abrupt drop in the current as the voltage is lowered below a critical value [123, 145, 114] (see Fig 4.1). This phenomenon is identical to the abrupt voltage drop seen in the SC transition at low temperatures as the current is lowered below a critical value. This state of apparent zero conductance was called superinsulator [145]. Further the transition to the zero conductance state was also observed in the linear response regime: the conductivity was observed to drop abrubtly below a critical temperature [113, 101].

The abrupt drop in the observed current-voltage characteristics was given a phenomenological explanation in Ref [8] as a consequence of electron overheating. But this phenomenological theory fails to explain the apparent transition to a zero conductance state that is observed in the linear response regime and in particular the emergence of the temperature scale at which the transition occurs. This finite temperature insulator transition was then proposed to be a possible manifestation of the phenomenon of many body localization (MBL) [113].

Diamantini *et al.* introduced the concept of a superinsulating state in the framework of the gauge theory of Josephson junction arrays (JJA)[45] as a realization of the Cooper pair-vortex duality [59, 56, 89], and later it was proposed in Ref [145] that the superinsulator is a low-temperature charge-BKT state. The zero temperature SIT then corresponds to the mutual termination of charge- and vortex BKT transitions at the self-dual point [56, 22].

The self-dual point separates a SC state that harbors Cooper pair condensate and pinned vortices from a superinsulating state where Bose condensation of vortices inhibits charge transport [89, 145]. The dual picture leads to similar vortex and Cooper pair dynamics on either side of the SIT [56]. The divergence of the dielectric constant near the SIT in strongly disordered superconductor thin films which in turn leads to 2D logarithmic Coulomb interactions between the Cooper pairs over appreciably macroscopic scales[145] provides a material platform for the realization of charge BKT physics. Further this also explains why the superinsulating transition is only observed for magnetic fields close to the SIT, since the shrinking of the SC islands beyond a field strength will bring down the effective dielectric constant and thus the logarithmic interaction between charge excitations wil no longer be valid.

Recent observations of the *charge* BKT critical behavior $R \propto \exp[b/\sqrt{1-T/T_{\rm BKT}}]$ [22, 101] is consistent with the dual BKT physics of the SIT [56]. Recent measurements [113] of the temperature dependence of the sheet resistance of InO_x thin films on the insulating side in the vicinity of a magnetic field-tuned SIT reported, however, a surprising observation of much more singular, the so called Vogel-Fulcher-Tammann (VFT)-like critical behavior of the resistance, $R_{\square}(T) \sim \exp[\text{const}/(T-T_{\rm VFT})]$. This VFT dependence is viewed as a standard critical behavior in glass-forming materials, but its origin remains a puzzle in spite of the decades-long search, (see Ref [118]) for a review. At the same time, an earlier suggestion made by Anderson [15] that the origin of the VFT law may also lie in logarithmic interactions between topological defects in the glass-forming materials, makes it appealing to revisit the theory of disordered superconductor films and to examine whether the VFT criticality may arise in the framework of the BKT physics. We will show that this is indeed the case.

We investigate here the nature of BKT criticality in strongly disordered superconductor thin films in the framework of the *disordered* Josephson-junction array (JJA) model that hosts both vortex and charge BKT transitions. Depending on the ratio of the characteristic Josephson coupling energy E_J and the Coulomb energy scale, E_C, one obtains either a SC phase for $E_J > E_C$, or insulating phase for $E_J < E_C$ [56]. For concreteness and also to connect with the recent experiment[113, 101], we focus here on the insulating regime. Apart from the well-studied effect of nucleating CP islands [55], we argue that potential disorder is also a source of quenched random dipole moments. We show that such disorder in the dipole moments, if sufficiently strong, turns the standard BKT critical behavior of conductivity

$$\sigma(T) \sim e^{-\text{const}/\sqrt{T-T_{\rm BKT}}} \tag{4.1}$$

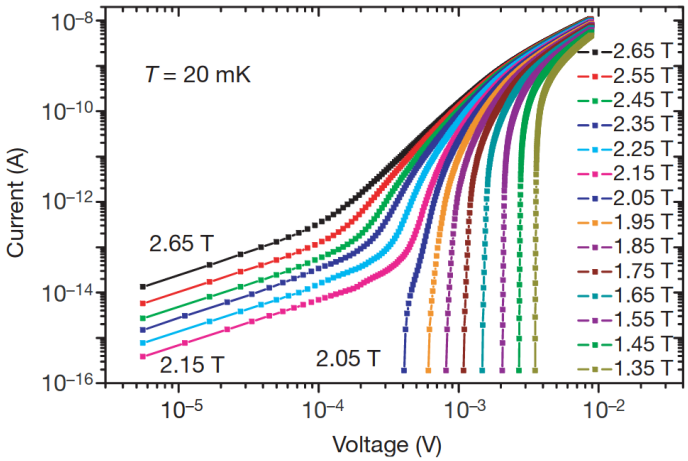

Figure 4.1 The observation of the superinsulating transition reported in Ref [145]. Here the transition is observed in the insulating side of a magnetic field tuned SIT. The abrubt drop in the current as the voltage is lowered to a critical value is observed up to a critical magnetic field strength. Beyond this a normal insulating behavior is seen. (Figure shown from Ref. [145] with permission.)

into the more singular VFT criticality

$$\sigma(T) \sim e^{-\text{const}/(T-T_{\text{VFT}})}. \tag{4.2}$$

The difference of critical behaviors comes from poorer electrostatic screening (in the VFT case) due to the freezing of charge dipole excitations that is known to occur [137] in the absence of interactions of the dipole-dipole kind once disorder strength exceeds a critical value. This critical strength is determined by the ratio of temperature and Coulomb interaction scales. Based on this consideration, we posit that the VFT and BKT phases respectively correspond to nonergodic and ergodic regimes of the superinsulator. The strong disorder criterion is $\eta > T/2E_C$, where dimensionless parameter η defines the strength of disorder via the correlation function of the coarse-grained random dipole potential, $\langle (V(\mathbf{r}) - V(\mathbf{r}'))^2 \rangle \approx 4\eta E_C^2 \ln(|\mathbf{r}-\mathbf{r}'|/R)$. We construct the disorder vs. temperature phase diagram of the superinsulator transition, and this, along with the critical behaviors given by Eqs. (4.1) and (4.2) and the physical understanding for the difference in the two critical behaviors are the main results of this chapter.

4.2 JJA model and disordered Coulomb gas description

We consider a homogeneously disordered two-dimensional superconductor on the insulating side of the SIT. Coarse-graining over the size of the Cooper pairs, we approximate the

disorder background charge distribution $\rho(\mathbf{r})$ as a Gaussian white noise correlation function, $\langle(\rho(\mathbf{r})-\bar{\rho})(\rho(\mathbf{r}')-\bar{\rho})\rangle = n_d\delta(\mathbf{r}-\mathbf{r}')$, where the average background charge density, $e\bar{\rho}$, equals the average charge density of the Cooper pairs, and n_d is the variance of the coarse-grained background charge distribution. The system is customarily viewed as a lateral JJA comprising SC droplets coupled by Josephson links as discussed in Chapter 2. The droplets nucleate at deep potential fluctuations resulting from intrinsic quenched charge disorder of the host. Near the SIT, the size of the droplets is expected to be of order of the SC coherence length and in any case exceed the characteristic localization length of single particles in the disordered potential [93, 55, 125]. In the JJA, the effective dielectric constant and, accordingly, the crossover length is expressed via the characteristic capacitances [56]. We will address the situation $\Lambda \gtrsim L$ so that the interactions between the charges is logarithmic.

The excess charge on a droplet interacts with the charge distribution of other droplets. The leading contribution to the energy is provided by the electric 'monopoles', the single excess charges $n_{\mathbf{i}}$ on the other droplets, $-\sum_{\mathbf{i}\neq\mathbf{j}} E_C n_{\mathbf{i}} n_{\mathbf{j}} \ln|(\mathbf{r_i}-\mathbf{r_j})/a|$, where a is a microscopic length scale (the size of the droplet), $E_C = q^2/2C$ is the characteristic energy for creation of a CP dipole ($q = 2e$) across neighboring droplets and C is the inter-droplet capacitance [56]. The next order contribution comes from the dipole moments of the grains, $\mathbf{P_i}$, which yield the random potential energy

$$V_{\mathbf{i}} = \sum_j \frac{q}{2\pi C}\frac{\mathbf{P}_j\cdot\mathbf{r}_{ij}}{r_{ij}^2}. \tag{4.3}$$

Using $\langle\mathbf{P}\rangle = 0$, we see that the dipole-induced random potential is logarithmically correlated:

$$\langle(V(\mathbf{r})-V(\mathbf{r}'))^2\rangle \approx 4\eta E_C^2 \ln\left(|\mathbf{r}-\mathbf{r}'|/R\right), \tag{4.4}$$

where $\eta = \pi\langle P^2\rangle/q^2R^2$, R is the typical radius of a grain and $\langle P^2\rangle \propto n_d$.

The effective action for JJA comprises both, the charge and phase degrees of freedom as discussed in Chapter 2.

$$S[n,v] = \int_0^\beta d\tau \sum_{\mathbf{i},\mathbf{j}} \Bigg(E_C n_{\mathbf{i}} U_{\mathbf{ij}} n_{\mathbf{j}} + E_J v_{\mathbf{i}} U_{\mathbf{ij}} v_{\mathbf{j}} + \imath n_{\mathbf{i}} \Theta_{\mathbf{ij}} \partial_\tau v_{\mathbf{j}} + \frac{1}{2E_J}\partial_\tau n_{\mathbf{i}} U_{\mathbf{ij}} \partial_\tau n_{\mathbf{j}} \Bigg) + \sum_i V_{\mathbf{i}} n_{\mathbf{i}}, \tag{4.5}$$

where $v_{\mathbf{i}}$ are the integer-valued vortex degrees of freedom, defined on the dual lattice, $\Theta_{\mathbf{ij}} = \arctan\left(\frac{y_i-y_j}{x_i-x_j}\right)$ and $U_{ij} = -\ln|\mathbf{r}_i-\mathbf{r}_j|$. In the insulating state where $E_J \ll E_C$, E_J being the typical strength of the Josephson coupling, we can treat the integer valued vortex fields

as continous fields and integrate them out to obtain the effective charge action as

$$S_e[n] = \int_0^\beta d\tau \sum_{\mathbf{i},\mathbf{j}} U_{\mathbf{ij}} \left(\frac{1}{E_J} \partial_\tau n_{\mathbf{i}} \partial_\tau n_{\mathbf{j}} + E_C n_{\mathbf{i}} n_{\mathbf{j}} \right) + \sum_i V_{\mathbf{i}} n_{\mathbf{i}} \,. \tag{4.6}$$

Hereafter we neglect the temporal fluctuations as they are irrelevant at low energies and do not alter the nature of the phase transition governed by the interplay of the long-range Coulomb interaction and disorder correlations. The parameters in the model are thus the temperature T, Coulomb energy scale E_C and the effective disorder strength η.

4.3 Results from scaling analysis

A scaling analysis of the classical 2D Coulomb gas Hamiltonian in Eq. (4.6) proceeds through analyzing the disorder averaged real-space Kosterlitz renormalization group (RG) equations as discussed in Chapter 3 and Appendix A. Following the discussion in chapter 3, we see that the phase boundary between the superinsulating (XY phase) and normal insulating (disordered) phases is given by

$$2 - \frac{E_C}{T} + \frac{\eta E_C^2}{T^2} = 0 \text{ for } T > T_g = E_C \sqrt{\frac{\eta}{2}}; \tag{4.7}$$

$$\eta = \eta_c = \frac{1}{8} \text{ for } T \leq T_g, \tag{4.8}$$

where E_C and η stand for the renormalized quantities at $\ell = \infty$.

Two distinct critical behaviors are identified on approach to the charge BKT transition. Near the phase boundary at small degrees of disorder, the correlation length exhibits the usual BKT criticality

$$\xi \sim e^{1/\sqrt{b/[(T/T_{\mathrm{BKT}})-1]}},\ (T - T_{\mathrm{BKT}})/E_C \ll 1\,, \tag{4.9}$$

where, $T_{\mathrm{BKT}} = E_C/2$ is the critical temperature of the charge-BKT transition [56] and b is a numerical constant of order unity. For finite but small disorder η, the dependence of T_{BKT} on η can be obtained from the solution of Eq. (4.7). Near the disorder-controlled phase boundary, the correlation length is

$$\xi \sim e^{1/(\eta - \eta_c)},\ T/E_C \ll 1, \eta - \eta_c \ll 1\,, \tag{4.10}$$

where $\eta_c = 1/8$ is the critical disorder strength at low temperatures for the transition.

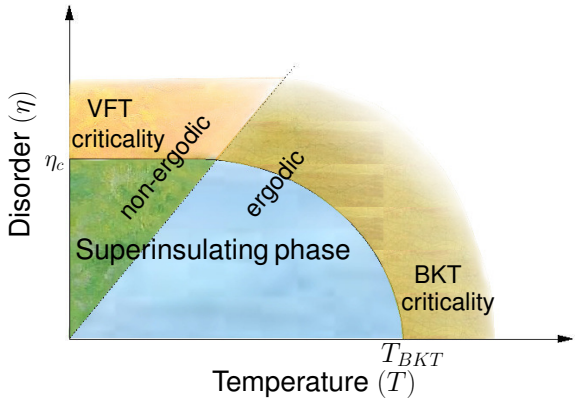

Figure 4.2 A sketch of the phase diagram of the superinsulating state and critical behaviours of a two-dimensional Josephson-junction disordered array in disorder-temperaure coordinates. Disorder being considered is the quenched random dipole moments of the grains. In the superinsulating phase, the probability of single charge excitations is zero. The transition to the conducting state occurs via the proliferation of the single charge excitations generated either thermally or by disorder. The former leads to the BKT criticality, given by Eq. (1), while the latter results in VFT behavior of Eq. (2). The dotted line $\eta = T/2E_C$, separates the nonergodic region (shaded green), where the charge dipoles freeze (their free energy becomes independent of temperature), from the ergodic region (shaded blue) where a finite entropy is associated with the charge dipoles which can appear anywhere. Likewise, the VFT critical region is nonergodic and conducting, while the BKT critical region is ergodic and conducting.

4.4 Ergodic and nonergodic regimes

To understand the physics underlying these two critical scenarios, we look at a dilute gas of charge dipoles subjected to disorder and neglect the dipole-dipole interations. Here, the distinct critical scenarios correspond to the system freezing into either the ergodic, at low disorder, or into the nonergodic, at strong disorder, respectively, superinsulating states as shown in the phase diagram in disorder-temperature coordinates in the Fig. 4.2. The dotted line $\eta^*(T) = T/2E_C$, marks the onset of freezing of isolated charge dipoles [137] where freezing means that the free energy of dipole excitations loses an explicit temperature dependence. To see this, consider a dilute gas of dipoles, where the inter-dipole distance D far exceeds the typical dipole size R. In this dilute limit, we focus on a region of linear size D containing a single dipole. The energy of this dipole is

$$E_d \sim 2(\ln Y + E_C \ln(R/a_0)) + (V^{(+)}(\mathbf{r}) - V^{(-)}(\mathbf{r}')), \tag{4.11}$$

where $V^{(\pm)}$ refer to the respective potential energies of the positive and negative charge constituting the dipole, $|\mathbf{r} - \mathbf{r}'| = R$. The first term is a uniform part and the latter term is

a random contribution. Although $V^{(+)}$ and $V^{(-)}$ individually have long-range correlations, their difference is short-range correlated beyond the scale R. The variance of this random potential difference is easily seen to be $\Delta = 4\eta E_C^2 \ln(r/a_0)$. Thus we effectively have a single particle (the dipole) subjected to a Gaussian white noise random potential with variance Δ. Factoring out the constant part of the energy, we construct the partition function for the random energies of different charge configurations,

$$Z = \sum_N \exp[-\beta E_d^i], \tag{4.12}$$

where i labels the charge configuration, $N \sim (D/a_0)^2 (R/a_0)^2$ is the total number of configurations. This random energy model has been extensively studied in the literature [42]. The free energy is known to have the following form,

$$F = -c(T,s)\ln N + O(\ln\ln N), \tag{4.13}$$

where,

$$c(T,s) = \begin{cases} T + s/2T & \text{for} T > T_g(s) \\ \sqrt{2s} & \text{for} T < T_g(s) \end{cases} \tag{4.14}$$

Here $s = \Delta/\ln N$ and $T_g(s) = \sqrt{s/2}$. Then for our case, we have,

$$s = \frac{2\eta E_C^2 \ln(R/a)}{\ln(R/a_0) + \ln(D/a_0)}. \tag{4.15}$$

The free energy is given by,

$$F_d(D,T) \sim 2(\ln Y + E_C \ln(R/a_0)) - 2c(T,s)\ln\left(\frac{DR}{a_0^2}\right) \tag{4.16}$$

The freezing now takes place at $T^* = T_g(s)$. The typical inter-dipole distance D can be determined from the condition, $F_d(D,T) = 0$. The D thus determined will then initially increase as T decreases and then lock to a value D^* as $T < T^*$. Thus T^* is obtained by self consistently solving the equation,

$$T^* = T_g(s^*), \tag{4.17}$$

with s^* given by (4.15) by putting $D = D^*$. The solution is then given by, $T^* = 2\eta E_C$.

Physically the distinction betweeen the two critical behaviors could be understood as follows (see also Fig 4.3). In the ergodic phase the dipoles can appear anywhere and thus assume the most efficient – for screening – configuration. In the nonergodic phase, the dipoles

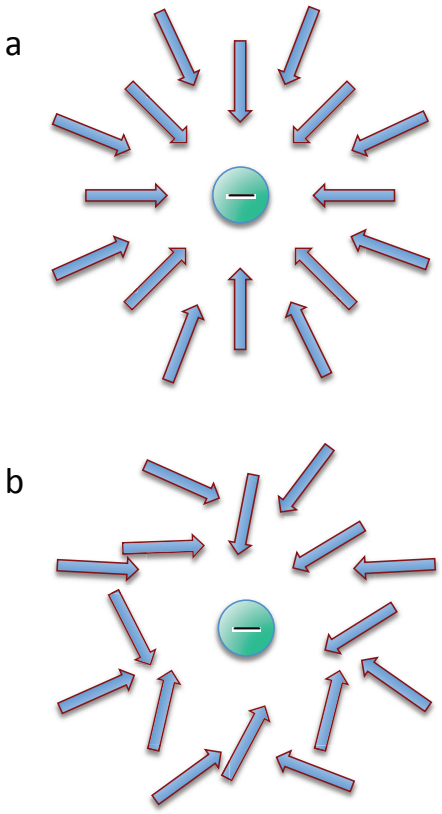

Figure 4.3 Schematic illustration of how freezing alters the usual BKT critical behavior. (a) In the ergodic phase the dipoles can appear anywhere and thus assume the most efficient – for screening – configuration. (b) In the nonergodic phase the dipoles are frozen and may not provide an efficient screening compared to that due to thermally generated dipoles. This inturn leads to the more singular VFT critical behavior.

are frozen, as they emerge mostly due to fluctuations in the random quenched potential, and hence may not provide an efficient screening as compared to the one due to thermally generated dipoles. This then leads to the more singular VFT-like critical behavior. In the presence of dipole-dipole interactions, it remains an open question as to whether the above transition remains a true one or becomes a crossover.

4.5 Charge transport in the critical region

The experimentally measurable quantity is conductivity, $\sigma \simeq \mu_c n_c$, where μ_c is the charge mobility and $n_c \sim 1/\xi^2$ is the density of free charges in the critical regime [76]. Then Eq. (4.9) leads us to our result in Eq. (4.1), i.e., the vanishing of conductivity in accordance with the BKT law.

We next address the conductivity in the strong disorder case described by Eq. (4.10). In Sec. 4.3, the disorder strength was treated as a temperature independent parameter. However in our description of the effective JJ model (see Sec. 4.2), η in general depends on the temperature. Physically, increasing the temperature increaes the ionization of the dopants. We assume an activated temperature dependence $n_d(T) = n_d(0) + N_d e^{-E_d/T}$, where E_d is the characteristic dopant-carrier binding energy for dopant levels near the conduction or valence bands. The temperature dependence of n_d imparts a temperature dependence to the disorder strength, η. Let T_c be the temperature at which $\eta(T_c) = \eta_c$. Expanding $n_d(T)$ in the vicinity of T_c, $n_d(T) \approx n_d(T_c)[1 + (T - T_c)(E_d/T_c^2)]$, we recover the VFT law for conductivity near the *disorder*-driven transition with $T_{\rm VFT} = T_c$ and constant $= 2T_c^2/(E_d\eta(T_c))$. Note that this result is obtained under the condition $T_c < E_C/2$, for otherwise the condition for the thermally-driven BKT transition is satisfied first with the increasing temperature and one obtains the BKT behavior of Eq. (4.1) as expected for the weak disorder case. Comparing VFT and BKT results one concludes that the transition from the VFT to the BKT behavior occurs at $\eta(T_{\rm BKT}) = \eta_{\rm c}$. Different critical behaviors in the strongly and weakly disordered regimes implies the existence of two distinct phases of the superinsulator.

4.6 Discussion

In summary, we have shown that in strongly disordered superconductor thin films, a logarithmically interacting 2D charge Coulomb gas may be realized in the vicinity of the SIT, where the dielectric constant tends to diverge. Apart from the well-known formation of SC islands, we proposed that quenched disorder also induces quenched random dipole moments of the charge distribution of the SC islands, which in turn, is the source of long-range (logarithmically) correlated potential fluctuations acting on the charge excitations. We also showed that the strength of the long-range correlated disorder increases with temperature. At low temperatures, a charge BKT (superinsulator) phase is realized, characterized by a vanishing conductivity. Increasing the temperature ultimately results in a BKT transition to a normal insulator phase. We showed that in the critical normal region, the conductivity continuously vanishes in accordance with two different laws - the usual BKT law for small disorder strengths, and a more singular VFT law for strong disorder strengths. We posit that these two distinct critical behaviors are manifestations respectively of ergodic and non-ergodic regimes of the superinsulator phase. The transition from the ergodic to nonergodic regimes is associated with the freezing of single charge dipole excitations.

By observing the critical behavior experimentally, we can understand if the system undergoes a transition to the ergodic or nonergodic superinsulating state. Based on the

existing data, we suggest that disordered SC TiN and NbTiN films [145, 22, 101] exhibit transition into the ergodic phase of the superinsulator, while the VFT criticality reported in InO films [113] suggests nonergodic behavior.

An analogous situation may also arise in the context of the SC transition in these systems in the presence of a finite magnetic field. Here, random Aharanov-Bohm phases associated with Cooper pair hopping lead to a (logarithmically) long-range correlated disorder for the vortex Coulomb gas [34, 116]. The crossover length separating 2D and 3D Coulomb regimes is now the Pearl screening length, $\lambda_P = \lambda^2/t$, where λ is the standard London penetration depth and t is the thickness of the SC film. Vortices tend to appear in regions of small local superfluid stiffness, and analogously to the residual charge dipoles discussed above, one now has residual vortex dipoles oriented along random directions. Since the (vortex) disorder parameter η is proportional to the density of randomly oriented vortex dipoles, increasing the temperature leads to the excitation of more dipoles in the weak-link regions thereby increasing η. Proceeding with the analysis we followed for the superinsulator phase, we arrive at essentially the same phase diagram and critical behavior for the superconductor phase. Owing to the vortex-charge duality, here the resistivity vanishes in accordance with either the BKT or VFT law upon approaching the SC phase boundary.

In Ref. [113], the authors propose that their finite temperature insulator transition could be a manifestation of the many-body localization (MBL) transition [73, 21]. The rationale behind this suggestion is that the CPs are only weakly coupled to the phonons, which is one of the prerequisites for observing an MBL transition. In what follows, we compare and contrast our picture with those obtained in the MBL framework. The critical behavior of $\sigma(T)$ on approaching the MBL transition proposed in Ref [73] is identical to our result for the ergodic BKT regime, while a recent result for conductivity in the vicinity of a many-body localized phase [72] resembles our nonergodic BKT behavior of Eq. (4.10).

A key difference is that in our picture, the zero conductivity phase is the result of long-range Coulomb interactions and turning up the disorder ultimately takes us out of this phase, while, in the MBL picture, the zero conductivity state is underpinned by disorder, and, Coulomb interactions provide the means to delocalize the charges. Historically, MBL studies have focused on the case with the short range interactions, but the recently proposed extension of MBL to a model with long-range interactions [104] challenges the earlier understanding that MBL does not occur for long range interactions [62]. We further note that while the MBL phase is essentially nonergodic, our superinsulating phase is ergodic for $T > 2\eta E_C$, and non-ergodic for $T < 2\eta E_C$. In the nonergodic region, the transition from the superinsulating phase to the conducting phase is reminiscent of the transition to nonergodic conducting

regime derived in the MBL framework [7]. The comparison of BKT and MBL pictures is summarized in Table I .

Property	Quantum many-body localization	2D disordered Coulomb gas
Role of disorder and interactions	Disorder underpins MBL, interactions provide a mechanism for delocalization.	Long-range (logarithmic) interactions responsible for superinsulation. Disorder facilitates transition from superinsulator to normal insulator.
Nature of interaction	Finite temperature insulator has been demonstrated for short range interactions. However a recent study claims that the MBL considerations can be extended to long range interactions also [104].	Logarithmic Coulomb interaction germane to finite temperature insulator. Further, VFT scaling for $\sigma(T)$ requires logarithmically correlated disorder.
Mechanism	$\sigma(T) = 0$ if the gap in the spectrum of many-particle bath excitations exceeds the corresponding inelastic scattering rate [73, 21]. Finite σ due to thermal activation above mobility edge not possible as mobility edge diverges with system volume [21].	(a) Low disorder ($\eta \ll \eta_c$): Transition from superinsulator phase $\sigma(T) = 0$ occurs when long-range Coulomb interaction gets screened by thermally generated low-energy charge dipole excitations. (b) High disorder ($\eta > \eta_c$): Transition occurs due to seeding of low-energy single charge excitations due to deep potential fluctuations.
Erogodicity	MBL phase is nonergodic. Recent work [7] suggests existence of a nonergodic delocalized phase near the MBL phase, and also that the transition between the nonergodic and ergodic delocalized phases resembles the classical glass transition.	Phase diagram has both ergodic and nonergodic regions with respect to the occurence of charge dipoles. Dilute gas of dipoles freezes [137] for $T/E_c < \eta$. Transition from XY to conducting phase can take place in both the ergodic and nonergodic regions resulting in KT-like or VF-like scaling respectively for $\sigma(T)$.
Cayley tree structure	Transition temperature and critical behaviour are obtained by an approximate mapping of the problem to an Anderson model in Fock space with a Cayley tree structure.	Scaling equation for charge fugacity in the disordered model can be recast in the form of the KPP equation [34] in relevant variables. The KPP equation arises naturally in studies of directed polymers on the Cayley tree [43].

Table 4.1 Comparison of two different theoretical routes to superinsulating behaviour based on (i) quantum many body localization and (ii) 2D disordered Coulomb gas.

Chapter 5

Keldysh field theory of nonequilibrium transport in a dissipative Mott insulator

5.1 Introduction

A central challenge in the area of dissipative quantum systems driven far from equilibrium relates to understanding the relaxation of initial conditions and the approach to nonequilibrium steady states. The temporal evolution is governed by the distribution of the initial disturbance over the many-body eigenmodes of the system, the nature of the bath and its coupling to the system, and the driving protocol. Mott insulator systems driven out of equilibrium are particularly interesting as they provide a meeting ground for quantum mechanics, strong interactions, dynamical processes and constraints. Many recent studies have attacked the problem of the nonequilibrium response of fermionic [65, 110, 108, 109, 50, 17, 140, 51, 111, 64, 94, 63, 46, 9, 18, 119, 103, 49, 85, 78, 107, 16, 52] or bosonic [121, 30, 35, 142, 92] Mott insulator systems subjected to a uniform and static electric field. One of the key questions concerns the fate of Bloch oscillations with increasing correlation strength [50, 51, 121, 35, 64, 63, 46, 16]. Another important question is regarding the role played by dissipation in the attenuation of the Bloch oscillations and the eventual approach to a nonequilibrium steady state (DC transport in particular) [94, 9, 17, 140, 16, 18]. A third crucial issue is related to the nature of nonequilibrium phase transitions in Mott insulator systems [121, 110, 109, 108, 17, 140, 119, 107, 52, 85, 78, 107, 16]. Different techniques have been employed in the literature that address some of these issues – these include numerical approaches such as solving time-dependent Schrödinger equations [110], nonequilibrium dynamical mean-field theory (NDMFT) [127, 111, 94, 63, 46, 9, 17, 18, 52, 16, 50, 51], time dependent density matrix renormalization group (TDMRG) [108, 49, 85, 78], as well as

analytic ones based on the Bethe ansatz [109, 107], including the phenomenological generalizations to $\mathscr{P}\mathscr{T}$-symmetric models [140, 65]. In this paper, we develop a new analytic field theoretical approach based on the Keldysh technique and address the above three questions. Our method also provides a general analytic framework to investigate novel and wide variety of nonequilibrium phenomena in strongly correlated systems.

It is long known that a noninteracting particle hopping on a periodic lattice subjected to a uniform electric field exhibits Bloch oscillations - the spectrum is discrete (Wannier-Stark ladder [146, 66]), and the particle motion is bounded. Correlations, dissipation and disorder can all suppress the Bloch oscillations by providing relaxation or breaking lattice translation symmetry. For field strengths such that the potential energy change between neighboring sites far exceeds correlation and other energy scales in the problem, Bloch oscillations have been found to persist [30, 35, 50, 51]. Physically, this can be understood from the fact that the noninteracting Wannier-Stark states are highly localized at the lattice sites at strong fields, and the correlations remain local in the Wanner-Stark basis. At fields where the potential energy drop in a bond is comparable to the interaction strength, study of the Bose-Hubbard model at integer filling establishes that the motion remains finite [121]. Recent numerical studies of fermionic Mott insulators show that at large fields, the electrons execute Bloch oscillations whose frequency approaches the noninteracting counterpart [50]. At smaller fields, the understanding for a long time was that interactions, through mixing of different momentum modes, attenuate the Bloch oscillations ultimately giving way to a steady state DC response[50, 51]. However recent work suggests that the apparent steady state DC behavior is only transient and ultimately gives way to finite (oscillatory) motion with a period different from that of the noninteracting Wannier-Stark states [16]. The current understanding is that dissipation is a necessary ingredient for establishing steady state DC response.

Bloch oscillations can be suppressed by dissipation through coupling the system to a bath. Earlier literature shows that even at a single-particle level, coupling the system to a phonon bath [53] or a fermionic bath [77] results in a finite DC response at any value of the coupling strength; however for the case of coupling to a phonon bath, signatures of the Wannier-Stark ladder are still evident in the spectral function, which are found to diminish with increasing electron-phonon coupling [39]. Recent works have also considered the effect of correlations in dissipative models. The dissipation is introduced either by coupling the system to a bath [17, 18, 94, 9] or by phenomenological means, for example, by introducing non-Hermitian terms in Hamiltonians preserving $\mathscr{P}\mathscr{T}$ symmetry [140, 65] or using Lindblad formulations [19]. The former (heat bath) case has been studied using a numerical Keldysh DMFT approach [17, 17], while the Bethe ansatz method is usually employed in the latter for one-dimensional systems [140]. Both these approaches yield a steady state nonequilibrium

response and nonequilibrium transitions from the Mott insulator state to a metallic state. In addition, an important observation was made in Ref. [17] that weak dissipation does not completely suppress quantum coherent oscillations - the numerically calculated single particle spectral function shows "Bloch islands" at beating frequencies involving the noninteracting Bloch oscillations and the Coulomb interaction strength. These features get suppressed as dissipation is increased. Despite these advances in the numerical studies of the microscopic model, many important issues have not yet been addressed; for instance, it is not known how the transient Bloch oscillations decay in time eventually establishing a DC current state, and how they get suppressed in the presence of dissipation. Phenomenological models such as the $\mathscr{P}\mathscr{T}$ symmetric Hubbard models are analytically tractable and give valuable insights such as the critical behavior near the nonequilibrium Mott insulator to metal transition; however relating the model parameters directly to experimentally relevant quantities has proved to be a challenge. Moreover, these models are designed to study the nonequilibrium steady state but not the transient response.

In band insulators, the linear response conductivity vanishes at zero temperature but electronic transport at finite electric fields is possible through the generation of low-energy particle-hole pairs by the Landau-Zener-Schwinger (LZS) mechanism [91, 148, 128], with the probability P of this process related to the electric field measured in terms of the potential energy drop, D, across a link, and the band-gap Δ as $P \sim \exp[-\Delta^2/cD]$, where c is a constant with the dimension of energy. For the fermionic Hubbard chain subjected to an electric field, a similar expression has been proposed in Ref. [108], with band-gap Δ being replaced by the Mott gap. Turning on a finite dissipation (coupling to a fermionic bath) under such nonequilibrium conditions, DMFT calculations of Ref. [17] show that the Hubbard bands leak into the Mott gap, and beyond some value of the dissipation strength, a quasiparticle feature, signaling a bad metallic phase appears, in the spectral function. The crucial question here is whether and under what circumstances this dielectric breakdown becomes a true nonequilibrium phase transition. Analysis of the phenomenological $\mathscr{P}\mathscr{T}$ symmetric fermionic Hubbard chain [140] suggests that this is a true nonequilibrium quantum phase transition and is associated with breaking of $\mathscr{P}\mathscr{T}$ symmetry in the metallic phase.

In this paper we develop an effective Keldysh field theory of a dissipative one-dimensional Mott insulator subjected to a uniform electric field and study it analytically to address the broad questions outlined above. Our microscopic model consists of a one-dimensional array of mesoscopic metallic quantum dots – each of these quantum dots contains a large number of electrons occupying the dot energy levels. The large number of degrees of freedom (DoF) in each mesoscopic dot effectively constitute a fermionic bath and provide a source of dissipation through the Landau damping mechanism. In addition, as we discuss

below, the large DoF acts as a large-$\mathscr{N}$ parameter (see also [147]) and facilitates a tractable analytic treatment of our model. The analytic tractability that our large-$\mathscr{N}$ formulation provides is analogous to that of large dimensionality in the DMFT approach to the Hubbard model. Under equilibrium conditions, the model is described by the following Hubbard-like Hamiltonian with multiple flavors (representing dot energy levels) of electrons at each site (we set electron charge $e = 1$, lattice spacing $a = 1$, $\hbar = 1$, $k_B = 1$):

$$\hat{H} = \hat{H}^0 + \hat{H}^C + \hat{H}^T, \text{ where} \tag{5.1}$$

$$\hat{H}^0 = \sum_{k,\alpha} \xi_\alpha c^\dagger_{j,\alpha} c_{j,\alpha}, \tag{5.2}$$

$$\hat{H}^C = \sum_k E_C \left[\left(\sum_\alpha c^\dagger_{k,\alpha} c_{k,\alpha} \right) - N_0 \right]^2, \tag{5.3}$$

$$\hat{H}^T = \sum_k \sum_{\alpha,\beta} \left(\tilde{t}^{k,k+1}_{\alpha\beta} c^\dagger_{k,\alpha} c_{k+1,\beta} + \text{h.c.} \right). \tag{5.4}$$

Here k labels the site index, α represents the different energy levels (E_α) within a dot, $\xi_\alpha = E_\alpha - \mu$ (μ being the Fermi level in the dot), $\tilde{t}^{k,k+1}_{\alpha\beta}$ is the inter-dot tunneling matrix element connecting levels α and β on dots labeled k and $k+1$ respectively, E_C is the Coulomb energy of single-electron charging, and N_0 is the equilibrium charge on a dot. The tunneling between the dots could be through an insulating barrier (as is the case in granular metals) or through ballistic point contacts (as may be the case in artificial quantum dot arrays). The Fermi energy in each dot is assumed to be the largest energy scale. In addition, we also have a small energy scale, δ, which is the mean level spacing in the dot and is approximately related to the volume of the dot, V, and the density of states at the Fermi level, $\nu(\mu)$ through $\delta \approx 1/(\nu(\mu)V)$. Elementary excitations in each isolated dot are of the low-energy particle-hole kind, which in the limit of large dot size, tend to become gapless. Interestingly, other models such as the Sachdev-Ye-Kitaev (SYK) [122, 86] model on a one-dimensional lattice [75, 41] interaction share a similar structure, and are also characterized by gapless excitations locally.

We study the model in Eq. (5.1) in the Mott insulator regime where $E_C \gg \delta, T$ and $g \lesssim 1$, where T is the temperature, and g is the dimensionless inter-dot tunneling conductance. For granular metals, the intergrain tunneling conductance is of the form $g \approx \pi^2 |\tilde{t}_{\alpha,\beta}|^2 (V\nu(\mu))^2 = \pi^2 |\tilde{t}_{\alpha,\beta}|^2/\delta^2$. For ballistic point contacts separating the quantum dots, the transverse (waveguide) momentum $\mathbf{k}_\perp$ is conserved during tunneling (i.e. $\tilde{t}_{\alpha,\beta} \equiv \tilde{t}_{\mathbf{k}_\perp}$) but the longitudinal momentum $k_\parallel$ is not, and g has the form, $g \approx \pi^2 \sum_{\mathbf{k}_\perp} |\tilde{t}_{\mathbf{k}_\perp}|^2 (\nu^{1D} L)^2$, where ν^{1D} is the one-dimensional density of states associated with the different sub-bands labeled by $\mathbf{k}_\perp$ and L is the dot size. In this Mott insulator regime, a conventional perturbation

expansion in the interaction is not possible. We therefore adopt a bosonization scheme well known in the literature as the Ambegaokar-Eckern-Schön (AES) [11, 23] model of granular metals - a class of Mott insulators. The AES model is, in effect, a rotor model with the difference that now the phases at each site in the AES model are dual to the total charge in the dot at that site. The AES model consists of a charging part that represents Coulomb blockade effects, and a dissipative tunneling part that describes inter-dot hopping of electrons. Unlike other dissipative models such as Caldeira-Leggett [32], the tunneling part of the AES model is periodic in the phase fields reflecting charge quantization. The large number of degrees of freedom on each dot makes the model analytically tractable, allowing one to discard terms in the effective action that are higher order than two in the inter-dot tunneling conductance. The model is tailor-made for studying transport, and consequently, information about the internal low-energy excitations at a site appears only at the level of the tunneling term.

In equilibrium or linear response situations, the AES model appears in diverse contexts including unusual transport phenomena in granular Mott insulators such as cotunneling dominated variable-range hopping [139, 23] and breakdown of the Wiedemann-Franz law by emergent bosonic modes [141] and the Kondo effect in quantum critical metals [129, 96]. A bosonic channel for thermal transport analogous to that in the AES model [141] has recently been reported for the SYK model [41]. It is also well-known that even in the regime of metal-like conduction ($g \gg 1$, $T \gg g\delta$), the low-energy excitations of the AES model are not quasiparticle-like, i.e., are not characterized by their momenta and spin, a property shared with the SYK model [41].

We generalize the AES model to the nonequilibrium case using the Keldysh formalism. For the case of a single mesoscopic quantum dot connected to noninteracting leads, a similar Keldysh generalization has been studied in the literature (see e.g. [3]). The granular chain, as we shall see, has significantly different physics from the single dot problem arising from the periodicity of the lattice and also the relevance of long-range tunneling processes since potential energy gain from cotunneling over multiple dots can offset the Coulomb blockade effects. In the equilibrium (Matsubara) treatment of the AES model, in order to properly treat charge quantization effects, essential in Coulomb blockade, finite winding numbers of the phase fields must be taken into account. In the real time Keldysh case, this is achieved by going to a mixed phase-charge representation (instead of a pure phase-only representation) and restricting the path integral over the classical component of the charge field to integer values.

We calculate the current response of our Keldysh AES model for the granular Mott insulator subjected to a uniform electric field at temperatures much smaller than D and E_C, and we further assume the mesoscopic dots are sufficiently large so that the temperature greatly

exceeds the mean level spacing δ. After the electric field is switched on, the leading order (in g) current response shows an oscillatory transient response whose primary components are the two beat frequencies, $\omega_\pm = |D \pm 2E_c|$:

$$J_{\rm tr} \approx -\frac{4g\Theta(\tau)}{(2\pi)^2 E_C}\frac{1}{\tau^2}\left[\frac{\omega_-}{\omega_+}\sin(\omega_+\tau)+\frac{\omega_+}{\omega_-}\sin(\omega_-\tau)\right]. \tag{5.5}$$

These oscillations arise, as we shall show in the paper, from a combination of the periodicity of the lattice, Coulomb correlations, and charge quantization. These beat frequencies have also been observed [17] in DMFT calculations of the dissipative Hubbard model in the form of "island" features in the spectral function, and in the dissipationless Bose-Hubbard model [30]. In the absence of correlations ($E_C = 0$), these oscillations would correspond to the Bloch oscillation frequency $\omega_B = |D|$. The amplitude of these oscillations decays in accordance with an inverse square law. Remarkably, the dissipation, which is responsible for the decay of the amplitude of these oscillations, is nevertheless unable to suppress the coherent quantum effects in a finite time scale. Apart from these oscillations, the current also has a finite DC component for $|D| > 2E_C$,

$$J_{\rm dc} = \frac{g\Theta(\tau)}{\pi}\left[(D-2E_C)\Theta(D-2E_C)+(D+2E_C)\Theta(-2E_C-D)\right], \tag{5.6}$$

and is a direct consequence of the presence of dissipation.

Next, to understand the nature of the DC response at small fields, $|D| < 2E_C$, we consider the long time limit of the current response. For this purpose, we take into account higher order cotunneling processes over multiple dots such that the Coulomb blockade is offset by the extra potential energy gain. We provide analytic expressions for the field dependence of current up to $O(g^2)$. The analysis of higher order terms at arbitrary field strengths rapidly becomes very complicated; however we infer some general features. In the zero temperature limit, there is a hierarchy of thresholds, $D_{\rm th}^{(n)} = 2E_C/n$, with the $n^{\rm th}$ order current corresponding to the matching of the Coulomb scale with the electrostatic potential energy gain from cotunneling over n successive dots. The leading order in g contributions to the current near these thresholds has the form

$$j^{(n)}(D) \sim nDg^n(1-2E_C/nD)^{2n-1}\Theta(nD-2E_C), \tag{5.7}$$

where Θ is the Heaviside step function. Based on this expression, we show that at low fields and small g, the field dependence of the current has the LZS form, $j(D) \sim D[g/\ln^2(1/g)]^{2E_C/D}$, but with qualitative differences from the LZS particle-hole pair production probability

$P \sim e^{-E_C^2/cD}$ for the non-dissipative Hubbard chain at half filling [109] deep in the Mott insulator phaes.

An important question relates to the nature of the transition from the Mott insulating state to a conducting state as a function of the field. In the dissipation free case, it is evident from the expression for the LZS pair production probability that it is a crossover, howsoever sharp, and not a true phase transition. A true phase transition to a metallic state is indicated if the perturbation expansion for the current made from within the Mott insulator phase diverges as a function of $g(\lesssim 1)$ or $D(< 2E_C)$. If the form of the current is assumed to have the form shown in Eq. (5.7) for a finite but small field strength away from the thresholds, then the criterion for divergence of the perturbation expansion for the current is

$$g = g_0 \left[1 - \frac{D}{2E_C}\right]^2, \quad D \ll 2E_C, \tag{5.8}$$

with g_0 a constant of order unity. However, as we have already mentioned above, the field dependence of high-n^{th} order terms is complicated for fields away from the respective thresholds $D^{(n)} = 2E_C/n$, and it is not currently clear to us how the above criterion would change.

The rest of the paper is organized as follows. In Sec. 5.2, beginning with the microscopic model of Eq. (5.1), we outline the derivation of our effective Keldysh-AES action. The electric field is introduced through a time-dependent vector potential. We also present the functional representation of the charge current in terms of the correlation functions of the phase fields. In Sec. 5.3, we analyze the leading order contribution to the current from the time the electric field is turned on. We show that there are Bloch-like oscillations whose amplitudes decay as a power-law in time. Further, the existence of a finite DC response at long times is also established. Sec. 5.4 is devoted to the analysis of the long-time DC behavior for small field strengths. For this purpose, the higher order cotunneling processes over multiple dots are considered in a perturbative expansion in small g, around the "atomic limit" of isolated dots. We discuss the LZS form of the current response at small fields, and the possible nonequilibrium phase transition to a metallic state. Finally, in Sec. 5.5 we conclude with a discussion of our results and open questions.

5.2 Keldysh-AES action

In this Section, we obtain the effective Keldysh-AES action from the microscopic Hamiltonian introduced in Eq. (5.1) and also provide functional representation of the charge current

that will be used throughout. Our derivation of the effective Keldysh-AES action parallels the one in Ref. [3] for the case of a single quantum dot connected to noninteracting leads.

The first step consists of Hubbard-Stratonovich decoupling of the part of the action corresponding to Eq. (5.1) that contains the Coulomb interaction term:

$$\begin{aligned} e^{-i\int_t H_C} &= \exp\left[-\imath\sum_k\int_t E_C\left(\sum_\alpha \bar\psi_{k,\alpha}\psi_{k,\alpha}-N_0\right)\left(\sum_\alpha \bar\psi_{k,\alpha}\psi_{k,\alpha}-N_0\right)\right] \\ &\propto \int DV\exp\left[\imath\sum_k\int_t\frac{1}{4E_C}\left(V-2E_C\left(\sum_\alpha \bar\psi_{k,\alpha}\psi_{k,\alpha}-N_0\right)\right)^2\right]e^{-i\int_t H_C} \end{aligned} \quad (5.9)$$

To study nonequilibrium transport, we put our action on the Keldysh contour and we label the fields with superscripts $+$ and $-$ corresponding respectively to the forward and backward time parts of the Keldysh contour. For incorporating the initial condition information (i.e. the initial density matrix) it is customary to work with a rotated classical-quantum basis in the Keldysh space:

$$V^c = \frac{1}{2}(V^+ + V^-)\,,\, V_q = V^+ - V^-, \quad (5.10)$$

$$\psi^c = \frac{1}{\sqrt{2}}(\psi^+ + \psi^-)\,,\, \psi^q = \frac{1}{\sqrt{2}}(\psi^+ - \psi^-), \quad (5.11)$$

$$\bar\psi^c = \frac{1}{\sqrt{2}}(\bar\psi^+ - \bar\psi^-)\,,\, \bar\psi^q = \frac{1}{\sqrt{2}}(\bar\psi^+ + \bar\psi^-), \quad (5.12)$$

$$\Psi = \begin{pmatrix}\psi^c\\ \psi^q\end{pmatrix}\,,\, \bar\Psi = \begin{pmatrix}\bar\psi^c & \bar\psi^q\end{pmatrix}. \quad (5.13)$$

We call the superscripts c and q the "classical" and "quantum" components respectively. The action S now assumes the form,

$$\begin{aligned} &S = S^0 + S^C + S^T\,, \text{ where} \\ &S^0 = \sum_{k,\alpha}\int_t \bar\Psi_{k,\alpha}\begin{bmatrix}\imath\partial_t + \imath\eta + \mu - E_\alpha - V_k^c & -\frac{V_k^q}{2} + 2\imath\eta F_k \\ -\frac{V_k^q}{2} & \imath\partial_t - \imath\eta + \mu - E_\alpha - V_k^c\end{bmatrix}\Psi_{k,\alpha}, \\ &S^C = \sum_k\int_t\left(\frac{1}{2E_c}V_k^cV_k^q + N_0V_k^q\right), \\ &S^T = \sum_{k,\alpha,\beta}\int_t\bar\Psi_{k\alpha}\begin{bmatrix}\tilde t_{\alpha,\beta}^{k,k+1} & 0\\ 0 & \tilde t_{\alpha,\beta}^{k,k+1}\end{bmatrix}\Psi_{k+1,\beta} + \text{c.c.} \end{aligned} \quad (5.14)$$

Here F_k is related to the distribution function for *noninteracting* electrons in the k^{th} dot and is, in general, a function of two time arguments, i.e., $F_k(t,t')$. For the case of thermal equilibrium, F_k depends only on the difference $t-t'$, and in frequency space, it has the form $F(\omega) \equiv 1-2f(\omega) = \tanh(\omega/2T)$, where $f(\omega)$ is the Fermi-Dirac distribution function and T is the temperature. The infinitesimally small positive constant, η, ensures the theory has the proper causal structure. At this stage, it would seem natural to integrate out the noninteracting fermions, and expand the resulting determinant to obtain an effective field theory for the Hubbard-Stratonovich fields. However, the Hubbard-Stratonovich fields effectively shift the entire band of electrons and, in fact, the shifts are large ($\sim E_C$) whenever tunneling events occur. We therefore perform a gauge transformation to eliminate the fluctuating Hubbard Stratanovich fields that appear in S^0

$$\Psi_{k,\alpha} \;\rightarrow\; e^{-\imath\hat{\phi}_k}\Psi_{k,\alpha}\,,\, \bar{\Psi}_{k,\alpha} \rightarrow \bar{\Psi}_{k,\alpha}e^{\imath\hat{\phi}_k}, \tag{5.15}$$

where

$$\hat{\phi}_k = \phi_k^c + \phi_k^q\frac{\sigma_1}{2}, \tag{5.16}$$

and the phase fields $\hat{\phi}_k$ are chosen such that their classical and quantum components obey

$$\partial_t\phi_k^{c,q} = V_k^{c,q}. \tag{5.17}$$

After the above gauge transformation, we have,

$$S^0 = \sum_{k,\alpha}\int_t \bar{\Psi}_{k,\alpha}\begin{bmatrix}\imath\partial_t+\imath\eta+\mu-E_\alpha & 2\imath\eta F_k \\ 0 & \imath\partial_t-\imath\eta+\mu-E_\alpha\end{bmatrix}\Psi_{k,\alpha}. \tag{5.18}$$

$$S^C = \sum_k\int_t\left(\frac{1}{2E_c}\partial_t\phi_k^c\partial_t\phi_k^q + N_0\partial_t\phi_k^q\right), \tag{5.19}$$

$$S^T = \sum_{k,\alpha,\beta}\int_t\left(\tilde{t}_{\alpha,\beta}^{k,k+1}\bar{\Psi}_{k\alpha}\exp(-\imath\hat{\phi}_{k,1})\Psi_{k+1,\beta}+\text{c.c.}\right)\,,\,\hat{\phi}_{k,1}=\hat{\phi}_{k+1}-\hat{\phi}_k, \tag{5.20}$$

The term in Eq. (5.19) proportional to N_0 is a Berry phase term. Our next step is to integrate out the fermions to obtain an effective action in terms of the phase fields. We denote the fermion-bilinear part of the action as $S_F = S^0+S^T = \hat{\bar{\Psi}}\hat{G}^{-1}\hat{\Psi}$, with

$$\hat{G}^{-1} = \hat{G}_0^{-1}+\hat{T}, \tag{5.21}$$

where

$$(\hat{G}_0)^{-1}_{k,\alpha;k,\alpha} = \begin{bmatrix} (g^R_{k,\alpha})^{-1} & 2\imath\eta F_k \\ 0 & (g^A_{k,\alpha})^{-1} \end{bmatrix}, \tag{5.22}$$

$$\hat{T}_{k,\alpha;k+1,\beta} = \tilde{t}^{k,k+1}_{\alpha,\beta} \exp(-\imath\hat{\phi}_{k,1}). \tag{5.23}$$

In Eq. (5.22), the diagonal elements are the usual inverse retarded and advanced Green functions,

$$(g^{R,A}_{k,\alpha})^{-1} = \imath\partial_t \pm \imath\delta + \varepsilon_F - E_\alpha. \tag{5.24}$$

The inter-dot hopping matrix $\hat{T}$ is diagonal in Keldysh space as well as in the time indices. Integrating out the fermions gives us $Z = \int D\phi \exp(\imath S^C[\phi] + \mathrm{tr}\ln(\imath\hat{G}^{-1}))$, and we use Eq. (5.21) to re-express the fermionic determinant as

$$\ln(\hat{G}^{-1}) = \ln(1 + \hat{G}_0\hat{T}) + \ln(\hat{G}_0^{-1}). \tag{5.25}$$

To obtain the effective action in terms of the phase fields, we discard the ϕ-independent $\ln(\hat{G}_0^{-1})$ make a Taylor expansion of $\ln(1+\hat{G}_0\hat{T})$. The first order term vanishes since $\mathrm{tr}(\hat{G}_0\hat{T}) = 0$ as $\hat{G}_0$ is diagonal in k and $T_{k;k} = 0$. Then, up to second order in $\hat{T}$ we have

$$Z = \int D\phi \exp(\imath S^C[\phi] + \imath S^{\mathrm{tun}}[\phi]) \ , \ S^{\mathrm{tun}}[\phi] = \frac{\imath}{2}\mathrm{tr}\left(\hat{G}_0\hat{T}\hat{G}_0\hat{T}\right). \tag{5.26}$$

Here $\hat{G}_0$ has the following structure in Keldysh space:

$$(\hat{G}_0)_{k,\alpha;k,\alpha}(t,t') = \begin{bmatrix} g^R_{k,\alpha} & F_k(g^R_{k,\alpha} - g^A_{k,\alpha}) \\ 0 & g^A_{k,\alpha} \end{bmatrix}(t,t'), \tag{5.27}$$

where

$$g^{R,A}_{k\alpha}(t,t') = \frac{1}{2\pi}\int_\omega g^{R,A}_{k,\alpha}(\omega)\exp(-\imath\omega(t-t')) = \int_\omega \frac{\exp(-\imath\omega(t-t'))}{\omega \pm \imath\delta + \mu - E_\alpha}. \tag{5.28}$$

We assume that the matrix elements of $\hat{T}$ are independent of the energy indices and also replace summation over the discrete states by corresponding integrals, $\sum_\alpha \leftrightarrow V\int_\varepsilon d\varepsilon\, \nu(\varepsilon)$, with $\nu(\varepsilon) = \frac{1}{V}\sum_\alpha \delta(\varepsilon - E_\alpha)$ the density of states in a dot. The summations over the energy indices gives quantities of the form $\sum_\alpha g^{R,A}_{k,\alpha}(\omega) = V\int_\varepsilon \nu(\varepsilon) g^{R,A}_{k,\alpha}(\omega) \approx \mp(\pi\imath)V\nu(\omega+\mu) \approx$

$\mp(\pi\imath)V\nu(\mu)$. With these approximations, we arrive at

$$\mathrm{tr}(\hat{G}_0\hat{T}\hat{G}_0\hat{T}) \approx -2\pi^2|\tilde{t}|^2(V\nu(\mu))^2\int_{t,t'}\sum_k \mathrm{tr}\Big[\Lambda_k(t-t')\exp(-\imath\hat{\phi}_{k,1}(t'))\Lambda_{k+1}(t'-t)\exp(\imath\hat{\phi}_{k,1}(t))\Big], \tag{5.29}$$

where

$$\Lambda_k(\omega) = (2\imath)\begin{bmatrix} G^R(\omega) & F_k(\omega)[G^R-G^A] \\ 0 & G^A(\omega)\end{bmatrix}, G^{R,A}(\omega) = \frac{1}{2\pi}\int_\varepsilon g^{R,A}_{k,\varepsilon}(\omega). \tag{5.30}$$

Thus,

$$S_{\mathrm{tun}} \approx -\imath g\int_{t,t'}\sum_k \mathrm{tr}\Big[\Lambda_k(t-t')\exp(-\imath\hat{\phi}_{k,1}(t'))\Lambda_{k+1}(t'-t)\exp(\imath\hat{\phi}_{k,1}(t))\Big]. \tag{5.31}$$

For a granular metal, we assume that the tunneling matrix connects any pair of levels in the neighboring grains with characteristic magnitude $|\tilde{t}|$, in which case, $g = \pi^2(V\nu(\mu))^2|\tilde{t}|^2 \sim |\tilde{t}|^2(\mathscr{N}/\mu)^2$. Here g is the dimensionless inter-dot tunneling conductance and $\mathscr{N}$ the total number of electrons in a dot. To give an estimate of the largeness of $\mathscr{N}$, for a 10nm metallic dot with conduction electron density of $\sim 10^{28}\mathrm{m}^{-3}$, we have $\mathscr{N}\sim 10^4$. Our regime of interest is $g \lesssim 1$, independent of the number of electrons in the dot. Thus for the granular metal we require the tunneling amplitudes to scale as $|\tilde{t}| \sim 1/\mathscr{N}$. Physically, this means that as the number of transmission channels increases, the individual tunneling amplitudes should scale inversely so as to keep g unchanged.

For the case of ballistic point contacts, we label the energy levels by transverse and longitudinal momenta, $\mathbf{k}_\perp$ and $k_\parallel$ respectively. The transverse momentum is conserved during tunneling but the longitudinal momentum is not. The tunneling matrix element thus connects any pair of longitudinal momenta, and we assume they all have a characteristic magnitude $|\tilde{t}|$. In this case, the dimensionless conductance $g = \pi^2\sum_{\mathbf{k}_\perp}|\tilde{t}|^2(\nu^{1D}L)^2 \sim |\tilde{t}|^2 N_{\mathrm{ch}}(\mathscr{N}_{1D}/\mu)^2$, where N_{ch} is the total number of transverse channels and $\mathscr{N}_{1D}$ is the typical number of electrons having the same transverse momentum. To keep $g \lesssim 1$, we require the tunneling amplitude to scale as $|\tilde{t}| \sim 1/(\sqrt{N_{\mathrm{ch}}}\mathscr{N}_{1D})$, and we show below that the large-$\mathscr{N}$ parameter in this case is $\mathscr{N} = N_{\mathrm{ch}}$.

We will present below a large-$\mathscr{N}$ justification for dropping higher order terms in the tunneling action.

5.2.1 Consequences of large-$\mathcal{N}$

Let us now discuss a couple of crucial consequences of having a large number of electrons in each dot. Consider first the $O(\tilde{t}^4)$ term in the tunneling action for the granular metal. The basic argument for disregarding such contributions has been presented in Ref [23] . Here we show that this is essentially a large-$\mathcal{N}$ argument. The fourth order tunneling terms are of the form $\mathrm{tr}(\hat{G}_0\hat{T}\hat{G}_0\hat{T}\hat{G}_0\hat{T}\hat{G}_0\hat{T})$. These processes involves two or three dots. Consider for example the three dot term (with consecutive dots labeled i,j,k),

$$\mathrm{tr}(\hat{G}_0\hat{T}\hat{G}_0\hat{T}\hat{G}_0\hat{T}\hat{G}_0\hat{T}) = \sum_{\substack{ijk \\ \alpha_{1,\ldots,}\alpha_4}} (\hat{G}_0)_{i,\alpha_1}\hat{T}^{ij}_{\alpha_1\alpha_2}(\hat{G}_0)_{j,\alpha_2}\hat{T}^{jk}_{\alpha_2\alpha_3}(\hat{G}_0)_{k,\alpha_3}\hat{T}^{kj}_{\alpha_3\alpha_4}(\hat{G}_0)_{j,\alpha_4}\hat{T}^{ji}_{\alpha_4\alpha_1}.$$

Now the tunneling amplitudes $\tilde{t}$ are of the form $\tilde{t}^{ij}_{\alpha\beta} = |\tilde{t}|e^{i\chi^{ij}_{\alpha\beta}}$, where $\chi^{ij}_{\alpha\beta}$ is a phase associated with the link ij and energy levels α,β. The key point is that for irregular dots, the phases $\chi^{ij}_{\alpha\beta}$ are random. For the case of a large number of levels, the random phases cause the vanishing of all terms except for the case $\alpha_4 = \alpha_2$ where the random phases cancel exactly. Thus there are only three independent energy indices to be summed over resulting in a factor of $\mathcal{N}^3$. However since the $\tilde{t}$ scale as $1/\mathcal{N}$, it is evident that the overall scaling of this term is $1/\mathcal{N}$. In general, the number of independent energy indices in the perturbative expansion of the tunneling action equals the number of dots involved in that term.

We now discuss the case of ballistic point contacts. The fourth order three-dot term can be written as

$$\mathrm{tr}(\hat{G}_0\hat{T}\hat{G}_0\hat{T}\hat{G}_0\hat{T}\hat{G}_0\hat{T}) = \sum_{\substack{ijl,\mathbf{k}_\perp \\ k_{1,\ldots,}k_4}} (\hat{G}_0)_{i,k_1}\hat{T}^{ij}_{k_1k_2}(\hat{G}_0)_{j,k_2}\hat{T}^{jl}_{k_2k_3}(\hat{G}_0)_{l,k_3}\hat{T}^{lj}_{k_3k_4}(\hat{G}_0)_{j,k_4}\hat{T}^{ji}_{k_4k_1},$$

where $k_1,\ldots,k_4$ are longitudinal momenta and we have suppressed the transverse momentum label $\mathbf{k}_\perp$ for brevity. Since the tunneling elements scale as $|\tilde{t}| \sim 1/(\sqrt{N_{\mathrm{ch}}}\mathcal{N}_{1D})$, each term in the above sum scales as $1/(N^2_{\mathrm{ch}}\mathcal{N}^4_{1D})$. Now the sum over the four longitudinal momenta brings a factor of $\mathcal{N}^4_{1D}$, and the sum over the transverse momentum gives a factor N_{ch}. Thus we find that the above fourth order contribution scales as $1/N_{\mathrm{ch}}$. In order to be able to neglect this fourth order term, we require $N_{\mathrm{ch}} \gg 1$,i.e., the width of the point contact should be much larger than the Fermi wavelength.

There is a second very important consequence of large-$\mathcal{N}$ that provides a crucial simplification in nonequilibrium situations and which has not been appreciated in the literature. This relates to the temporal variation of the F_k under general nonequilibrium conditions. It is convenient to work with the Wigner representation, $F_k(t,t') \equiv \int (d\varepsilon)F_k(\varepsilon,\tau)e^{-i\varepsilon(t-t')}$, where

$\tau = (t+t')/2$, and the relation with the time-dependent distribution function is $F_k(\varepsilon,t) = 1-2f_k(\varepsilon,t)$. The total number of electrons in the k^{th} dot is $N_0 + n_k^c(t) = \int d\varepsilon\, \nu(\varepsilon) f(\varepsilon,t)$, where $n_k^c(t)$ is the classical component of the number field conjugate to the quantum component of the phase, ϕ_k^q. In the rest of the paper, we will be specifically interested in the case of constant N_0. More general, time-dependent N_0 can if a time-dependent gate voltage is applied to the quantum dots. Thus in our case we have

$$\frac{dn_k^c}{dt} = V \int d\varepsilon\, \nu(\varepsilon) \frac{df_k(\varepsilon,t)}{dt}. \tag{5.32}$$

The RHS of Eq. (5.32) is, by using the continuity equation, simply the net current into the dot, and is given by the functional derivative $\langle \delta S/\delta \phi_k^q(t)\rangle_\phi$, which has the form $g\int d\varepsilon\, h(\varepsilon,t) \equiv j_{k-1,k}(t) - j_{k,k+1}(t)$. Consequently, the continuity equation leads us to a kinetic equation for the distribution $f_k(\varepsilon,t)$ of the form $V\nu(\mu) df_k/dt + gh(\varepsilon,t) = 0$. The quantity h is a functional of the distributions $\{f_k\}$ and also depends on the tunneling conductance and electric field. Recognizing $V\nu(\mu) = 1/\delta$, we find that the distribution function evolves with a large characteristic time scale that is proportional to $1/g\delta$ and increases linearly with the total number of electrons in the grain ($\delta \sim 1/\mathcal{N}$). We now assume that the grains are coupled to an external thermal bath, whose effect we model by an additional relaxation term in the kinetic equation, i.e.,

$$\frac{df_k}{dt} = -g\delta h[f] + \frac{f_k - f_k^{\text{eq}}}{\tau_{eb}}, \tag{5.33}$$

where f_k^{eq} is the equilibrium Fermi-Dirac distribution function and τ_{eb} is the electron-bath relaxation time. If $1/\tau_{eb} \gg g\delta$, then the distribution functions f_k may be approximated by their equilibrium values. We will now proceed with this, and hence $F_k(\varepsilon) = \tanh(\varepsilon/2T)$. In contrast, in the usual Hubbard models, the electron distribution function at every site is a time dependent quantity under general nonequilibrium conditions since in that case there is no large-$\mathcal{N}$ mitigating factor.

5.2.2 Keldysh-AES action

We resume our derivation of the effective Keldysh AES action. Henceforth we will describe tunneling in both the granular metal as well as the point contact cases by the action in Eq. (5.31) and note that g can have different forms for the two cases. Now let us manipulate S_{tun}

to a more dealable form. We introduce new fields C and S defined as

$$C = \exp(\imath\phi^c)\cos\left(\frac{\phi_q}{2}\right) \quad , \quad S = \exp(\imath\phi^c)\sin\left(\frac{\phi_q}{2}\right). \tag{5.34}$$

These are related to the $\hat{\phi}$ fields in Eq. (5.16) through

$$\exp(\imath\hat{\phi}) = C + \imath S\sigma_1 \quad , \quad \exp(-\imath\hat{\phi}) = \bar{C} - \imath\bar{S}\sigma_1. \tag{5.35}$$

The tunneling action under equilibrium conditions then takes the form

$$S_{\rm tun} = 4g\sum_k \int_{t,t'} \begin{bmatrix}\bar{C}_{k,1} & -\imath\bar{S}_{k,1}\end{bmatrix}_t \begin{bmatrix}0 & \Sigma^A_{k,1}\\ \Sigma^R_{k,1} & \Sigma^K_{k,1}\end{bmatrix}_{t-t'} \begin{bmatrix}C_{k,1}\\ \imath S_{k,1}\end{bmatrix}_{t'}, \tag{5.36}$$

where

$$\Sigma^{R(A)}_{k,1}(t) = \imath\left(G^{R(A)}(t)G^K_k(-t) + G^K_{k+1}(t)G^{A(R)}(-t)\right), \tag{5.37}$$

$$\Sigma^K_{k,1}(t) = \imath\left(G^K_k(-t)G^K_{k+1}(t) - (G^R - G^A)_t(G^R - G^A)_{-t}\right), \tag{5.38}$$

with $G^K_k = F_k(G^R - G^A)$. It is evident from Eq. (5.37) that $\Sigma^{R(A)}$ also have a causal structure, i.e., $\Sigma^R(t) \propto \Theta(t)$ etc. Under general nonequilibrium conditions, the quantities $\Sigma^{R,A,K}(t,t')$ describing particle-hole excitations in the dots depend on both the time arguments, and not just their difference.

Let $F_b(\varepsilon) = \coth(\varepsilon/2T) = 1 + 2f_b$, where f_b is the equilibrium Bose distribution function. We make use of the following identities,

$$\left(G^R - G^A\right)_\varepsilon = -\imath, \tag{5.39}$$

$$\int_\varepsilon \frac{1}{2\pi}\left(F(\varepsilon+\omega) - F(\varepsilon)\right) = \frac{\omega}{\pi}, \tag{5.40}$$

$$\int_\varepsilon \frac{1}{2\pi}\left(1 - F(\varepsilon-\omega)F(\varepsilon)\right) = \frac{\omega}{\pi}F_b(\omega). \tag{5.41}$$

to obtain,

$$\left(\Sigma^R_{k,1} - \Sigma^A_{k,1}\right)_\omega = \imath\int_\varepsilon \frac{1}{2\pi}\left(F_{k+1}(\varepsilon) - F_k(\varepsilon-\omega)\right) = \frac{\imath}{\pi}\omega, \tag{5.42}$$

$$(\Sigma^K_{k,1})_\omega = \imath\int_\varepsilon \frac{1}{2\pi}\left(1 - F_{k+1}(\varepsilon)F_k(\varepsilon-\omega)\right) = \frac{\imath}{\pi}\omega F_b(\omega). \tag{5.43}$$

We will later find it convenient to work in the $\pm$ Keldysh contour. Hence we re-express our phase action in this contour. We ignore N_0 by assuming that it can be set to zero by some gate voltage. We have,

$$S_C[n,\phi] = E_C \sum_k \int_t [(\partial_t \phi_k^+)^2 - (\partial_t \phi_k^-)^2], \tag{5.44}$$

$$S_{\rm tun}[\phi] = g \sum_k \int_{t,t'} \left(\exp(-\imath \phi_{k,1}^+) \quad \exp(-\imath \phi_{k,1}^-) \right)_t L_{k,1}(t-t') \begin{pmatrix} \exp(\imath \phi_{k,1}^+) \\ \exp(\imath \phi_{k,1}^-) \end{pmatrix}_{t'}, \tag{5.45}$$

$$L = \frac{1}{4} \begin{pmatrix} \Sigma^R + \Sigma^A + \Sigma^K & \Sigma^R - \Sigma^A - \Sigma^K \\ -\Sigma^R + \Sigma^A - \Sigma^K & -\Sigma^R - \Sigma^A + \Sigma^K \end{pmatrix}. \tag{5.46}$$

Note that the diagonal elements of the matrix L written in the $\pm$ basis contain the combination $\Sigma^R + \Sigma^A$ and the off-diagonal elements contain $\Sigma^R - \Sigma^A$. In the (equilibrium) Matsubara formalism, finite winding numbers of the phase fields must be considered to bring out the charge quantization effects. In our continuous time formalism, the charge quantization effects are brought out by a procedure discussed, for example, in Ref. [3] that we briefly describe below.

5.2.3 Phase windings and charge quantization

We are interested in the small tunneling regime, $g \lesssim 1$. In this regime, the phases in each dot fluctuate strongly and hence we represent the action in terms of the conjugate variables, i.e., the number fields. For this, we first perform a Hubbard-Stratanovich decoupling of the charging term, which leads to the following action in the phase-charge representation:

$$S[n,\phi] = \sum_k \int_t \left([n_k^c + N_0] \partial_t \phi_k^q + n_k^q \partial_t \phi_k^c - 2E_C n_k^c n_k^q \right) + S_{\rm tun}[\phi]. \tag{5.47}$$

To properly understand the quantization of the charge degrees of freedom, we first work in a contour, $t \in [0,P]$. The requirement that $\phi^-(0) = \phi^+(0) + 2\pi W$ (W is an integer) leads us to an unconstrained field, ϕ^c, and,

$$\phi_q(t) = \tilde{\phi}_q(t) + \frac{2\pi W}{P}(t-P), \tag{5.48}$$

with Dirichlet conditions, $\tilde{\phi}^q(0) = \tilde{\phi}^q(P) = 0$. Consider first the situation where tunneling is absent. Using Eq. (5.48) in the first term of Eq. (5.47), we see that the partition function has contributions of the form $\sum_W e^{\imath 2\pi (n^c + N_0) W}$,which vanishes unless $n^c + N_0$ is an integer. Writing $N_0 = [N_0] + n_g$, where $[N_0]$ is the integer part of N_0 and $n_g \in [0,1)$ is the residual

"gate charge" on a dot, the integration over the Hubbard-Stratonovich field n^c is equivalent to a sum over integers, $\sum_{[n^c]-n_g}$, where $[n^c]$ is the integer part of n^c. Making a change of variables, $n^c \to n^c - n_g$, the sum becomes one over integer values of n^c. Now the part of the action containing the time derivative of the classical phase field is a function only of the boundary values of the field. Performing the path integral over the boundary fields gives us the constraint that $n^q = 0$ at the boundaries. Let's now imagine turning on the tunneling at some time. From the structure of the tunneling action, Eq. (5.45), it is clear that n^+ and n^- can change only in integer steps. This quantization condition is independent of the time boundary or the length of the time interval. Translated back in the language of the Keldysh closed-time contour, the condition that the *initial* values of n^c can only take integer values together the fact that boundary values of n^q are zero, one concludes that $n^+(-\infty) = n^-(-\infty) \in Z$, and both change in only in integer steps during tunneling events. In this paper, we are interested in the Mott insulator regime with zero gate charge, i.e., $n_g = 0$ (or integer N_0) and therefore we drop the $N_0 \partial_t \phi^q$ term in the action. The point $n_g = 1/2$ is special due to degeneracy between $n^c = 0, 1$. The gate charge, n_g, can also be made to fluctuate in time by using a time-dependent gate voltage. These different scenarios can also be studied using our formalism and will be taken up elsewhere.

5.2.4 Functional representation of charge current

Here we obtain the functional representation for the charge current in the presence of a constant electric field. The electric field is introduced in the form of a time-dependent vector potential that is turned on at some instant of time, say $t = 0$. In every link, the classical component of the vector potential has the form

$$A^c_{k,1}(t) = \Theta(t) D t, \tag{5.49}$$

where D is the potential energy change across a link as already mentioned in Sec. 5.1. This changes the tunneling part of the action by incorporating the Peierls shifts in the phase differences, $\phi^{c,q}_{k,1}(t) \to \phi^{c,q}_{k,1}(t) + A^{c,q}_{k,1}(t)$. The tunneling part of the action now has the form

$$S_{\text{tun}}[\phi, A^c, A^q] = g \sum_k \int_{t,t'} \begin{bmatrix} (e^+_{k,1}(t))^* & (e^-_{k,1}(t))^* \end{bmatrix} L(t-t') \begin{bmatrix} e^+_{k,1}(t') \\ e^-_{k,1}(t') \end{bmatrix}, \tag{5.50}$$

where, $e^\pm_{k,1}(t) = \exp(\imath \phi^\pm_{k,1}(t) - \imath A^\pm_{k,1}(t))$. The functional representation of the classical component of the charge current in a link, $\hat{J}_{k,1}[A^c(t)]$, is obtained by taking the functional

derivative with respect to $A^q_{k,1}(t)$, and setting this quantum source term to zero:

$$\hat{J}_{k,1}(\tau) = -\imath g \int_t \left[(e^+_\tau)^* L^{++}_{\tau t} e^+_t - (e^+_t)^* L^{++}_{t\tau} e^+_\tau + (e^+_\tau)^* L^{+-}_{\tau t} e^-_t + (e^+_t)^* L^{+-}_{t\tau} e^-_\tau \right.$$
$$\left. -(e^-_\tau)^* L^{-+}_{\tau t} e^+_t - (e^-_t)^* L^{-+}_{t\tau} e^+_\tau - (e^-_\tau)^* L^{--}_{\tau t} e^-_t + (e^-_t)^* L^{--}_{t\tau} e^-_\tau \right]. \quad (5.51)$$

Here we have suppressed the site indices and written the time arguments as subscripts for brevity.

5.3 Transient current response

In this Section, we obtain the current response to leading order (in g) upon turning on the uniform electric field by performing the average of the current functional in Eq. (5.51) over the phase fields. This primarily involves a calculation of the bond correlators defined as

$$\Pi_{\sigma\sigma'}(\tau,\tau') = \left\langle \exp\left[-\imath\phi^\sigma_{j,1}(\tau) + \imath\phi^{\sigma'}_{j,1}(\tau') \right] \right\rangle. \quad (5.52)$$

Here $\langle ... \rangle$ denotes averaging with the full action, $S[n,\phi]$.

We calculate the bond correlators as a perturbation series in the tunneling conductance g, by treating the charging action as the bare action and expanding the tunneling part in the exponential to various orders in g. We denote $\langle ... \rangle_0$ to represent averaging with the bare action. The bare bond correlator, $\Pi^{(0)}_{\sigma\sigma'}$ factorizes into a product of two single site correlators,

$$\Pi^{(0)}_{\sigma\sigma'}(\tau,\tau') = C_{\sigma\sigma'}(\tau,\tau') C_{\sigma'\sigma}(\tau',\tau), \quad (5.53)$$

where

$$C_{\sigma\sigma'}(\tau,\tau') = \left\langle e^{-\imath(\phi^\sigma(\tau) - \phi^{\sigma'}(\tau'))} \right\rangle_0. \quad (5.54)$$

Let us first consider $C_{+-}(\tau-\tau')$. Performing the functional integral over the phase fields $\phi^\pm$ we get the equations,

$$\partial_t n^+ = -\delta(t-\tau)\ ,\ \partial_t n^- = -\delta(t-\tau'). \quad (5.55)$$

The solution depends on the boundary conditions at $t=-\infty$. We assume that in the remote past, the system is in thermal equilibrium, and hence the probability distribution for n^c is $P(n^c) = \exp(-\beta(n^c)^2 E_C)/\sum_{n=-\infty}^{\infty}\exp(-\beta E_C n^2)$. In the zero temperature limit, $P(n^c) = \delta_{n^c,0}$. Furthermore since $n^q(-\infty)=0$, we have $n^+(-\infty) = n^-(-\infty) = 0$. Thus the solution

to Eq. (5.55) is

$$n^{+}(t) = -\Theta(t-\tau)\,,\, n^{-}(t) = -\Theta(t-\tau^{'}). \tag{5.56}$$

Plugging this back, we get,

$$C_{+-}(\tau,\tau^{'}) = \exp(\imath E_C(\tau-\tau^{'})). \tag{5.57}$$

Similarly,

$$C_{-+}(\tau,\tau^{'}) = \exp(-\imath E_C(\tau-\tau^{'})), \tag{5.58}$$

$$C_{\pm\pm}(\tau,\tau^{'}) = \exp(\mp\imath E_C|\tau-\tau^{'}|). \tag{5.59}$$

Using these site correlators in Eq. (5.52) for the bond correlators in Eq. (5.51), and using the causal structure of $\Sigma^{R(A)}$, we obtain the following expression for the leading order nonequilibrium current

$$J(\tau) = \frac{g}{2\pi}\int_{-\infty}^{\tau} \mathrm{d}t \left[e^{\imath D(\tau\Theta(\tau)-t\Theta(t))} \left\{ 2\Sigma^{R}(\tau-t)\cos(2E_C(\tau-t)) \right.\right. \\ \left.\left. -2\imath\Sigma^{R}(\tau-t)\cos(2E_C(\tau-t)) \right\} + \text{c.c.} \right]. \tag{5.60}$$

Since the upper limit of the integral is $t=\tau$ and $\Sigma^{A}(t)$ has a $\Theta(-t)$ structure, we can replace

$$\Sigma^{R}(\tau-t) \to \Sigma^{R}(\tau-t) - \Sigma^{A}(\tau-t), \tag{5.61}$$

and use the relation for the Fourier transform, Eq. (5.42). For $\tau<0$, the average current clearly vanishes. Let us split the integral in Eq. (5.60) into two parts, $J = J_{<} + J_{>}$, where $J_{<}$ involves integration from $t=-\infty$ to 0 and in $J_{>}$, $t=0$ to τ :

$$J_{<}(\tau) = \frac{g e^{\imath D\tau}\Theta(\tau)}{(2\pi)^2}\int_{-\infty}^{\infty}\mathrm{d}\omega\int_{-\infty}^{0}\mathrm{d}t \left[e^{\imath(2E_C-\omega)(\tau-t)}(\omega-|\omega|) \right. \\ \left. + e^{-\imath(2E_C+\omega)(\tau-t)}(\omega+|\omega|) + \text{c.c.} \right],$$

$$J_{>}(\tau) = \frac{g\Theta(\tau)}{(2\pi)^2}\int_{-\infty}^{\infty}\mathrm{d}\omega\int_{0}^{\tau}\mathrm{d}t \left[e^{\imath(2E_C-\omega+D)(\tau-t)}(\omega-|\omega|) \right. \\ \left. + e^{-\imath(2E_C+\omega-D)(\tau-t)}(\omega+|\omega|) + \text{c.c.} \right]. \tag{5.62}$$

After performing the time integration and some simple manipulations, we get

$$\begin{aligned} J_<(\tau) &= -\frac{4\imath g e^{\imath D\tau}\Theta(\tau)}{(2\pi)^2}\int_0^\infty d\omega \frac{\omega\cos((\omega+2E_C)\tau)}{\omega+2E_C} + \text{c.c.}, \\ J_>(\tau) &= \frac{2\imath g\Theta(\tau)}{(2\pi)^2}\left[\int_0^\infty d\omega\frac{\omega e^{\imath(\omega+2E_C+D)\tau}}{\omega+2E_C+D} + \int_0^\infty d\omega\frac{\omega e^{-\imath(\omega+2E_C-D)\tau}}{\omega+2E_C-D}\right. \\ &\qquad \left. -\int_0^\infty d\omega\frac{\omega(4E_C+2\omega)}{(2E_C+\omega)^2-D^2}\right] + \text{c.c.}. \end{aligned} \tag{5.63}$$

Now, using

$$\begin{aligned} \int_0^\infty d\omega\frac{\omega e^{\imath\omega\tau}}{\omega+x} &= \frac{\imath}{\tau} - x\int_x^\infty du\frac{e^{\imath(u-x)\tau}}{u}, \\ &= \frac{\imath}{\tau} - xe^{-\imath x\tau}(\imath\pi\Theta(x) - \text{Ei}(\imath x\tau)), \end{aligned} \tag{5.64}$$

the expression for the current simplifies to

$$\begin{aligned} J(\tau) = \frac{2\imath g\Theta(\tau)}{(2\pi)^2}\,&[(2E_C+D)(\text{Ei}(\imath(2E_C+D)\tau) - \text{Ei}(-\imath(2E_C+D)\tau)) \\ &-(2E_C-D)(\text{Ei}(\imath(2E_C-D)\tau) - \text{Ei}(-\imath(2E_C-D)\tau)) \\ &-2\imath E_C\sin(D\tau)(\text{Ei}(\imath 2E_C\tau) + \text{Ei}(-\imath 2E_C\tau)) \\ &-2\pi\imath(2E_C+D)\Theta(2E_C+D) + 2\pi\imath(2E_C-D)\Theta(2E_C-D)]\,. \end{aligned} \tag{5.65}$$

The current response at long times $\tau \gg \tau_+ = \max[|D+2E_C|^{-1}, |D-2E_C|^{-1}]$ has two components ($J(\tau \gg \tau_0) = J_{\text{dc}} + J_{\text{tr}}$): a dc part,

$$J_{\text{dc}} = \frac{g\Theta(\tau)}{\pi}\left[(D-2E_C)\Theta(D-2E_C) + (D+2E_C)\Theta(-2E_C-D)\right] \tag{5.66}$$

and a transient part,

$$J_{\text{tr}} \approx -\frac{4g\Theta(\tau)}{(2\pi)^2 E_C}\frac{1}{\tau^2}\left[\left(\frac{D-2E_C}{D+2E_C}\right)\sin((D+2E_C)\tau) + \left(\frac{D+2E_C}{D-2E_C}\right)\sin((D-2E_C)\tau)\right], \tag{5.67}$$

that oscillates with the two beat frequencies $\omega_\pm = |D\pm 2E_C|$, and slowly decays in accordance with an inverse square law in time. Such oscillations are absent in classical *RC* networks subjected to a constant electric field, where only exponential relaxation may occur. The amplitudes of the two oscillation frequencies are inversely related. Close to a resonance, $D = \pm 2E_C$, the amplitude of the faster mode tends to vanish and the slower mode dominates.

At high fields, $|D| \gg 2E_C$, the beat frequencies are approximately $\omega_\pm \approx |D| = \omega_B$, where ω_B is the Bloch oscillation frequency for noninteracting electrons. It is instructive to compare with the fermionic Hubbard chain at half-filling - a quantum model that is the dissipation-free counterpart of ours. At strong electric fields, the Bloch oscillations in this model also occur [50] at ω_B, and which has a simple physical explanation. Consider a noninteracting model of fermions hopping on a one-dimensional lattice:

$$H_{\rm el}^{(0)} = -t \sum_{\langle ij\rangle\sigma} [c_{i\sigma}^\dagger c_{j\sigma} + \text{h.c.}] + \sum_{i\sigma} \varepsilon_i n_{i\sigma}, \tag{5.68}$$

where $\varepsilon_j = Dj$ is the linearly varying potential energy in the presence of a constant electric field. As is well-known [see eg. [53]], the above Hamiltonian is easily diagonalized by the transformation

$$f_n = \sum_i J_{i-n}(2t/D) c_i, \tag{5.69}$$

which gives us a discrete spectrum, the Wannier-Stark ladder, with energies $E_n = nD$, with n an integer. The wave function corresponding to E_n is localized, centered around the site n, and with a spatial extent of the order of $L = 2t/D$. Since there is no matrix element connecting different Wannier-Stark levels, no net current flows in the system. If the gain in potential energy across a link, D, greatly exceeds the tight binding hopping energy, then the Wannier-Stark states are highly localized. Introducing now a small local Hubbard repulsion term of strength E_C in Eq. (5.68), we find that the interaction remains approximately local even in the Wannier-Stark basis. For $D \gg E_C$, the energy levels are approximately nD, which leads to Bloch oscillations at frequency ω_B.

Consider now the short-time current response. Above the threshold field, $D_T > 2E_C$, a finite dc response exists unlike the dissipationless Hubbard chain at half filling. However, the Bloch-like oscillations are present both above and below the threshold field. At short times $\tau \ll \tau_- = \min[|D+2E_C|^{-1}, |D-2E_C|^{-1}]$, the current response is

$$J(\tau) \approx \frac{g\Theta(\tau)}{\pi} D - \frac{8g\Theta(\tau)}{(2\pi)^2} D(2E_C\tau)\left[\ln(1/2E_C\tau) + 2 - \gamma\right], \tag{5.70}$$

where $\gamma \approx 0.577$ is the Euler-Mascheroni constant. Remarkably, the initial current response, $J = gD/\pi$ is independent of the charging energy, E_C, and appears to be physically related to the fact that sudden changes in the potential effectively short-circuit a capacitor. Plots of

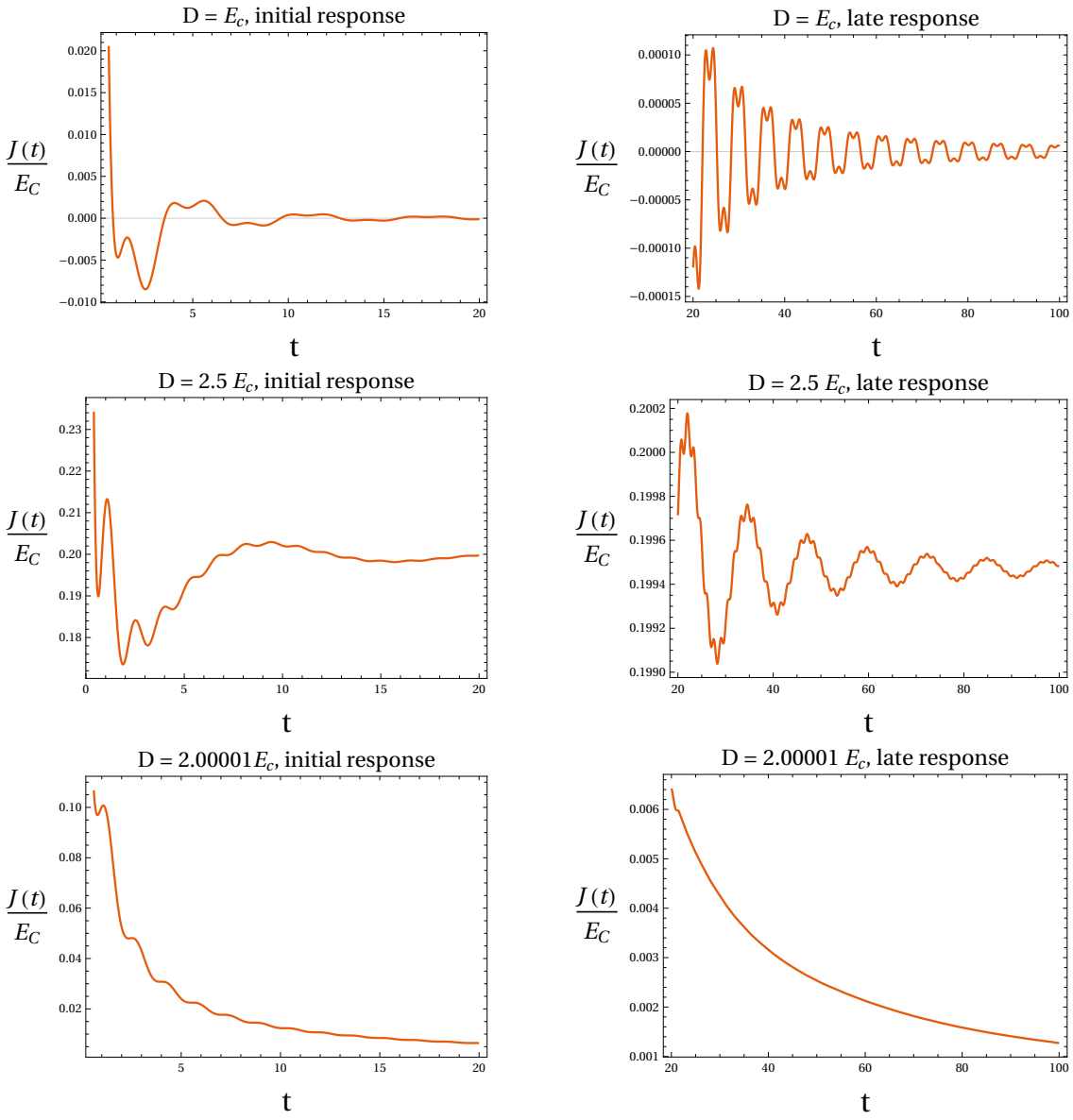

Figure 5.1 The current response to leading order in g after an electric field is turned on as described by Eq. 5.65. The plots to the left show the initial time response and those to the right show the late time response where the power law decay of the oscillatory behavior is seen. The effect of correlations in the late time response is seen in the form of beating frequencies. A finite steady state DC response exists only for $D > 2E_C$

the current response for different applied electric field strengths are given in Fig. 5.1 The transient current response is a central result of this paper.

A higher order perturbation expansion (in g) can be made for the current response using the procedure described above. Calculating the transient response now involves multiple processes (single site vs. multi-site tunneling) and time scales. At high fields and small values of g, these higher order contributions can be ignored. However at small fields and g not very small compared to unity, the current response is dominated by higher order tunneling terms involving multiple sites. In the following Section, we will study the effect of higher order processes on the steady state part of the current.

5.4 DC current at low fields: higher order processes

We are interested in the long time steady state response here, for which we turn on the electric field at $t = -\infty$ and for all later times, the vector potential is simply $A_{k,1}(t) = Dt$ (i.e. without the theta function in time). In this case, the expression for current given in Eq. (5.51) assumes a simpler form,

$$J = 2\imath g \int d\tau \left[e^{-iD\tau} \Pi^{+-}(\tau) L^{+-}(\tau) - e^{iD\tau} \Pi^{-+}(\tau) L^{-+}(\tau) \right], \tag{5.71}$$

since the terms involving Eq. (5.51) involving the bond correlators Π^{++} and Π^{--} cancel out. Furthermore, for a given sign of D, only one of the two terms in the integrand contributes. In the rest of the paper, we will assume $D > 0$ unless otherwise stated, and in this case, only the first term in the integrand in Eq. (5.71) needs to be calculated. The perturbative expansion of J is now obtained by expanding the bond correlators in increasing orders in g,

$$\Pi_{\sigma,\sigma'} = \Pi^{(0)}_{\sigma,\sigma'} + \Pi^{(1)}_{\sigma,\sigma'} + \cdots .$$

From Sec. 5.3, we have the leading order contribution to current as $J^{(1)} = (g/\pi)[(D - 2E_C)\Theta(D - 2E_C) - (D + 2E_C)\Theta(-D - 2E_C)]$. We now consider the contribution to the current in the second order in the tunneling conductance g.

5.4.1 Second order steady state response

The first order correction to the bare bond correlator of the link labeled $(k, 1)$ is

$$\Pi^{(1)}_{\mu,\mu'}(\tau,\tau') = \imath g \sum_{n,\sigma\sigma'} \int_{t,t'} W^{k,n}_{\mu\mu'\sigma\sigma'}(\tau,\tau',t,t') L^{\sigma\sigma'}(t-t') e^{-\imath D(t-t')}, \tag{5.72}$$

where

$$W^{k,n}_{\mu\mu'\sigma\sigma'}(\tau,\tau',t,t') = \left\langle \exp\left[-\imath\phi^{\mu}_{k,1}(\tau)+\imath\phi^{\mu'}_{k,1}(\tau')-\imath\phi^{\sigma}_{n,1}(t)+\imath\phi^{\sigma'}_{n,1}(t')\right]\right\rangle_{S_C}. \tag{5.73}$$

Let us define the four-point site correlators,

$$C_{\mu\mu'\sigma\sigma'}(\tau,\tau',t,t') = \left\langle \exp\left[-\imath\phi^{\mu}(\tau)+\imath\phi^{\mu'}(\tau')-\imath\phi^{\sigma}(t)+\imath\phi^{\sigma'}(t')\right]\right\rangle_{S_C}. \tag{5.74}$$

We now express the function $W^{k,n}_{\mu\mu'\sigma\sigma'}(\tau,\tau',t,t')$ in terms of the two and four point site correlators. For $n = k\pm 1$,

$$W^{k,n}_{\mu\mu'\sigma\sigma'}(\tau,\tau',t,t') = C_{\sigma'\sigma}(t'-t)C_{\mu'\mu\sigma\sigma'}(\tau',\tau,t,t')C_{\mu\mu'}(\tau-\tau'), \tag{5.75}$$

while for $n = k$,

$$W^{k,n}_{\mu\mu'\sigma\sigma'}(\tau,\tau',t,t') = C_{\mu'\mu\sigma'\sigma}(\tau',\tau,t',t)C_{\mu\mu'\sigma\sigma'}(\tau,\tau',t,t'). \tag{5.76}$$

The correlator W is nonzero only for $n = k\pm 1\,k$. For the calculation of current we only need the $W_{\mu\mu'\sigma\sigma'}$ with $\mu,\mu' = \{+,-\}$. These involve the following four-point site correlators:

$$C_{+-++}(\tau,\tau',t,t') = \exp\left[-\imath E_C\left(-|t-\tau|+|t'-\tau|+|t-t'|-t-\tau+t'+\tau'\right)\right], \tag{5.77}$$

$$C_{+-+-}(\tau,\tau',t,t') = \exp\left[-\imath E_C\left(-|t-\tau|+|t'-\tau'|-2(t-t'+\tau-\tau')\right)\right], \tag{5.78}$$

$$C_{+--+}(\tau,\tau',t,t') = \exp\left[-\imath E_C\left(|t'-\tau|-|t-\tau'|\right)\right], \tag{5.79}$$

$$C_{+---}(\tau,\tau',t,t') = \exp\left[-\imath E_C\left(-|t-\tau'|+|t'-\tau'|-|t-t'|-t-\tau+t'+\tau'\right)\right], \tag{5.80}$$

$$C_{-+++}(\tau,\tau',t,t') = \exp\left[-\imath E_C\left(|t-\tau'|-|t'-\tau'|+|t-t'|+t+\tau-t'-\tau'\right)\right], \tag{5.81}$$

$$C_{-++-}(\tau,\tau',t,t') = \exp\left[-\imath E_C\left(|t-\tau'|-|t'-\tau|\right)\right], \tag{5.82}$$

$$C_{-+-+}(\tau,\tau',t,t') = \exp\left[-\imath E_C\left(|t-\tau|-|t'-\tau'|+2(t-t'+\tau-\tau')\right)\right], \tag{5.83}$$

$$C_{-+--}(\tau,\tau',t,t') = \exp\left[-\imath E_C\left(|t-\tau|-|t'-\tau|-|t-t'|+t+\tau-t'-\tau'\right)\right]. \tag{5.84}$$

The four-point site correlators clearly satisfy the identities

$$\begin{aligned} C_{\mu\mu'\sigma\sigma'}(\tau,\tau',t,t') &= C_{\sigma\sigma'\mu\mu'}(t,t',\tau,\tau'),\\ C_{\mu\mu'\sigma\sigma'}(\tau,\tau',t,t') &= C_{\bar\mu\bar\mu'\bar\sigma\bar\sigma'}(\tau,\tau',t,t'), \end{aligned} \tag{5.85}$$

where the bar on the subscripts interchanges the $+$ and $-$ indices.

From the structure of the four-point site correlators, we see that the expression for the bond correlators has nonanalytic terms of the type $e^{\imath E_C|t_1-t_2|}$. To deal with these, we make use of the identity,

$$e^{-\imath E_C|t|} = \lim_{\eta\to 0} \frac{\imath E_C}{\pi} \int_{-\infty}^{\infty} \frac{d\omega\, e^{-\imath\omega t}}{(\omega - E_C + \imath\eta)(\omega + E_C - \imath\eta)}.$$

We then express $L^{\sigma\sigma'}(t-t')$ in the Fourier basis and then perform the t, t' integrals in Eq.(5.72). After some effort we get the following expression for $\Pi^{(1)}_{+-}$:

$$\begin{aligned}\Pi^{(1)}_{+-}(\tau) = \frac{4\imath E_C^2 g}{\pi} \lim_{\eta\to 0} \int d\omega \Bigg[& \frac{L^{+-}(\omega - D) e^{\imath 2E_C\tau}(e^{-\imath\omega\tau} - 1)}{(\omega^2+\eta^2)((\omega - 2E_C)^2 + \eta^2)} \\ & + \frac{H^{+-}(\omega - D) e^{i2E_C\tau}(1 - e^{\imath(4E_C+\omega)\tau})}{((\omega + 4E_C)^2 + \eta^2)((\omega + 2E_C)^2 + \eta^2)} \\ & + \frac{2L^{+-}(\omega - D) e^{\imath 2E_C\tau}(e^{-\imath(\omega - 6E_C)\tau} - 1)}{((\omega - 6E_C)^2 + \eta^2)((\omega - 2E_C)^2 + \eta^2)} \\ & + \frac{2H^{+-}(\omega - D)(e^{\imath 2E_C\tau} - e^{\imath\omega\tau})}{((\omega - 2E_C)^2 + \eta^2)((\omega + 2E_C)^2 + \eta^2)} \Bigg], \end{aligned} \tag{5.86}$$

where $H^{+-}(\omega) = \Sigma^+(\omega) - \Sigma^-(\omega) + \Sigma^K(\omega)$. Using Eq. (5.86) in Eq. (5.71), we obtain the second order contribution to the current:

$$\begin{aligned} J^{(2)} = -\frac{8g^2E_C^2}{\pi} \lim_{\eta\to 0} \int d\omega \Bigg[& \frac{L^{+-}(\omega - D)[L^{+-}(2E_C - D - \omega) - L^{+-}(2E_C - D)]}{(\omega^2+\eta^2)((\omega - 2E_C)^2 + \eta^2)} \\ & + \frac{H^{+-}(\omega - D)[L^{+-}(2E_C - D) - L^{+-}(\omega + 6E_C - D)]}{((\omega + 4E_C)^2 + \eta^2)((\omega + 2E_C)^2 + \eta^2)} \\ & + 2\frac{L^{+-}(\omega - D)[L^{+-}(8E_C - D - \omega) - L^{+-}(2E_C - D)]}{((\omega - 6E_C)^2 + \eta^2)((\omega - 2E_C)^2 + \eta^2)} \\ & + 2\frac{H^{+-}(\omega - D)[L^{+-}(2E_C - D) - L^{+-}(\omega - D)]}{((\omega - 2E_C)^2 + \eta^2)((\omega + 2E_C)^2 + \eta^2)} \Bigg]. \end{aligned} \tag{5.87}$$

From the step-like structure of the L^{+-} and H^{+-} functions, we find that $J^{(2)} = 0$ for $D < E_C$; thus, $J^{(2)}$ has a smaller threshold compared to $J^{(1)}$, which vanishes below $2E_C$. For $E_C \leq D < 2E_C$, the calculation of the current simplifies considerably since only one term makes a nonzero contribution in Eq. (5.87), and we have

$$J^{(2)} = -\frac{8g^2E_C^2}{\pi} \lim_{\eta\to 0} \int d\omega \frac{L^{+-}(\omega - D)L^{+-}(2E_C - D - \omega)}{(\omega^2+\eta^2)((\omega - 2E_C)^2 + \eta^2)}, \quad E_C \leq D < 2E_C, \tag{5.88}$$

and upon performing the integration we arrive at

$$J^{(2)} = \frac{2g^2}{\pi^3 E_C}\left((D-E_C)^2+E_C^2\right)\log\left[\frac{D^2}{(D-2E_C)^2}\right] - \frac{8g^2}{\pi^3}(D-E_C), \quad E_C \le D < 2E_C. \tag{5.89}$$

Just above the threshold for $J^{(2)}$, $D = E_C$, the current has a power-law behavior,

$$J^{(2)} \approx \frac{8g^2 E_C}{\pi^3}\left(\frac{D}{E_C}-1\right)^3, \tag{5.90}$$

which is to be contrasted with the linear behavior of $J^{(1)}$ above its threshold. At the other end, $D = 2E_C$, the expression for $J^{(2)}$ has a logarithmic divergence. Physically, this is a manifestation of a resonance: $D = 2E_C$ is the condition for creating a particle-hole dipole excitation in neighboring grains. For higher fields, $D > 2E_C$, more terms in Eq. (5.87) will now contribute to $J^{(2)}$; however, none of these terms eliminate the logarithmic singularity.

The second order perturbation correction to the current is justified provided one does not get too close to the singular point, i.e.,

$$g\ln\left|\frac{D}{2E_C-D}\right| \lesssim 1. \tag{5.91}$$

Similar logarithmic divergence is also evident in $\Pi^{(1)}(\tau)$. On the other hand, the bond correlator, $\Pi = \Pi^{(0)} + \Pi^{(1)} + \cdots$, by definition is bounded by ± 1. This clearly shows that the divergence in current at the resonance is the result of a perturbative treatment about the bare charging action. The region of validity of the perturbative treatment could be increased in principle by a resummation of the leading singular terms to all orders in g. Unfortunately, the number of processes contributing to current in higher orders increases rapidly with the order, rendering the calculation of the current at intermediate fields (sufficiently larger than the lowest threshold) quite complicated. The other possibility is a phase transition from the Mott phase to a conducting, metallic phase whose boundary is given by the condition $g\ln(2E_C/\varepsilon) = 1$, with $\varepsilon = 2E_C - D \ll E_C$. The resummation and possible phase transition will be studied in detail elsewhere. Incidentally, the energy scale $\varepsilon = E_C e^{-1/g}$ also appears in the scaling analysis of the single site equilibrium AES model close to the degeneracy point, $n_g = 1/2$ [54]. Below this scale, phase fluctuations renormalize the gate charge to the fixed point value, $n_g = 1/2$, which corresponds to resonant transmission. Finally, for very small values of $2E_C - D$, we expect that the energy level discreteness of the dots will begin

to matter, and at resonance, the lower cutoff for $|2E_C - D|$ should at least be of the order of the mean level spacing δ, i.e., we need $g < 1/\ln(2E_C/\delta)$.

5.4.2 Higher order contributions and current response at low fields

At low fields, finite contributions to the current appear only at higher orders. An order-n process has a threshold field $D_{\rm th}^{(n)} = 2E_C/n$. Physically, a large-distance cotunneling process provides the potential energy gain required to overcome Coulomb blockade. During the cotunneling process between sites labeled i and $i+n$, the classical charges, n^c, at the $n-1$ intermediate sites only have virtual transitions and thus the only Coulomb blockade cost appears at the sites i and $i+n$. The pure cotunneling process gives the lowest threshold value, $D_{\rm th}^{(n)}$, at any order. The contribution to the current from this process can be shown to be

$$J^{(n)} = \imath 2ng\left(\frac{\imath 2gE_C^2}{\pi}\right)^{n-1} K^{(n)}, \tag{5.92}$$

where

$$K^{(n)} = \int \prod_{i=1}^{n-1} d\omega_i \left[\prod_{j=1}^{n-1} \frac{L^{+-}(\omega_j - D)}{\omega_j^2(\omega_j - 2E_C)^2}\right] L^{+-}(2E_C - D - \sum_{p=1}^{n-1}\omega_p). \tag{5.93}$$

The L^{+-} functions constrain the frequency integration and we have

$$\begin{aligned} K^{(n)} = &\left(\frac{\imath}{2\pi}\right)^n \int_{2E_C-(n-1)D}^{D} d\omega_1 \int_{2E_C-(n-2)D-\omega_1}^{D} d\omega_2 \cdots \int_{2E_C-D-\sum_{p=1}^{n-2}\omega_p}^{D} d\omega_{n-1} \\ &\times \frac{(\omega_1 - D)(\omega_2 - D)\cdots(\omega_{n-1} - D)(2E_C - D - \sum_{p=1}^{n-1}\omega_p)}{\omega_1^2 \ldots \omega_{n-1}^2(\omega_1 - 2E_C)^2 \ldots (\omega_{n-1} - 2E_C)^2}. \end{aligned} \tag{5.94}$$

The integral gets the dominant contribution from the vicinity of $\omega_i = D$, and is approximately

$$K^{(n)} \approx \left(-\frac{\imath}{2\pi}\right)^n \frac{n^{(2n-1)}}{(2n-1)!} \frac{(D - D_{\rm th}^{(n)})^{(2n-1)}}{D^{2(n-1)}(2E_C - D)^{2(n-1)}} \Theta(D - D_{\rm th}^{(n)}), \quad \frac{D - D_{\rm th}^{(n)}}{D_{\rm th}^{(n)}} \ll 1. \tag{5.95}$$

Combining Eqs. (5.92) and (5.95), and making the Stirling approximation for factorials, we obtain, for large n,

$$J^{(n)} \sim n g^n \left(\frac{e}{2\pi}\right)^{2n-1} \left(\frac{2E_C}{D(2E_C - D)}\right)^{2(n-1)} \left(D - D_{\rm th}^{(n)}\right)^{2n-1} \Theta(D - D_{\rm th}^{(n)}) \tag{5.96}$$

$$\approx anb^n D \left(1 - \frac{n_D}{n}\right)^{2n-1} \Theta\left(1 - \frac{n_D}{n}\right), \tag{5.97}$$

where

$$a = \frac{2\pi}{e}\left(1 - \frac{1}{n_D}\right)^2,$$

$$b = g\left(\frac{e}{2\pi}\right)^2 \left(\frac{1}{1 - n_D^{-1}}\right)^2,$$

$$n_D = \frac{2E_C}{D}. \tag{5.98}$$

Denoting $[n_D]$ to be the least integer $\geq n_D$, the expression for the total current is given by,

$$J = \sum_{n=[n_D]}^{\infty} J^{(n)}. \tag{5.99}$$

For $D \ll E_C$, from the large n form of $J^{(n)}$ in Eq. (5.97), we see that the expression for the total current is divergent for $b \geq 1$. We identify the onset of this divergence as the breakdown of our perturbation theory which is developed to work in the Mott phase and thus signals the nonequilibrium phase transition to a metallic phase. Thus, for small values of the electric field, the phase boundary for the nonequilibrium phase transition to this metallic phase is given by setting $b = 1$:

$$g = g_0 \left[1 - \frac{D}{2E_C}\right]^2, \quad D \ll 2E_C, \tag{5.100}$$

with g_0 a constant of order unity.

Let us now look into the form of current within the Mott phase for small D. From Eq.(5.97), we see that the expression for J in eq.(5.99) can be approximated by a saddle point approximation if $b \ll 1$. For this we first rewrite Eq. (5.99) as

$$J = aD \sum_{n=[n_D]}^{\infty} \exp\left[\ln n + n \ln b + (2n-1) \ln\left(1 - \frac{n_D}{n}\right)\right]. \tag{5.101}$$

The saddle point condition is (neglecting some small terms):

$$\ln b + 2\ln\left(1-\frac{n_D}{n}\right)+\frac{2n_D}{n-n_D}=0. \tag{5.102}$$

In terms of $x = n_D/n$, an approximate solution of the above equation can be written as

$$x = x^* - (1-x^*)^2\ln(1-x^*), \tag{5.103}$$

where, $x^* = \left(1-\frac{2}{\ln b}\right)^{-1}$. The form of current then turns out to be (for $D < D_c = 2E_C(1-\sqrt{g/g_0})$ and $D_c \ll 2E_c$),

$$J \sim a\begin{cases} D\exp\left[-(4E_C/D)\ln\left[\sqrt{\frac{g_0}{g}}\left(1-\frac{D}{2E_C}\right)\right]\right], & D \ll D_c \\ D_c\left(\frac{D_c}{D_c-D}\right)^2, & \frac{D_c-D}{D_c} \ll 1. \end{cases} \tag{5.104}$$

Thus as the critical field D_c is approached, the perturbation series for the current diverges, signaling the breakdown of the Mott insulator state.

5.5 Discussion

In summary, we developed an effective Keldysh field theory for studying the nonequilibrium response of dissipative Mott insulator systems, and used it to study the nonequilibrium current response to a uniform electric field switched on at some instant of time. Our model, a Keldysh generalization of the AES model for Mott insulators, is in effect a bosonization of the Hubbard model with a large number ($\mathscr{N}$) of electron flavors at the lattice sites. The effective degrees of freedom are the excess charges at the sites and the phases conjugate to these. The large-$\mathscr{N}$ is simultaneously a source of dissipation through the Landau damping mechanism and also affords significant simplification of the effective action (in comparison with the usual Hubbard model) by suppressing all terms that are higher than second order in the interdot tunneling amplitude.

The main quantum effect that survives in the large-$\mathscr{N}$ limit is charge quantization, which is respected at every stage in the analysis of our problem. The charge quantization is reflected in sustained Bloch-like oscillations that decay as an inverse square power-law in time despite the presence of dissipation. The effect of correlations is to split the Bloch oscillation frequency into two beating frequencies whose difference is of the order of the Coulomb repulsion scale.

A major challenge in the area has been to demonstrate a DC current response in lattice translationally invariant Hubbard models. We identified the role played by dissipation in suppressing the Bloch oscillations (even if as a power law in time) and enabling a finite DC current response. We analyzed the DC current response taking into account higher order cotunneling processes that allow a trade-off between the reduced probability of a long-distance cotunneling and energy gain from the applied electric field. The response at small electric fields is found to be of the LZS form, $J \sim D[g/\ln^2(1/g)]^{2E_C/D}$, although the exponent is proportional to the Mott gap E_C instead of the usual $e^{-E_C^2/D}$ expected for pair-production probability in the dissipation-free case [108]. We do not find a threshold field below which DC conduction is absent since at any small field, DC conduction is possible through sufficiently high order cotunneling. At higher fields, the perturbation expansion of the current in powers of the small tunneling conductance breaks down, and from this we obtain the phase boundary for the electric field driven Mott insulator to a conducting state.

The AES model regards the interdot tunneling processes to be of the Fermi Golden-Rule type, which breaks down when the characteristic energies of particle-hole excitations in the dots approach the mean level spacing, δ. Therefore the typical potential drop between neighboring sites or the temperature should exceed δ. This imposes a cutoff on the regime of validity of our analysis.

We conclude with a brief discussion of future directions. Our approach can also be useful for the study of other far from equilibrium problems of current interest. For example, it is an interesting question as to how an initial non-thermal distribution of dot charges would evolve with time - in particular whether the long-time behavior retains any memory of the initial conditions. Similar questions have been posed, for example, in the context of relaxation of initial charge distribution in bosonic cold atom systems [26] and the approach to thermal equilibrium in fermionic quantum chains [31]. Our Keldysh-AES model can also be used to study the energy transport. The problem we have attacked in our paper is the current response to a uniform DC electric field; however, the approach is readily generalized to problems involving time-dependent drives. In this context, it would be interesting to compare with periodically driven Hubbard chains in the absence of dissipation [143]. As we noted in our paper, there are two special values of the background charge on a dot - integer and half odd integer. The integer case that we studied in detail corresponds to a Mott insulator, while the latter is a correlated "bad" metal. The nonequilibrium response close to half odd integer background charges is an open question. Another interesting direction would be to study the nonequilibrium response of driven Josephson-junction arrays. This direction, especially after taking into account long-range Coulomb interactions, would shed more light to understand the sudden jumbs observed in the I-V characteristics of disordered superconductors that

are in the insulating side and in the proximity of superconductor to insulator transition [145, 113, 101, 126].

Chapter 6

Summary

I summarize the main findings of the three research projects.

1. Magneto-response of strongly disordered superconductor thin films
In this project I studied the shrinking of the SC islands in disordered superconductor thin films subjected to a perpendicular magnetic field using a method similar to that of *Liftshitz tails*. The field dependence of the typical size of the islands, the typical distance between the islands, the typical Josephson coupling etc. were obtained and these were used to construct a JJ model with field dependent parameters. Analyzing the model in three extreme parameter regimes – dominated by either 1. Coloumb blockade 2. Thermal fluctuations or 3. AB phase disorder – the form of magnetoresistance and superfluid stiffness were obtained.

2. Disordered BKT transition and superinsulation
In this project it was shown that the superinsulation transition can be understood as a charge BKT transition. Strong enough disorder (via random quenched dipole moments of the SC islands) alters the critical behavior of the resistivity from the usual BKT critical form to a more singular VFT critical form. This work also provides a microscopic derivation of the VFT crtical behavior. The physical origin of the VFT behavior is traced to the freezing phenomenon of charge dipole excitations.

The results of these two projects share some similarties since the theoretical model used in studying them have origins in the coupled Coulomb gas model in Eq. (2.37). In the first project we studied vortex BKT transition by considering the limit $J \gg E_C$. On the other hand, in the second project we studied charge BKT transition by considering the limit $E_C \gg J$. The

similarities could be seen in the structure of the obtained phase diagrams and in the critical forms of conductivity or resistivity and is related to the self-duality of the coupled Coulomb gas model [56]

3. Keldysh field theory of nonequilibrium transport in a dissipative Mott insulator In this project I developed an effective Keldysh theory of a one dimensional granular metal array. The developed effective Keldysh action is essentialy a Keldysh generalization of the AES action. This action was used to study the electric current response upon switching on an uniform electric field. The leading order current shows oscillatory response with "beat frequencies" and decays as inverse square of time to a steady state DC response. The contribution of higher order tunneling processes to the DC current is analyzed. A perturbation series in powers of the intergrain tunneling conductance is obtained for the current. In the zero temperature limit, different orders show a hierarchy of thresholds and the form of the current near the threshold is estimated. Dielectric breakdown is predicted from the divergence of the perturbation series for the current.

References

[1] Abrahams, E., Anderson, P., Licciardello, D., and Ramakrishnan, T. (1979). Scaling theory of localization: Absence of quantum diffusion in two dimensions. *Physical Review Letters*, 42(10):673.

[2] Altland, A. and Egger, R. (2009). Nonequilibrium dephasing in coulomb blockaded quantum dots. *Physical review letters*, 102(2):026805.

[3] Altland, A. and Simons, B. D. (2010). *Condensed matter field theory*. Cambridge University Press.

[4] Altman, E., Kafri, Y., Polkovnikov, A., and Refael, G. (2004). Phase transition in a system of one-dimensional bosons with strong disorder. *Physical Review Letters*, 93(15):150402.

[5] Altman, E., Kafri, Y., Polkovnikov, A., and Refael, G. (2008). Insulating phases and superfluid-insulator transition of disordered boson chains. *Physical review letters*, 100(17):170402.

[6] Al'tshuler, B. and Aronov, A. (1979). Sov. phys. jetp 50, 968 (1979). *Sov. Phys. JETP*, 50:968.

[7] Altshuler, B., Cuevas, E., Ioffe, L., and Kravtsov, V. (2016). Non-ergodic phases in strongly disordered random regular graphs. *arXiv preprint arXiv:1605.02295*.

[8] Altshuler, B. L., Kravtsov, V. E., Lerner, I. V., and Aleiner, I. L. (2009). Jumps in current-voltage characteristics in disordered films. *Physical review letters*, 102(17):176803.

[9] Amaricci, A., Weber, C., Capone, M., and Kotliar, G. (2012). Approach to a stationary state in a driven hubbard model coupled to a thermostat. *Physical Review B*, 86(8):085110.

[10] Ambegaokar, V. and Baratoff, A. (1963). Tunneling between superconductors. *Physical Review Letters*, 10(11):486.

[11] Ambegaokar, V., Eckern, U., and Schön, G. (1982). Quantum dynamics of tunneling between superconductors. *Physical Review Letters*, 48(25):1745.

[12] Anderson, P., Muttalib, K., and Ramakrishnan, T. (1983). Theory of the" universal" degradation of t c in high-temperature superconductors. *Physical Review B*, 28(1):117.

[13] Anderson, P. W. (1958). Absence of diffusion in certain random lattices. *Physical review*, 109(5):1492.

[14] Anderson, P. W. (1959). Theory of dirty superconductors. *Journal of Physics and Chemistry of Solids*, 11(1-2):26–30.

[15] Anderson, P. W. (1979). Lectures on amorphous systems. *II condensed matter Les Houches*, (XXXI):159–261.

[16] Aoki, H., Tsuji, N., Eckstein, M., Kollar, M., Oka, T., and Werner, P. (2014). Nonequilibrium dynamical mean-field theory and its applications. *Reviews of Modern Physics*, 86(2):779.

[17] Aron, C. (2012). Dielectric breakdown of a mott insulator. *Physical Review B*, 86(8):085127.

[18] Aron, C., Kotliar, G., and Weber, C. (2012). Dimensional crossover driven by an electric field. *Physical review letters*, 108(8):086401.

[19] Arrigoni, E., Knap, M., and von der Linden, W. (2013). Nonequilibrium dynamical mean-field theory: An auxiliary quantum master equation approach. *Physical review letters*, 110(8):086403.

[20] Bardeen, J., Cooper, L. N., and Schrieffer, J. R. (1957). Theory of superconductivity. *Physical Review*, 108(5):1175.

[21] Basko, D. M., Aleiner, I. L., and Altshuler, B. L. (2006). Metal - insulator transition in a weakly interacting many-electron system with localized single-particle states. *Annals of Physics*, 321:1126–1205.

[22] Baturina, T. I. and Vinokur, V. M. (2013). Superinsulator-superconductor duality in two dimensions. *Annals of Physics*, 331:236–257.

[23] Beloborodov, I., Lopatin, A., Vinokur, V., and Efetov, K. (2007). Granular electronic systems. *Reviews of Modern Physics*, 79(2):469.

[24] Berezinskii, V. (1971). Destruction of long-range order in one-dimensional and two-dimensional systems having a continuous symmetry group i. classical systems. *Sov. Phys. JETP*, 32(3):493–500.

[25] Biscaras, J., Bergeal, N., Hurand, S., Feuillet-Palma, C., Rastogi, A., Budhani, R., Grilli, M., Caprara, S., and Lesueur, J. (2013). Multiple quantum criticality in a two-dimensional superconductor. *Nature Materials*, 12(6):542–548.

[26] Bordia, P., Lüschen, H., Scherg, S., Gopalakrishnan, S., Knap, M., Schneider, U., and Bloch, I. (2017). Probing slow relaxation and many-body localization in two-dimensional quasiperiodic systems. *Physical Review X*, 7(4):041047.

[27] Bouadim, K., Loh, Y. L., Randeria, M., and Trivedi, N. (2011). Single-and two-particle energy gaps across the disorder-driven superconductor–insulator transition. *Nature Physics*, 7(11):884.

[28] Bramson, M. (1983). Convergence of solutions of the kolmogorov equation to traveling waves. *Memoirs of the American Mathematical Society*, 44(285):1–190.

[29] Breznay, N. P., Steiner, M. A., Kivelson, S. A., and Kapitulnik, A. (2016). Self-duality and a hall-insulator phase near the superconductor-to-insulator transition in indium-oxide films. *Proceedings of the National Academy of Sciences*, 113(2):280–285.

[30] Buchleitner, A. and Kolovsky, A. R. (2003). Interaction-induced decoherence of atomic bloch oscillations. *Physical review letters*, 91(25):253002.

[31] Bulchandani, V. B., Vasseur, R., Karrasch, C., and Moore, J. E. (2017). Solvable hydrodynamics of quantum integrable systems. *Physical review letters*, 119(22):220604.

[32] Caldeira, A. O. and Leggett, A. J. (1981). Influence of dissipation on quantum tunneling in macroscopic systems. *Physical Review Letters*, 46(4):211.

[33] Carpentier, D. and Le Doussal, P. (1998). Disordered xy models and coulomb gases: renormalization via traveling waves. *Physical Review Letters*, 81(12):2558.

[34] Carpentier, D. and Le Doussal, P. (2000). Topological transitions and freezing in xy models and coulomb gases with quenched disorder: renormalization via traveling waves. *Nuclear Physics B*, 588(3):565–629.

[35] Carrasquilla, J., Manmana, S. R., and Rigol, M. (2013). Scaling of the gap, fidelity susceptibility, and bloch oscillations across the superfluid-to-mott-insulator transition in the one-dimensional bose-hubbard model. *Physical Review A*, 87(4):043606.

[36] Cha, M.-C. and Fertig, H. (1995). Disorder-induced phase transitions in two-dimensional crystals. *Physical review letters*, 74(24):4867.

[37] Chakrabarti, A. and Dasgupta, C. (1988). Phase transition in positionally disordered josephson-junction arrays in a transverse magnetic field. *Physical Review B*, 37(13):7557.

[38] Chand, M., Saraswat, G., Kamlapure, A., Mondal, M., Kumar, S., Jesudasan, J., Bagwe, V., Benfatto, L., Tripathi, V., and Raychaudhuri, P. (2012). Phase diagram of the strongly disordered s-wave superconductor nbn close to the metal-insulator transition. *Physical Review B*, 85(1):014508.

[39] Cheung, A. K. C. and Berciu, M. (2013). Phonon-assisted carrier motion on the wannier-stark ladder. *Physical Review B*, 88(3):035132.

[40] Crane, R., Armitage, N., Johansson, A., Sambandamurthy, G., Shahar, D., and Grüner, G. (2007). Survival of superconducting correlations across the two-dimensional superconductor-insulator transition: A finite-frequency study. *Physical Review B*, 75(18):184530.

[41] Davison, R. A., Fu, W., Georges, A., Gu, Y., Jensen, K., and Sachdev, S. (2017). Thermoelectric transport in disordered metals without quasiparticles: The sachdev-ye-kitaev models and holography. *Physical Review B*, 95(15):155131.

[42] Derrida, B. (1981). Random-energy model: An exactly solvable model of disordered systems. *Physical Review B*, 24(5):2613.

[43] Derrida, B. and Spohn, H. (1988). Polymers on disordered trees, spin glasses, and traveling waves. *Journal of Statistical Physics*, 51(5-6):817–840.

[44] Dhar, D. (1981). On the topological characterization of two-dimensional phase transitions. *Physics Letters A*, 81(1):19–22.

[45] Diamantini, M. C., Sodano, P., and Trugenberger, C. A. (1996). Gauge theories of josephson junction arrays. *Nuclear Physics B*, 474(5):641 – 677.

[46] Dias, W., Nascimento, E., Lyra, M., and De Moura, F. (2007). Frequency doubling of bloch oscillations for interacting electrons in a static electric field. *Physical Review B*, 76(15):155124.

[47] Dubi, Y., Meir, Y., and Avishai, Y. (2006). Theory of the magnetoresistance of disordered superconducting films. *Physical Review B*, 73(5):054509.

[48] Dubi, Y., Meir, Y., and Avishai, Y. (2007). Nature of the superconductor–insulator transition in disordered superconductors. *Nature*, 449(7164):876.

[49] Dutta, S., Lakshmi, S., and Pati, S. K. (2007). Effect of electric field on one-dimensional insulators: a density matrix renormalization group study. *Journal of Physics: Condensed Matter*, 19(32):322201.

[50] Eckstein, M., Oka, T., and Werner, P. (2010). Dielectric breakdown of mott insulators in dynamical mean-field theory. *Physical review letters*, 105(14):146404.

[51] Eckstein, M. and Werner, P. (2011). Damping of bloch oscillations in the hubbard model. *Physical review letters*, 107(18):186406.

[52] Eckstein, M. and Werner, P. (2013). Dielectric breakdown of mott insulators–doublon production and doublon heating. In *Journal of Physics: Conference Series*, volume 427, page 012005. IOP Publishing.

[53] Emin, D. and Hart, C. (1987). Phonon-assisted hopping of an electron on a wannier-stark ladder in a strong electric field. *Physical Review B*, 36(5):2530.

[54] Falci, G., Schön, G., and Zimanyi, G. T. (1995). Unified scaling theory of the electron box for arbitrary tunneling strength. *Physical review letters*, 74(16):3257.

[55] Falco, G., Nattermann, T., and Pokrovsky, V. L. (2009). Weakly interacting bose gas in a random environment. *Physical Review B*, 80(10):104515.

[56] Fazio, R. and Schön, G. (1991). Charge and vortex dynamics in arrays of tunnel junctions. *Physical Review B*, 43(7):5307.

[57] Feigel'man, M., Ioffe, L., Kravtsov, V., and Yuzbashyan, E. (2007). Eigenfunction fractality and pseudogap state near the superconductor-insulator transition. *Physical review letters*, 98(2):027001.

[58] Finkel'stein, A. (1984). Metal–insulator transition in a disordered system. *Zh. Eksp. Teor. Fiz*, 86:367–380.

[59] Fisher, M. P. (1990). Quantum phase transitions in disordered two-dimensional superconductors. *Physical Review Letters*, 65(7):923.

[60] Fisher, M. P., Weichman, P. B., Grinstein, G., and Fisher, D. S. (1989). Boson localization and the superfluid-insulator transition. *Physical Review B*, 40(1):546.

[61] Fistul, M., Vinokur, V., and Baturina, T. (2008). Collective cooper-pair transport in the insulating state of josephson-junction arrays. *Physical review letters*, 100(8):086805.

[62] Fleishman, L. and Anderson, P. W. (1980). Interactions and the Anderson transition. *Physical Review B*, 21(6):2366–2377.

[63] Freericks, J. (2008). Quenching bloch oscillations in a strongly correlated material: Nonequilibrium dynamical mean-field theory. *Physical Review B*, 77(7):075109.

[64] Freericks, J., Turkowski, V., and Zlatić, V. (2006). Nonequilibrium dynamical mean-field theory. *Physical review letters*, 97(26):266408.

[65] Fukui, T. and Kawakami, N. (1998). Breakdown of the mott insulator: Exact solution of an asymmetric hubbard model. *Physical Review B*, 58(24):16051.

[66] Fukuyama, H., Bari, R. A., and Fogedby, H. C. (1973). Tightly bound electrons in a uniform electric field. *Physical Review B*, 8(12):5579.

[67] Fukuyama, H., Ebisawa, H., and Maekawa, S. (1984). Bulk superconductivity in weakly localized regime. *Journal of the Physical Society of Japan*, 53(10):3560–3567.

[68] Galitski, V. and Larkin, A. (2001). Disorder and quantum fluctuations in superconducting films in strong magnetic fields. *Physical Review Letters*, 87(8):087001.

[69] Galitski, V. M., Refael, G., Fisher, M. P., and Senthil, T. (2005). Vortices and quasiparticles near the superconductor-insulator transition in thin films. *Physical Review Letters*, 95(7):077002.

[70] Ghosal, A., Randeria, M., and Trivedi, N. (2001). Inhomogeneous pairing in highly disordered s-wave superconductors. *Physical Review B*, 65(1):014501.

[71] Giamarchi, T. and Schulz, H. (1988). Anderson localization and interactions in one-dimensional metals. *Physical Review B*, 37(1):325.

[72] Gopalakrishnan, S. and Nandkishore, R. (2012). Mean-field theory of nearly many-body localized metals. *Phys. Rev. B*, 90:224203–224215.

[73] Gornyi, I. V., Mirlin, A. D., and Polyakov, D. G. (2005). Interacting electrons in disordered wires: Anderson localization and low-t transport. *Phys. Rev. Lett.*, 95:2006603–2006606.

[74] Gor'Kov, L. (1960). Theory of superconducting alloys in a strong magnetic field near the critical temperature. *Soviet Physics JETP*, 10:998.

[75] Gu, Y., Qi, X.-L., and Stanford, D. (2017). Local criticality, diffusion and chaos in generalized sachdev-ye-kitaev models. *Journal of High Energy Physics*, 2017(5):125.

[76] Halperin, B. and Nelson, D. R. (1979). Resistive transition in superconducting films. *Journal of Low Temperature Physics*, 36(5-6):599–616.

[77] Han, J. E. (2013). Solution of electric-field-driven tight-binding lattice coupled to fermion reservoirs. *Physical Review B*, 87(8):085119.

[78] Heidrich-Meisner, F., González, I., Al-Hassanieh, K., Feiguin, A., Rozenberg, M., and Dagotto, E. (2010). Nonequilibrium electronic transport in a one-dimensional mott insulator. *Physical Review B*, 82(20):205110.

[79] Hrahsheh, F. and Vojta, T. (2012). Disordered bosons in one dimension: From weak-to strong-randomness criticality. *Physical review letters*, 109(26):265303.

[80] Ioffe, L. and Larkin, A. (1981). Properties of superconductors with a smeared transition temperature.

[81] Josephson, B. D. (1962). Possible new effects in superconductive tunnelling. *Physics letters*, 1(7):251–253.

[82] Kamlapure, A., Das, T., Ganguli, S. C., Parmar, J. B., Bhattacharyya, S., and Raychaudhuri, P. (2013). Emergence of nanoscale inhomogeneity in the superconducting state of a homogeneously disordered conventional superconductor. *Scientific reports*, 3:2979.

[83] Keldysh, L. (1979). Coulomb interaction in thin semiconductor and semimetal films. *Soviet Journal of Experimental and Theoretical Physics Letters*, 29:658.

[84] Kim, K. and Stroud, D. (2008). Quantum monte carlo study of a magnetic-field-driven two-dimensional superconductor-insulator transition. *Physical Review B*, 78(17):174517.

[85] Kirino, S. and Ueda, K. (2010). Nonequilibrium current in the one dimensional hubbard model at half-filling. *Journal of the Physical Society of Japan*, 79(9):093710.

[86] Kitaev, A. (2015). A simple model of quantum holography, talk given at the kitp program: entanglement in strongly-correlated quantum matter. *USA April*, 7.

[87] Kosterlitz, J. (1974). The critical properties of the two-dimensional xy model. *Journal of Physics C: Solid State Physics*, 7(6):1046.

[88] Kosterlitz, J. M. and Thouless, D. J. (1973). Ordering, metastability and phase transitions in two-dimensional systems. *Journal of Physics C: Solid State Physics*, 6(7):1181.

[89] Krämer, A. and Doniach, S. (1998). Superinsulator phase of two-dimensional superconductors. *Physical Review Letters*, 81(16):3523 – 3527.

[90] Landau, L. (1959). On the theory of the fermi liquid. *Sov. Phys. JETP*, 8(1):70.

[91] Landau, L. D. (1932). Zur theorie der energieubertragung ii. *Z. Sowjetunion*, 2:46–51.

[92] Lankhorst, M., Poccia, N., Stehno, M. P., Galda, A., Barman, H., Coneri, F., Hilgenkamp, H., Brinkman, A., Golubov, A. A., Tripathi, V., et al. (2018). Scaling universality at the dynamic vortex mott transition. *Physical Review B*, 97(2):020504.

[93] Larkin, A. and Vinokur, V. (1995). Bose and vortex glasses in high temperature superconductors. *Physical review letters*, 75(25):4666.

[94] Li, J., Aron, C., Kotliar, G., and Han, J. E. (2015). Electric-field-driven resistive switching in the dissipative hubbard model. *Physical review letters*, 114(22):226403.

[95] Lifshitz, I. (1968). Theory of fluctuation levels in disordered systems. *Soviet Physics JETP*, 26(2).

[96] Loh, Y., Tripathi, V., and Turlakov, M. (2005). Magnetic droplets in a metal close to a ferromagnetic quantum critical point. *Physical Review B*, 71(2):024429.

[97] Lopatin, A. and Vinokur, V. (2007). Hopping transport in granular superconductors. *Physical Review B*, 75(9):092201.

[98] Ma, M. and Lee, P. A. (1985). Localized superconductors. *Physical Review B*, 32(9):5658.

[99] Maekawa, S. and Fukuyama, H. (1982). Localization effects in two-dimensional superconductors. *Journal of the Physical Society of Japan*, 51(5):1380–1385.

[100] Mermin, N. D. and Wagner, H. (1966). Absence of ferromagnetism or antiferromagnetism in one-or two-dimensional isotropic heisenberg models. *Physical Review Letters*, 17(22):1133.

[101] Mironov, A. Y., Silevitch, D. M., Proslier, T., Postolova, S. V., Burdastyh, M. V., Gutakovskii, A. K., Rosenbaum, T. F., Vinokur, V. V., and Baturina, T. I. (2018). Charge berezinskii-kosterlitz-thouless transition in superconducting nbtin films. *Scientific reports*, 8(1):4082.

[102] Misra, S., Urban, L., Kim, M., Sambandamurthy, G., and Yazdani, A. (2013). Measurements of the magnetic-field-tuned conductivity of disordered two-dimensional mo 43 ge 57 and ino x superconducting films: Evidence for a universal minimum superfluid response. *Physical Review Letters*, 110(3):037002.

[103] Murakami, Y. and Werner, P. (2018). Nonequilibrium steady states of electric field driven mott insulators. *Physical Review B*, 98(7):075102.

[104] Nandkishore, R. M. and Sondhi, S. (2017). Many-body localization with long-range interactions. *Physical Review X*, 7(4):041021.

[105] Nattermann, T., Scheidl, S., Korshunov, S. E., and Li, M. S. (1995). Absence of reentrance in the two-dimensional xy-model with random phase shift. *Journal de Physique I*, 5(5):565–572.

[106] Oganesyan, V., Huse, D. A., and Sondhi, S. (2006). Theory of diamagnetic response of the vortex liquid phase of two-dimensional superconductors. *Physical Review B*, 73(9):094503.

[107] Oka, T. (2012). Nonlinear doublon production in a mott insulator: Landau-dykhne method applied to an integrable model. *Physical Review B*, 86(7):075148.

[108] Oka, T. and Aoki, H. (2005). Ground-state decay rate for the zener breakdown in band and mott insulators. *Physical review letters*, 95(13):137601.

[109] Oka, T. and Aoki, H. (2010). Dielectric breakdown in a mott insulator: Many-body schwinger-landau-zener mechanism studied with a generalized bethe ansatz. *Physical Review B*, 81(3):033103.

[110] Oka, T., Arita, R., and Aoki, H. (2003). Breakdown of a mott insulator: a nonadiabatic tunneling mechanism. *Physical review letters*, 91(6):066406.

[111] Okamoto, S. (2007). Nonequilibrium transport and optical properties of model metal–mott-insulator–metal heterostructures. *Physical Review B*, 76(3):035105.

[112] Onnes, H. K. (1911). The disappearance of the resistivity of mercury. *Comm. Leiden*, 122:2.

[113] Ovadia, M., Kalok, D., Tamir, I., Mitra, S., Sacépé, B., and Shahar, D. (2015). Evidence for a finite-temperature insulator. *Scientific reports*, 5:13503.

[114] Ovadia, M., Sacépé, B., and Shahar, D. (2009). Electron-phonon decoupling in disordered insulators. *Physical review letters*, 102(17):176802.

[115] Paalanen, M., Hebard, A., and Ruel, R. (1992). Low-temperature insulating phases of uniformly disordered two-dimensional superconductors. *Physical Review Letters*, 69(10):1604.

[116] Petković, A., Vinokur, V. M., and Nattermann, T. (2009). Transport properties of clean and disordered josephson-junction arrays. *Physical Review B*, 80(21):212504.

[117] Pokrovsky, V., Falco, G., and Nattermann, T. (2010). Phase diagram of electron systems near the superconductor-insulator transition. *Physical Review Letters*, 105(26):267001.

[118] Rault, J. (2000). Origin of the vogel–fulcher–tammann law in glass-forming materials: the α–β bifurcation. *Journal of Non-Crystalline Solids*, 271(3):177–217.

[119] Rozenberg, M., Sanchez, M. J., Weht, R., Acha, C., Gomez-Marlasca, F., and Levy, P. (2010). Mechanism for bipolar resistive switching in transition-metal oxides. *Physical Review B*, 81(11):115101.

[120] Sacépé, B., Chapelier, C., Baturina, T., Vinokur, V., Baklanov, M., and Sanquer, M. (2008). Disorder-induced inhomogeneities of the superconducting state close to the superconductor-insulator transition. *Physical review letters*, 101(15):157006.

[121] Sachdev, S., Sengupta, K., and Girvin, S. (2002). Mott insulators in strong electric fields. *Physical Review B*, 66(7):075128.

[122] Sachdev, S. and Ye, J. (1993). Gapless spin-fluid ground state in a random quantum heisenberg magnet. *Physical review letters*, 70(21):3339.

[123] Sambandamurthy, G., Engel, L., Johansson, A., Peled, E., and Shahar, D. (2005). Experimental evidence for a collective insulating state in two-dimensional superconductors. *Physical review letters*, 94(1):017003.

[124] Sambandamurthy, G., Engel, L., Johansson, A., and Shahar, D. (2004). Superconductivity-related insulating behavior. *Physical review letters*, 92(10):107005.

[125] Sankar, S. and Tripathi, V. (2016). Low-field magnetoresponse of strongly disordered two-dimensional superconductors. *Phys. Rev. B*, 94:054520–054527.

[126] Sankar, S., Vinokur, V., and Tripathi, V. (2018). Disordered berezinskii-kosterlitz-thouless transition and superinsulation. *Physical Review B*, 97(2):020507.

[127] Schmidt, P. and Monien, H. (2002). Nonequilibrium dynamical mean-field theory of a strongly correlated system. *arXiv preprint cond-mat/0202046*.

[128] Schwinger, J. (1951). On gauge invariance and vacuum polarization. *Physical Review*, 82(5):664.

[129] Sengupta, A. M. (2000). Spin in a fluctuating field: the bose (+ fermi) kondo models. *Physical Review B*, 61(6):4041.

[130] Shangina, E. L. and Dolgopolov, V. T. (2003). Quantum phase transitions in two-dimensional systems. *Physics-Uspekhi*, 46(8):777–787.

[131] Shimshoni, E., Auerbach, A., and Kapitulnik, A. (1998). Transport through quantum melts. *Physical Review Letters*, 80(15):3352.

[132] Shklovskii, B. (2008). Variable range hopping in thin film with large dielectric constant. *arXiv preprint arXiv:0803.3331*.

[133] Spivak, B. and Zhou, F. (1995). Mesoscopic effects in disordered superconductors near h c 2. *Physical Review Letters*, 74(14):2800.

[134] Steiner, M. A., Boebinger, G., and Kapitulnik, A. (2005). Possible field-tuned superconductor-insulator transition in high-t c superconductors: Implications for pairing at high magnetic fields. *Physical review letters*, 94(10):107008.

[135] Stewart, M., Yin, A., Xu, J., and Valles, J. M. (2007). Superconducting pair correlations in an amorphous insulating nanohoneycomb film. *Science*, 318(5854):1273–1275.

[136] Syzranov, S., Efetov, K., and Altshuler, B. (2009). dc conductivity of an array of josephson junctions in the insulating state. *Physical Review Letters*, 103(12):127001.

[137] Tang, L.-H. (1996). Vortex statistics in a disordered two-dimensional xy model. *Physical Review B*, 54(5):3350–3366.

[138] Teitel, S. and Jayaprakash, C. (1983). Josephson-junction arrays in transverse magnetic fields. *Physical Review Letters*, 51(21):1999.

[139] Tran, T., Beloborodov, I., Lin, X., Bigioni, T., Vinokur, V., and Jaeger, H. (2005). Multiple cotunneling in large quantum dot arrays. *Physical review letters*, 95(7):076806.

[140] Tripathi, V., Galda, A., Barman, H., and Vinokur, V. M. (2016). Parity-time symmetry-breaking mechanism of dynamic mott transitions in dissipative systems. *Physical Review B*, 94(4):041104.

[141] Tripathi, V. and Loh, Y. (2006). Thermal conductivity of a granular metal. *Physical review letters*, 96(4):046805.

[142] Trotzky, S., Chen, Y.-A., Flesch, A., McCulloch, I. P., Schollwöck, U., Eisert, J., and Bloch, I. (2012). Probing the relaxation towards equilibrium in an isolated strongly correlated one-dimensional bose gas. *Nature Physics*, 8(4):325.

[143] Tsuji, N., Oka, T., Aoki, H., and Werner, P. (2012). Repulsion-to-attraction transition in correlated electron systems triggered by a monocycle pulse. *Physical Review B*, 85(15):155124.

[144] Van der Zant, H., Elion, W., Geerligs, L., and Mooij, J. (1996). Quantum phase transitions in two dimensions: Experiments in josephson-junction arrays. *Physical Review B*, 54(14):10081.

[145] Vinokur, V. M., Baturina, T. I., Fistul, M. V., Mironov, A. Y., Baklanov, M. R., and Strunk, C. (2008). Superinsulator and quantum synchronization. *Nature*, 452(7187):613.

[146] Wannier, G. H. (1960). Wave functions and effective hamiltonian for bloch electrons in an electric field. *Physical Review*, 117(2):432.

[147] Zaránd, G., Zimányi, G. T., and Wilhelm, F. (2000). Two-channel versus infinite-channel kondo models for the single-electron transistor. *Physical Review B*, 62(12):8137.

[148] Zener, C. (1934). A theory of the electrical breakdown of solid dielectrics. *Proc. R. Soc. Lond. A*, 145(855):523–529.

Appendix A

Replica RG analysis of the disordered XY model

In this section I show the essential steps followed for obtaining the phase diagram of the two-dimensional XY model with phase disorder. A comprehensive study can be found in Ref. [34].

The partition function of the replicated Coulomb gas with *m-vector* charges after averaging over the bare disorder is

$$\overline{Z^m} = 1 + \sum_{p=2}^{\infty} \sum_{\mathbf{n}_1,\ldots,\mathbf{n}_p} \int_{|\mathbf{r}_i - \mathbf{r}_j| > a_0} \exp(-\beta H^{(m)}[\mathbf{n},\mathbf{r}]),$$

where the sum is over all distinct neutral configurations and

$$\beta H^{(m)} = \sum_{i \neq j} K_{ab} n_i^a \ln\left(\frac{|\mathbf{r}_i - \mathbf{r}_j|}{a_0}\right) n_j^b + \sum_i \ln Y[\mathbf{n}_i].$$

Here, $Y[\mathbf{n}] = \exp(-n^a \gamma K_{ab} n^b)$, where $K_{ab} = \beta J \delta_{ab} - \sigma \beta^2 J^2$. Significant contribution to the partition function only comes from charges $\pm 1, 0$ and hence we restrict to these. We increase the hard core cutoff $a_0 \to a_0 e^{(dl)}$ and retain the original form of the partition function in terms of scale dependent coupling constants $(K_l)_{ab}$ and fugacities $Y_l[\mathbf{n}]$. To $O(Y[\mathbf{n}]^2)$, we obtain the following RG flow equations[34]:

$$\partial_l (K_l^{-1})_{ab} = 2\pi^2 \sum_{\mathbf{n} \neq 0} n^a n^b Y[\mathbf{n}] Y[-\mathbf{n}] \tag{A.1}$$

$$\partial_l Y[\mathbf{n} \neq 0] = (2 - n^a K_{ab} n^b) Y[\mathbf{n}] + \sum_{\mathbf{n}' \neq 0, \mathbf{n}} \pi Y[\mathbf{n}'] Y[\mathbf{n} - \mathbf{n}'] \tag{A.2}$$

Equation(A.1) comes from the annihilation of dipoles of opposite vector charges in the annulus $a_0 < |r_i - r_j| < a_0 e^{dl}$. It gives the renormalization of the interaction and of the disorder. Simple rescaling gives the first part of equation (A.2). The second part comes from the possibility of fusion of two replica vector charges upon coarse graining. Some examples of fusion are given below.

$$\begin{pmatrix}\vdots\\ +1\\ \vdots\\ +1\\ \vdots\\ 0\\ \vdots\end{pmatrix}+\begin{pmatrix}\vdots\\ 0\\ \vdots\\ 0\\ \vdots\\ -1\\ \vdots\end{pmatrix}\rightarrow\begin{pmatrix}\vdots\\ +1\\ \vdots\\ +1\\ \vdots\\ -1\\ \vdots\end{pmatrix},\quad\begin{pmatrix}\vdots\\ +1\\ \vdots\\ -1\\ \vdots\\ 0\\ \vdots\end{pmatrix}+\begin{pmatrix}\vdots\\ 0\\ \vdots\\ +1\\ \vdots\\ 0\\ \vdots\end{pmatrix}\rightarrow\begin{pmatrix}\vdots\\ +1\\ \vdots\\ 0\\ \vdots\\ 0\\ \vdots\end{pmatrix}$$

Replica permutation symmetry, which we will assume here and which is preserved by the RG, together with $n^a = 0, \pm 1$ implies that $Y[\mathbf{n}]$ depends only on the numbers n_+ and n_- of $+1/-1$ components of $\mathbf{n}$. We parameterize $Y[\mathbf{n}]$ by introducing a function of two arguments $\Phi(z_+, z_-)$, where $z_\pm(\mathbf{r}) = \exp(\pm\beta v_\mathbf{r})$, such that:

$$Y[\mathbf{n}] = \left\langle z_+^{n_+} z_-^{n_-} \right\rangle_\Phi \tag{A.3}$$

where we denote $< A >_\Phi = \int dz_+ dz_- A\Phi(z_+, z_-)$. After some manipulations [34], in the limit $m \to 0$, we can write eq(A.2) in terms of, $P = \phi/(\int_{z_+, z_- > 0} \phi)$, which can be interpreted as a probability distribution, as

$$\partial_l P(z_+, z_-) = \mathscr{O}P - 2P(z_+, z_-) + 2\left\langle \delta\left(z_+ - \frac{z_+^{'} + z_+^{''}}{1 + z_-^{'} z_+^{''} + z_+^{'} z_-^{''}}\right)\delta\left(z_- - \frac{z_-^{'} + z_-^{''}}{1 + z_-^{'} z_+^{''} + z_+^{'} z_-^{''}}\right)\right\rangle_{P'P''}, \tag{A.4}$$

where, $\mathscr{O} = \beta J(2 + z_+\partial_{z_+} + z_-\partial_{z_-}) + \sigma(\beta J)^2(z_+\partial_{z_+} - z_-\partial_{z_-})^2$. The $m \to 0$ limit of eq(A.1) similarly yields,

$$T\frac{dJ^{-1}}{dl} = 8\left\langle \frac{z_+^{'} z_-^{''} + z_-^{'} z_+^{''} + 4 z_+^{'} z_+^{''} z_-^{'} z_-^{''}}{(1 + z_+^{'} z_-^{''} + z_-^{'} z_+^{''})^2}\right\rangle_{PP} \tag{A.5}$$

$$\frac{d\sigma}{dl} = 8\left\langle \frac{(z_+^{'} z_-^{''} - z_-^{'} z_+^{''})^2}{(1 + z_+^{'} z_-^{''} + z_-^{'} z_+^{''})^2}\right\rangle_{PP} \tag{A.6}$$

Equations (A.4),(A.5) and (A.6) form the complete set of RG equations.

Numerical study[34] of the RG equations indicate the existence of an XY phase at low temperatures and below some critical disorder. Guided by the RG flow observed numerically within and near the boundaries of the XY phase, we can approximate the full RG equations by a simpler equation involving only the single fugacity distribution, $P_l(z) = \int dz_+ P_l(z_+, z) = \int dz_- P_l(z, z_-)$. In the low T regime, the distribution $P_l(z_+, z_-)$ is broad and the physics is dominated by rare favorable regions ($z_+ \sim 1$ or $z_- \sim 1$). Here we identify a parameter that allows to organise perturbation theory as: $P_l(1) \equiv P_l(z \sim 1) \sim P_l(z_+ \sim 1, z_- \sim 0) = P_l(z_+ \sim 0, z_- \sim 1)$We also observe that $P_l(1,1) \equiv P_l(z_+ \sim 1, z_- \sim 1) \sim P_l(1)^2$. Using these we can see schematically the RG equation (A.4) as a correction to $P_l(1)$ of order $P_l(1)$ by the first term and order $P_l(1)^2$ by the second term; in RG equation (A.5),(A.6) as a correction to order $P_l(1)^2$ to J_l and σ_l. Again working to order $P_l(1)^2$, we see that the denominators in the delta functions in (A.4) could be neglected. This approximation also simplifies equations (A.5) and (A.6).

Introducing

$$G_l(x) = 1 - \int_{-\infty}^{\infty} du \tilde{P}_l(u) exp(-e^{\beta(u-x+E_l)}), \tag{A.7}$$

where $u = 1/\beta \ln(z)$ and $E_l = \int_0^l J(l')dl'$, we see that (A.4) can be written as $\frac{1}{2}\partial_l G = \frac{\sigma J^2}{2}\partial_x^2 G + G(1-G)$. If σ and J are l independent we identify the above with Kolmogorov-Petrovskii-Piscounov (KPP) equation, whose general form is , $\frac{1}{2}\partial_l G = D\partial_x^2 G + f(G)$, where D is a constant and f satisfies $f(0) = f(1) = 0$, f positive between 0 and 1 and $f'(0) = 1, f'(G) \leq 1$ between 0 and 1. Since at large l, both J and σ converge and effectively becomes l independent, we see that we can use results from the study of KPP equation in our case at large l.

For a large class of initial conditions, the solutions of the KPP equation are known to converge uniformly towards traveling wave solutions of the form: $G_l(x) \to h(x - m_l)$. The velocity of the wave is given by $c = \lim_{l\to\infty} \partial_l m_l$. A theorem due to Bramson[28] shows that the asymptotic traveling wave is determined by the behavior at $x \to \infty$ of the initial condition $G_{l=0}(x)$ in the following manner. If $G_{l=0}(x)$ decays faster than $e^{-\mu x}$ where $\mu = 1/\sqrt{D}$, then $c = \sqrt{D}$. If $G_{l=0}(x)$ decays slower than $e^{-\mu x}$ where $\mu < 1/\sqrt{D}$, then $c = 2(D\mu + \mu^{-1})$. The parameterization(A.7) implies that the distribution $\tilde{P}_l(u)$ itself converges to a traveling front solution

$$\tilde{P}_l(u) \to_{l\to\infty} \tilde{p}(u - X_l)\ , X_l = m_l - E_l. \tag{A.8}$$

Since $\partial_l E_l \to_{l\to\infty} J_R$, we see that the asymptotic velocity of the front of $\tilde{P}_l(u)$ is $c - J_R$, where c is the KPP front velocity. The center of the front corresponds to the maximum of the distribution $\tilde{P}(u)$.

The asymptotic velocity clearly decides the phase of the system: since we start with a distribution peaked at some small z, if the velocity is positive, then $P_l(1)$ will increase and this would imply that the system is in the disordered phase. On the other hand negative velocity implies that the system is in the XY phase. The velocity vanishes at the phase boundary. By construction, the initial condition $G_{l=0}(x)$ decays for large x as $< z >_{P_0} e^{-\beta x}$. Hence we identify $\mu = \beta$. Based on the results discussed above about the front velocity selection in KPP equation we can conclude the following about the phase diagram of the model:

(a) For $T > T_g = J_R\sqrt{\sigma_R/2}$, $c = T\left(2 + \frac{\sigma_R J_R^2}{T^2}\right)$. Thus here the XY phase would exist for

$$2 - \frac{J_R}{T} + \frac{\sigma_R J_R^2}{T^2} < 0. \tag{A.9}$$

(b) For $T \leq T_g$, $c = J_R\sqrt{8\sigma_R}$. Thus here the XY phase would exist for $\sigma_R < \sigma_c = \frac{1}{8}$.

Critical behavior at zero temperature: The zero temperature phase transition from the XY phase to the disordered phase occurs at $\sigma_R = 1/8$. The center of the front is located at $u = X_l$ near the transition. It follows from [28] that, $X_l \approx (4\sqrt{D} - J)l - 3/2\sqrt{D}\ln l + X_0$.Hence in the critical region to leading order, we get,

$$\partial_l X_l \sim 4\sqrt{D} - J - \frac{3\sqrt{D}}{2l}. \tag{A.10}$$

After some manipulations the RG equations for J and σ in the critical region reads,

$$\partial_l(J^{-1}) = k\int du\tilde{p}_l(u - X_l)\tilde{p}_l(-u - X_l) \tag{A.11}$$

$$\partial_l\sigma = k\int_{u+u^{'}>-2X_l} \tilde{p}_l(u)\tilde{p}_l(u^{'}), \tag{A.12}$$

where k is some constant. Using the asymptotic form of $\tilde{p}_l(u)$discussed in [28] and working upto leading order in $(\sigma - \sigma_c)$, we can simplify the above equations to get,

$$\partial_l(J^{-1}) \sim \frac{C}{\sqrt{D}} X_l^3 \exp\left(\frac{2X_l}{\sqrt{D}}\right) \tag{A.13}$$

$$\partial_l\sigma \sim C X_l^3 \exp\left(\frac{2X_l}{\sqrt{D}}\right), \tag{A.14}$$

where C is a constant. To estimate the form of correlation length, we first introduce the small parameter,$g_l = \exp(X_l/\sqrt{D})$. Then (A.10) reads,

$$\partial_l g \sim \left(16(\sigma - \sigma_c) - \frac{3}{2l}\right) g \tag{A.15}$$

Now starting away from criticality, $\varepsilon = \sigma_c - \sigma_R > 0$, we find, $g_l \sim l^{-3/2} \exp(16\varepsilon l)$. Identifying the correlation length ξ as when $g_\xi \sim 1$, we find,

$$\xi \sim \exp\left(\frac{b}{|\sigma - \sigma_c|}\right), \tag{A.16}$$

where b is some constant. We then see that the universality class of this transition is clearly different from the BKT universality class.

Appendix B

Normalization of the Keldysh-AES partition function

A key property of the Keldysh partition function is that in the absence of source fields, the partition function is normalized. Demonstrating this for the Keldysh-AES action requires one to take into account the correct causal structure of the Green functions. We expand $\exp[\imath S_{\text{tun}}[\phi]]$ in powers of g. To leading order, we get,

$$Z^{(0)} = \int [D\phi][Dn] \exp\left[\imath \left(S_C[n,\phi]\right)\right] \tag{B.1}$$

Doing the functional integration over ϕ, we see that the constraints $\partial_t n^+ = 0$ and $\partial_t n^- = 0$ are imposed and then it immediately follows from the boundary condition , $n^+(-\infty) = n^-(-\infty)$, that $Z^{(0)} = 1$.

Order g

$$Z^{(1)} = \imath g \sum_k \int_{-\infty}^{\infty} \int_{-\infty}^{\infty} \text{dt dt' } L^{\sigma\sigma'}(t-t') \left\langle \exp\left[-\imath \phi_{k,1}^{\sigma}(t) + \imath \phi_{k,1}^{\sigma'}(t')\right] \right\rangle_0, \tag{B.2}$$

where $<>_0$ denotes averaging with respect to the bare action. Thus,

$$Z^{(1)} = \imath g \sum_k \int_{-\infty}^{\infty} \int_{-\infty}^{\infty} \text{dt dt' } L^{\sigma\sigma'}(t-t') \Pi_{\sigma\sigma'}(t-t'). \tag{B.3}$$

We have the site correlators,

$$C_{++}(t-t^{'}) = \exp\left[-\imath E_C|t-t^{'}|\right], \tag{B.4}$$

$$C_{+-}(t-t^{'}) = \exp\left[\imath E_C(t-t^{'})\right], \tag{B.5}$$

$$C_{-+}(t-t^{'}) = \exp\left[-\imath E_C(t-t^{'})\right], \tag{B.6}$$

$$C_{--}(t-t^{'}) = \exp\left[\imath E_C|t-t^{'}|\right]. \tag{B.7}$$

Then we get the bond correlators,

$$\Pi_{++}(t-t^{'}) = \exp\left[-2\imath E_C|t-t^{'}|\right], \tag{B.8}$$

$$\Pi_{+-}(t-t^{'}) = \exp\left[2\imath E_C(t-t^{'})\right], \tag{B.9}$$

$$\Pi_{-+}(t-t^{'}) = \exp\left[-2\imath E_C(t-t^{'})\right], \tag{B.10}$$

$$\Pi_{--}(t-t^{'}) = \exp\left[2\imath E_C|t-t^{'}|\right]. \tag{B.11}$$

From the bond correlators we immediately see that the term involving Σ^K vanishes. Now lets look at the term with Σ^+. In the time representation, we have to keep in mind that it comes with the causality factor $\theta(t)$ and hence we write it as $\Sigma(t)\theta(t)$. The term involving this reads as,

$$\Sigma^+(t)\theta(t)\left[\exp(\imath E_C t)-\exp(-\imath E_C t)-\exp(\imath E_C|t|)+\exp(-\imath E_C|t|)\right]. \tag{B.12}$$

Because of the presence of the Theta function, we see that we can remove the modulus sign from the last two terms and then clearly this contribution vanishes. Similarly we see that the contribution from terms involving Σ^- also vanishes. Hence we see that the order g contribution to the partition function vanishes. We assume that all the higher order g contributions to the partition function vanishes too and thus the partition function is truly equal to 1.

Appendix C

Overview of BCS theory

In this appendix, I discuss the fundamentals of the BCS theory of superconductivity. In the main text I have discussed the phonon mediated attractive interaction between electrons near the Fermi surface. For simplicity we now consider a local attractive interaction between the electrons characterized by a coupling constant g. The Hamiltonian for this system is (represented in the momentum space),

$$\hat{H} = \sum_{\mathbf{k}\sigma} \varepsilon_{\mathbf{k}} \hat{n}_{\mathbf{k}\sigma} - \frac{g}{V} \sum_{\mathbf{k},\mathbf{k}',\mathbf{q}} c^{\dagger}_{\mathbf{k}+\mathbf{q}\uparrow} c^{\dagger}_{-\mathbf{k}\downarrow} c_{-\mathbf{k}'+\mathbf{q}\downarrow} c_{\mathbf{k}'\uparrow}. \tag{C.1}$$

This model Hamiltonian is commonly referred to as the BCS Hamiltonian.

C.1 Instability towards Cooper pairing

To understand the existence of the instability near the Fermi surface towards formation of CPs lets look at the four point correlation function,

$$\Pi(\mathbf{q},\tau) = \frac{1}{V^2} \sum_{\mathbf{k}\mathbf{k}'} \left\langle \bar{\psi}_{\mathbf{k}+\mathbf{q}\uparrow}(\tau) \bar{\psi}_{-\mathbf{k}\downarrow}(\tau) \psi_{\mathbf{k}'+\mathbf{q}\downarrow}(0) \psi_{-\mathbf{k}'\uparrow}(0) \right\rangle \tag{C.2}$$

It is convenient to switch to a frequency representation, $\Pi(q) = T \int_0^{\beta} d\tau e^{-\imath\omega_m\tau} \Pi(\mathbf{q},\tau)$, where $q = (\mathbf{q},\omega_m)$. To calculate the correlation function diagrammatically, we assume that the density of the electron gas would play the role of a large parameter and thus retain only those diagrams that appear with one free momentum summation per interaction. See Fig C.1. The vertex of the propagator obeys the Bethe-Salpeter equation,

$$\Gamma_q = g + \frac{gT}{V} \sum_P G_{p+q} G_{-p} \Gamma_q. \tag{C.3}$$

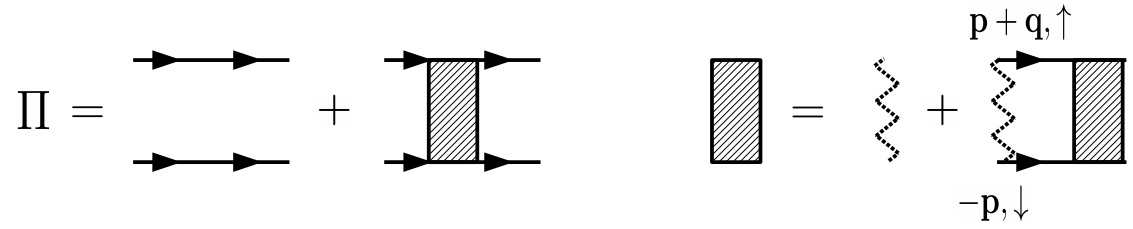

Figure C.1 Diagrams contributing to the four point correlation function with only one free momentum summation per interaction. The two green function lines defining each rung of the ladder carry momenta $p+q$ and $-p$ respectively. The vertex of the propagator obeys the Bethe Salpeter equation defined in Eq. (C.3)

The solution is given by,

$$\Gamma_q = \frac{g}{1 - \frac{gT}{V} G_{p+q} G_{-p}}. \tag{C.4}$$

We now look the case of zero external momentum, $q = (0,0)$. After some calculations [3], we can show that,

$$\Gamma_{0,0} \simeq \frac{g}{1 - g\nu \ln(\frac{\omega_D}{T})}, \tag{C.5}$$

where ν is the single particle DoS at the Fermi energy. The above form highlights one of the main points of the Cooper instability: the attractive interaction constant appears in combination with the single particle DoS; thus even for a small attractive interaction, the presence of a large single particle DoS, results in the Cooper instability. The above form suggests a critical temperature $T_c = \omega_D e^{-1/g\nu}$, where the vertex develops a singularity which signals the breakdown of a perturbative approach based on the Fermi sea of noninteracting electrons. To further understand this we now resort to a mean field treatment.

C.2 Mean field theory

We assume that the operator $\sum_{\mathbf{k}} c_{-\mathbf{k}\downarrow} c_{\mathbf{k}\uparrow}$ acquires a non-vanishing ground state expectation value in the SC state. Let us define the SC order parameter,

$$\Delta = \frac{g}{V} \sum_{\mathbf{k}} \left\langle 0 | c_{-\mathbf{k}\downarrow} c_{\mathbf{k}\uparrow} | 0 \right\rangle, \tag{C.6}$$

where $|0\rangle$ refers to the ground state. We now write

$$\sum_{\mathbf{k}} c_{-\mathbf{k}+\mathbf{q}\downarrow} c_{\mathbf{k}\uparrow} = \frac{V\Delta}{g} + \left[\sum_{\mathbf{k}} c_{-\mathbf{k}+\mathbf{q}\downarrow} c_{\mathbf{k}\uparrow} - \frac{V\Delta}{g} \right], \tag{C.7}$$

and consider the term in the square brackets to be small. We then substitute this back into the microscopic Hamiltonian retaining only the terms quadratic in the Fermionic operators. The mean-field Hamiltonian then takes the form,

$$\hat{H} - \mu\hat{N} \simeq \sum_{\mathbf{k}} \left[\xi_{\mathbf{k}} c^{\dagger}_{\mathbf{k}\sigma} c_{\mathbf{k}\sigma} - \left(\bar{\Delta} c_{-\mathbf{k}\downarrow} c_{\mathbf{k}\uparrow} + \Delta c^{\dagger}_{\mathbf{k}\uparrow} c^{\dagger}_{-\mathbf{k}\downarrow} \right) \right] + \frac{V|\Delta|^2}{g}. \tag{C.8}$$

This Hamiltonian is called the Bogoliubov-de Gennes (BdG) Hamiltonian. In terms of the Nambu spinors defined as,

$$\Psi_{\mathbf{k}} = \begin{pmatrix} c_{\mathbf{k}\uparrow} \\ c^{\dagger}_{-\mathbf{k}\downarrow} \end{pmatrix}, \tag{C.9}$$

the BdG Hamiltonian can be written as,

$$\hat{H} - \mu\hat{N} = \sum_{\mathbf{k}} \Psi^{\dagger}_{\mathbf{k}} \begin{pmatrix} \xi_{\mathbf{k}} & -\Delta \\ -\bar{\Delta} & -\xi_{\mathbf{k}} \end{pmatrix} \Psi_k + \sum_{\mathbf{k}} \xi_{\mathbf{k}} + \frac{V|\Delta|^2}{g}. \tag{C.10}$$

The BdG Hamiltonian can be diagonalized by the unitary transformation

$$\Xi_{\mathbf{k}} \equiv \begin{pmatrix} \alpha_{\mathbf{k}\uparrow} \\ \alpha^{\dagger}_{-\mathbf{k}\downarrow} \end{pmatrix} = U_{\mathbf{k}} \Psi_{\mathbf{k}}; \qquad U_{\mathbf{k}} = \begin{pmatrix} \cos\theta_{\mathbf{k}} & \sin\theta_{\mathbf{k}} \\ \sin\theta_{\mathbf{k}} & -\cos\theta_{\mathbf{k}} \end{pmatrix}. \tag{C.11}$$

Choosing Δ to be real and setting $\tan(2\theta_{\mathbf{k}}) = -\Delta/\xi_k$, the diagonalized Hamiltonian can be written as

$$\hat{H} - \mu\hat{N} = \sum_{\mathbf{k}\sigma} \lambda_{\mathbf{k}} \alpha^{\dagger}_{\mathbf{k}\sigma} \alpha_{\mathbf{k}\sigma} + \sum_{\mathbf{k}} (\xi_{\mathbf{k}} - \lambda_{\mathbf{k}}) + \frac{\Delta^2 V}{g}, \tag{C.12}$$

where,

$$\lambda_{\mathbf{k}} = \left(\Delta^2 + \xi^2_{\mathbf{k}} \right)^{1/2}. \tag{C.13}$$

The elementary excitations created by $\alpha^{\dagger}_{\mathbf{k}\sigma}$ are called Bogoliubov quasiparticles. They have a minimum energy Δ and is called the energy gap that is mentioned in the main text. Thus the elementary excitations from the SC ground state are well separated by this energy gap and this results in the rigidity of the SC ground state. The SC ground state wave function is determined by the vacuum of the algebra $\{\alpha_{\mathbf{k}}, \alpha^{\dagger}_{\mathbf{k}}\}$,

$$|\Omega_s\rangle \sim \prod_{\mathbf{k}} \left(\cos\theta_{\mathbf{k}} - \sin\theta_{\mathbf{k}} c^{\dagger}_{\mathbf{k}\uparrow} c^{\dagger}_{-\mathbf{k}\downarrow} \right) |\Omega\rangle, \tag{C.14}$$

where $|\Omega\rangle$ is the ground state of the Fermion algebra. In the mean-field treatment Δ has been a input parameter so far and we need to determine it self-consistently from Eq. (C.6). We

have

$$\begin{aligned} \Delta &= \frac{g}{2V}\sum_{\mathbf{k}}\frac{\Delta}{(\Delta^2+\xi_{\mathbf{k}}^2)^{1/2}} \\ &\simeq \frac{g\Delta}{2}\int_{-\omega_D}^{\omega_D}\frac{\nu(\xi)d\xi}{(\Delta^2+\xi^2)^{1/2}} = g\Delta\nu\sinh^{-1}(\omega_D/\Delta), \end{aligned} \tag{C.15}$$

where we have made use of the assumption that the pairing interaction uniformly extends over an energy scale ω_D and have also taken the single particle DoS to be constant in that range. The DoS for the excitations from the SC ground state is obtained as,

$$\rho(\varepsilon) = \int d\xi\,\nu(\xi)\delta(\varepsilon-\lambda(\xi)) \sim 2\nu\Theta(\varepsilon-\Delta)\frac{\varepsilon}{\left(\varepsilon^2-\Delta^2\right)^{1/2}} \tag{C.16}$$

where $\lambda(\xi) = (\xi^2+\Delta^2)^{1/2}$.

The above equation for the gap (Eq. (C.16)) is obtained only for the zero temperature case. For a finite temperature T, the gap equation gets modified as,

$$\Delta = \frac{gT}{V}\sum_{\mathbf{k},n}\frac{\Delta}{|\Delta|^2+\xi_{\mathbf{k}}^2+\omega_n^2}, \tag{C.17}$$

where n is the index of the Fermionic Matsubara frequency ω_n. After performing the Matsubara summation, we get the BCS gap equation

$$\Delta = g\Delta\nu\int_0^{\omega_D} d\xi\,\frac{\tanh(\lambda(\xi)/2T)}{\lambda(\xi)}. \tag{C.18}$$

We can estimate the critical temperature for the SC transition from the gap equation by looking at the point where the gap vanishes. We obtain

$$T_c = c\,\omega_D e^{-1/g\nu}, \tag{C.19}$$

where c is a constant of order unity. For temperatures close and below T_c , Δ obeys the form, $\Delta \sim \sqrt{T_c(T_c-T)}$.